Study on the effect of different sols on high alumina castable refractory

Akhilesh Kr. Singh

Department of Ceramic Engineering,

National Institute of Technology, Rourkela

Study on the effect of different sols on high alumina castable refractory

Dissertation submitted in partial fulfillment
of the requirements of the degree of

Doctor of Philosophy

in

Ceramic Engineering

By

Akhilesh Kr. Singh (Roll No. 512CR108)

based on research carried out
under the supervision of

Dr. Ritwik Sarkar & Dr. Sumit Kr. Pal

Department of Ceramic Engineering,

National Institute of Technology,

Rourkela, Odisha, India

(April 2017)

Ceramic Engineering Department
National Institute of Technology, Rourkela

April 2017

Certificate of Examination

Roll Number: 512CR108

Name: Akhilesh Kr. Singh

Title of Dissertation: Study on the effect of different sols on high alumina castable refractory

We the below signed, after checking the dissertation mentioned above and the official record book(s) of the student, hereby state our approval of the dissertation submitted in partial fulfillment of the requirements of the degree of Doctor of Philosophy in Ceramic Engineering at National Institute of Technology Rourkela. We are satisfied with the volume, quality, correctness, and originality of the work.

Dr. Sumit Kr. Pal
Co-Supervisor

Dr. Ritwik Sarkar
Principal Supervisor

Dr. Shantanu Kr. Behera
Member, DSC

Dr. Sunipa Bhattacharya
Member, DSC

Dr. Anil Kr. Singh
Member, DSC

Dr. Atanu Ranjan Pal
External Examiner

Dr. Swadesh Kr. Pratihar
Chairperson, DSC

Dr. Bibhuti Bhusan Nayak
Head of the Department

Ceramic Engineering Department
National Institute of Technology, Rourkela

April 2017

Supervisor's Certificate

This to certify that the thesis entitled "**Study on the effect of different sols on high alumina castable refractory**" being submitted by **Mr. Akhilesh Kr. Singh** for the award of the degree of **Doctor of Philosophy** in Ceramic Engineering of NIT Rourkela is a record of bona fide research work carried out by him under our supervision and guidance. Akhilesh Kr. Singh has worked for more than four years on the above topic. His research work at the Department of Ceramic Engineering from National Institute of Technology, Rourkela has reached the standard fulfilling the requirements and the regulations relating to the degree. The contents of this thesis, in full or part, have not been submitted to any other university or institution for the award of any degree.

Dr. Sumit K Pal
Assistant Professor
Department of Ceramic Engg,
NIT, Rourkela.

Dr. Ritwik Sarkar
Associate Professor
Department of Ceramic Engg,
NIT, Rourkela

In loving memory of my beloved father

…“Shri Shivpujan Prasad”…

This thesis is dedicated to my family

“For their endless love, support and encouragement”

Declaration of Originality

I, **Akhilesh Kr. Singh**, Roll Number 512CR108 hereby declare that this dissertation entitled "**Study on the effect of different sols on high alumina castable refractory**" represents my original work carried out as a doctoral student of NIT Rourkela and, to the best of my knowledge, it contains no material previously published or written by another person, nor any material presented for the award of any other degree or diploma of NIT Rourkela or any other institution. Any contribution made to this research by others with whom I have worked at NIT Rourkela or elsewhere is explicitly acknowledged in the dissertation. Works of other authors cited in this dissertation have been duly acknowledged under the section "Bibliography". I have also submitted my original research records to the scrutiny committee for the evaluation of my dissertation.

I am fully aware that in the case of any non-compliance detected in future, the Senate of NIT Rourkela may withdraw the degree awarded to me on the basis of the present Dissertation.

April 2017

Akhilesh Kr. Singh
NIT Rourkela

Acknowledgement

This manuscript would not have been possible without the help of my empathetic and supportive guide **Dr. Ritwik Sarkar**. I heartfelt thank him for his unconditional help, constant effort for improving my work, providing time to time feedback and never giving upon me. It has been an honor to be his first Ph.D. student. You have been a tremendous mentor for me. I would like to thank you for encouraging my research and for allowing me to grow as a research scientist.

I would also like to express my gratitude to my co-supervisor **Dr. Sumit Kr. Pal** for his help and guidance throughout my research. I am indebted to my Doctoral Scrutiny Committee (DSC) chairman **Dr. Swadesh Kr**. **Pratihar** and members **Dr. Shantanu Behera, Dr. Sunipa Bhattacharya** of Ceramic Engineering department and **Dr. Anil Kr. Singh** of Physics Department.

I am highly obliged to **Dr. A. Biswas**, Director, and **Dr. S. K. Sarangi**, Ex-Director, National Institute of Technology (NIT), Rourkela and **Dr. Bibhuti Bhusan Nayak,** Head of the Department, of Ceramic Engineering, for the academic support and the facilities to carry out the research work efficiently at the institute.

I also express my thankfulness to all the faculty and staff members of the Department of Ceramic Engineering for their continuous encouragement and suggestions. Special thanks to my friend **Kanchan, Abhishek, Satya, Venkatesh**, my seniors, and juniors for their kind cooperation during the research work.

April 2017

Akhilesh Kr. Singh

NIT Rourkela

Abstract

Ever-increasing demand and application of unshaped refractories replacing shaped ones have inspired the scientists and manufacturers to investigate these materials in depth for further improving the quality and performance. Among the various unshaped refractories, castables lead in all the areas of research, development, manufacturing and application. Physical, mechanical, chemical and thermo-mechanical characteristics of various castable systems as well as their processing and bonding mechanisms are the focus of such investigations. Among the different bonding materials, calcium aluminate cement (CAC) is most common, but the introduction of CaO in the refractory castable system by the use of CAC produces low melting phases on reaction with Al_2O_3 and SiO_2 of the refractory systems and finally resulting in poor high temperature properties. To avoid the crisis, decrease in cement content and use of alternate bonding system were widely experimented. Among alternate bonding materials, development of sol-gel technique has opened a new horizon in bonding system for refractory technologists. The principle behind sol-gel bonding is the formation of a 3-dimensional network (gel) of particles that surrounds the refractory materials and which on subsequent heating develop strength by formation of ceramic bonding through sintering.

In the present work, four different precursor sol systems have been synthesized, namely alumina, boehmite, mullite, and spinel by wet chemical synthesis. The sol systems were chosen in such a way that they generate high temperature withstanding refractory oxides on firing (alumina, mullite, and spinel). These synthesized sols are used as a sole binder in high alumina castable systems, with two different particle size distributions, containing no cement. The castables were processed conventionally and evaluated at different temperatures for the various refractory properties. Phase analysis and microstructural development are also studied to investigate the reasoning for the development of the properties. These synthesized sol based castable compositions were further compared with commercially available silica sol and cement-containing compositions using similar raw materials, particle size distributions and processed under exactly similar conditions.

The synthesized sol bonded castables showed well-sintered density and strength compared to traditional cement and silica sol bonded castables. The densities (3.0-3.2 g/cc) obtained signifies a well compact microstructure, as also observed in the microstructural analysis. Considerably high hot strength and higher thermal shock and corrosion resistances were observed for the developed sol containing compositions, higher than the commercial binders, mainly due to the absence of any impurity phase. Among the developed sol bonding systems, mullite and spinel sols were found to have improved hot properties and greater resistances against corrosion and thermal shock. All the developed sol containing compositions showed no deformation or any considerable shrinkage even on firing at 1650^0C, indicating its application at and above this temperature without any difficulty. However, conventional cement and silica containing compositions resulted in poor properties due to the formation of low melting compounds in the system.

Keywords: *sol-gel, high alumina castable, alumina sol, boehmite sol, mullite sol, spinel sol, characterization.*

Contents

List of Figures

List of Tables

Dissertation layout

The present thesis is the outcome of the research work on Synthesis of different sol systems and using them as sole binder for the development of cement free refractory castable compositions. For systematic description and discussion of the entire work, the thesis has been divided into 6 Chapters. The brief contents of the different Chapters have been described below:

Chapter-1

Chapter 1 describes the Introduction to the work and starts with a brief introduction to ceramics and refractories followed by a general description of unshaped refractories. A brief introduction of refractory castables with various bonding systems available for castables is then detailed, followed by brief description of commercial sol-gel bonding system, colloidal silica. Later, some new bonding systems are mentioned which are under research during last decade and have a potential for commercial exploitation. Finally, the application areas of different refractory castables are mentioned in brief.

Chapter-2

This chapter describes the available Literature in the area of refractory castables. The chapter begins with a brief introduction about the refractory materials followed by unshaped refractories with a focus on castables. The history and present perspective of various bonding systems for castables are discussed next. The next section deals with the sol-gel bonding system, the advantages and drawbacks of silica sol followed by the requirement of other sols as a binding system and difficulties associated with them. The next section discusses the available literature for sol making processes of alumina, mullite and spinel systems and studies of these sols in castable systems followed by the importance of particle size distribution in castables.

Chapter-3

This chapter points out the various factors from the literature study which Motivates to choose the current topic and the various Objectives set to carried out the proposed research work.

Chapter-4

This Chapter discusses in detail about the Experimental Work carried out to conduct the research work. The initial part describes the synthesis of various sol (alumina, boehmite, mullite, and Mg-Al spinel) systems followed by different characterizations done on the synthesized sols. This is followed by preparation of high alumina castables, with two different particle size distribution patterns, using the synthesized sols as sole binder. The next section discusses the various characterization techniques to evaluate the properties of developed castables. The further section discusses the preparation of high alumina castables with commercial binders for a comparative study with each of the developed sol bonded castables having optimized properties. The final part lists the various instruments used in the research work.

Chapter-5

This chapter discusses the various results obtained from the research work and is divided into five sections. The first section deals with the results and discussion for developed alumina sol bonded high alumina castable composition. The first part of this section discusses the various results obtained from alumina sol characterization and the second part discusses the results obtained for various castable characterizations. Both the parts are summarized finally in the last.

Similarly the second, third and fourth sections of this chapter deals with the results and discussion on the properties of the developed boehmite, mullite, and spinel sols and also on the properties obtained for the high alumina castables prepared by using these sols respectively. The final fifth section of this chapter discusses the comparative study of the optimized batches from previous four sections against the castables prepared by using commercial binders, cement and silica sol, prepared by using exactly similar raw materials and processing conditions.

Chapter-6

In this final chapter, the entire work is summarized, and the outline for the future work has also been provided.

Further, it is important to note that all the references have been compiled together as a separate Reference list after 6^{th} Chapter. All the references for a given chapter are provided under the chapter heading.

Chapter 1

Introduction

1.1 Ceramics- materials for advanced technology

Ceramics are inorganic, non-metallic solid materials wherein the atoms are bonded together by ionic or covalent bonds. The ceramic material ranges from highly crystalline to semi-crystalline and is often completely amorphous by nature such as glasses. They are synthesized either from a molten mass by solidification, which is formed and matured by the heat treatment or synthesized chemically by hydrothermal or sol-gel synthesis at low temperatures. The ceramics history can be dated as back as 27,000 years old pottery objects, including figurines made of clay which is hardened and sintered by fire. But ceramics are not only about pottery and dishes; bricks, tiles, cement and glass are other known examples. The last century witnessed the development of new ceramic materials for use in a wide range of industries, like aerospace, biomedical, mining, refinery, chemical, electronics, etc. [1.1, 1.2].

The properties of ceramics, like any other materials, are dependent on the types of constituent atoms, the bonding nature of the atoms, and the structural arrangement of those atoms. The nature of bonding and the structural arrangement of the atoms determines the properties acquired by a material. The combination of strong ionic and covalent bonds present in a ceramic material usually resulted in high melting points, high hardness and elastic modulus, low thermal expansion and higher chemical resistance. On the other hand, they are often brittle (unless toughened by any reinforcements), which can lead to fracture.

The special properties possessed by ceramics give rise to many applications in diverse engineering fields such as materials, electrical, chemical and mechanical, etc. Also, the high heat resistant of ceramic materials prefers them over metal and polymers which are unsuitable for such tasks [1.2]. For example, in industries like metals, cement, glasses, petrochemicals, even in nuclear power plants and in space shuttles, special ceramic materials, resistant to very high temperatures, are required. Commonly known as refractory materials, these special high temperature ceramics are one of the most important classes of materials which have recently got attention among the research community.

1.2 Refractories: High temperature ceramics

Refractories are special materials which are primarily used to expedite the production of various other materials by enabling the utilization of heat since Bronze Age [1.3]. The various scientific and technical developments that have taken place over the last 100 years would not have been possible without the refractories. The development of refractories industry over the last few decades are directly influenced by the developments in other materials processing industries, particularly the iron and steel industry, which utilizes currently more than 60% of all the refractories produced [1.4]. They are mostly used in iron and steel industries along with cement, glass, copper, aluminium and petrochemical industries and play a very crucial role in cost and quality of the products.

Improved process technology resulting in easier production methods and higher productivity or better quality products resulting in longer campaign lives by improving high temperature properties are the primary driving force for the change in refractory technology. Moreover, some new criteria are added recently, like environmental friendliness, waste utilization, etc. The later criteria can better be understood from the replacement of the chromium bearing refractories in cement kiln applications. Trivalent chromium ions may convert to hexavalent one during the kiln operation due to various chemical environments. The same is also true for the change in the refractory carbonaceous binder from pitch and tar to the resin, to reduce the poisonous fumes from these binders [1.5].

In metallurgical industries, refractories are usually employed as the internal linings of furnaces, reactors, kilns and other vessels for holding and transportation of hot metal and slag. In non-metallurgical industries, it is mostly used in coke calciner, cracking furnaces, sulfur furnaces, catalytic cracking units, utility boilers, incinerators, fired heaters, ammonia primary and secondary reformers, hydrogen reformers, ducting, stacks, air heaters, etc. Most of these equipment function at high pressure and temperature can ranges from 500 to 1600^0C or even more. Thus refractory materials which can withstand these conditions are required for proper functioning of these equipment [1.6].

The operating conditions where refractories are used vary considerably, and hence a range of refractory materials with different properties are required to meet the challenge. Depending on their application, refractory materials are manufactured in various combinations and shapes. A refractory material, in general, must have the following properties [1.7]:

- Sustainability for high temperature
- Ability to withstand sudden temperature change
- Resistance for molten metal, slag, etc.
- Load bearing capacity at service conditions.
- Resistance to abrasive forces
- Heat conserving capability
- Volume stability at higher temperatures
- Should have high chemical resistance

1.3 Properties of a refractory material

The physical, chemical and mineralogical characteristics of a refractory material decide the quality and its suitability for a particular application. The properties [1.6-1.8] that are taken into consideration while selecting an optimum refractory lining configuration are as follows-

- Bulk density: It is the amount of refractory material within a given volume. A refractory material with higher bulk density has a denser structure, resulting in better chemical resistance, lower metal penetration, higher abrasion resistance, besides other related advantages.
- Apparent porosity: It is the percent volume of the open pores in comparison to the total volume of the refractory. This is essentially an important property for the refractories which remain in contact with molten charge and slag. A refractory with lower apparent porosity better prevents the penetration of the molten material.
- Cold crushing strength (CCS): The CCS of a refractory material is its capacity to provide resistance against any compressive load at the room temperature. It is the maximum load which a refractory can resist before it breaks and is generally measured in pounds per inch square or kilogram per centimeter square.

- Hot modulus of rupture (HMOR): It is the flexural resistance of any refractory against loading at an elevated temperature or over a range of temperatures. The HMOR is an essential property from which the suitability of a refractory at a certain temperature can be determined.
- Pyrometric cones and Pyrometric cones equivalent (PCE): Pyrometric cones are used in ceramic industries to test the refractoriness and state of maturity of the refractory material composition after firing. They consist of a mixture of oxides that are known to melt at a specific narrow temperature range.
- Refractoriness under load (RUL): The refractoriness of a material is its ability to sustain at an elevated temperature without undergoing any deformation. The RUL of any material indicates the temperature at which it will collapse, during service under similar load.
- Creep at high temperature: It is a time-dependent property of a refractory material, which governs the deformation in the material, at a given temperature within a given time, when the material is under a certain load. In other words, it is the heat-activated plastic deformation in the body under stress as a function of time.
- Reversible thermal expansion: Heating any material leads to its expansion, and it contracts when cooled. The reversible thermal expansion of a material reflects the phase transformations which takes place during heating and cooling.
- Thermal conductivity: It is defined as the amount of heat flow through a unit area, in a direction normal to the surface area, in a defined time, with a known temperature gradient. Thermal conductivity depends on the chemical and mineralogical composition, porosity and on the application temperature. High thermal conductivity of a refractory is desirable when heat transfer though brickwork is required, for example in recuperators, regenerators, muffles, etc. Low thermal conductivity is desirable when the heat has to be conserved.

1.4 Refractories classification:

Refractories can be classified on various bases like chemical composition, chemical nature or behavior, end use of refractory, methods of manufacture or in terms of physical shape [1.6-1.10].

- **Based on Chemical Composition:** According to this, the refractories are classified on the basis of the major chemical constituent present in the refractory system. For e.g.
  - **Silica bricks:** Silica brick (or Dinas) is a refractory that contains at least 93 percent SiO_2.
  - **Fireclay refractories:** Fireclay refractories consist of aluminum silicates with varying silica (SiO_2) content of up to 78 percent and Al_2O_3 content of up to 44 percent.
  - **High alumina refractories:** Alumina silicate refractories containing more than 45 percent alumina are generally termed as high alumina materials.
  - **Mullite refractories:** A refractory body consisting of 71.8% alumina and 28.2% silica, if fired at equilibrium conditions, will be composed of the mullite only.
  - **Corundum refractories:** The refractories with more than 99% alumina is called corundum refractories. They consist of only single-phase, polycrystalline alpha alumina.
  - **Magnesite:** Magnesite refractories are chemically basic materials, which contains at least 85 percent magnesium oxide (MgO).
  - **Dolomite:** The naturally occurring double carbonate of calcium and magnesium (Dolomite, $CaCO_3.MgCO_3$) on high temperature firing converts to refractory dolomite (CaO- MgO). High purity dolomite consists of more than 97% CaO and MgO.
  - **Chromite refractories:** Two types of chromite refractories are distinguished:
    - Chrome-Magnesite refractories, which usually contain 15-35 percent Cr_2O_3 and 42-50 percent MgO.
    - Magnesite-Chromite refractories, which contain at least 60 percent MgO and 8-18 percent Cr_2O_3.
  - **Zirconia refractories:** The very high strength of zirconia at room temperature is maintained even up to the temperature of 1500^0C and thus is useful as high temperature construction material.
- **Based on Chemical nature or behavior: O**n the basis of refractories chemical behavior towards slags i.e. their reaction to a particular slag, they are classified as:

- **Acidic refractories**: They are chemically stable to acidic slags and in the acidic atmosphere but are attacked by alkalis e.g. Silica, Semi-silica, Aluminosilicate refractories.
- **Basic refractories**: They are chemically stable to basic slags and in the basic atmosphere but reacts with acids e.g. Magnesite, Chrome-Magnesite, Magnesite-Chromite, Dolomite refractories.
- **Neutral refractories**: They are chemically stable to both acidic and basic slags and are used in either atmosphere e.g. Fireclay bricks, Pure Alumina and Chrome refractories.
- **Special refractories**: Silicon Carbide, Zirconia and Carbon refractories.

❖ Based on end use, they may be classified as Blast furnace, casting pit, etc.

❖ Based on manufacturing method, the classification is Dry press process, fused cast, hand molded, formed (normal, fired or chemically bonded) and unformed (monolithic, gunning castable, plastic, ramming mass and spraying, etc.)

❖ **Based on the physical form:** Classification on the basis of physical form, in which they are used, is more common and are classified as shaped refractories commonly known as bricks and unshaped or monolithic refractories which are loose powdered material without any definite shape and only given shape during application.

Shaped and Unshaped refractories:

Physically refractories are shaped or unshaped. The refractories which delivered to the end user in a fixed shape are known as shaped refractories and are commonly known as bricks. The shaped refractories or bricks may further be divided into standard shapes and special shapes. Standard shaped bricks come with a dimension that most refractory manufacturers follows and are applicable to furnaces and kilns of the same type. Special bricks are specifically designed for a particular furnace or kiln and may not applicable to others. Shaped refractories are generally prepared by a pressing machine. The machine applies a static pressure to shape the bricks in the mold. A high uniformity in properties is achieved in these shaped refractories. Special shapes are usually hand-molded and hence a slight variation in properties are expected in these [1.6].

Unshaped refractories have no predefined shape or size and are supplied to user industries as a mixture of different aggregates, binders, and additives. They can take the shape of a single (mono) structure (lithus) without any joints and are thus also called monolithics. Unshaped or monolithic refractories have wide commercial applications throughout the iron and steel, cement, non-ferrous metallurgy, petrochemical and waste incinerators. These refractories are available in many forms as per their application techniques with wide compositional variations. Chemical inertness, mechanical integrity, abrasion and corrosion resistances and thermal shock resistance at high temperatures are the main feature of these refractories. Monolithic refractories are gradually replacing conventional shaped ones due to various advantages like joint-less lining, easier installation method, skill not required, simple handling and transportation, better volume stability, high spalling resistance and ability to install in "hot standby" mode [1.11, 1.12].

1.5 Classification of Unshaped refractories:

They can further be classified on the basis of application as castables, refractory mortars, ramming mass, gunning mass, plastic mass, shotcrete, etc. [1.11, 1.12].

- Castables: They consists of precision graded coarse and fine refractory grains and are consolidated by a binding system at green stage. After heating, the binder either volatizes or transforms into finer particles, facilitating ceramic bond formation by sintering. The commonly used binder for castables is high alumina cement. Hydratable alumina and colloidal silica are other binders that are often used. These materials are installed by casting and are also known as refractory concretes.
- Plastic Refractories: These unshaped refractories are tempered with water and/or added with a binder to have sufficient plasticity such that it can be pounded or rammed onto place. They are mixtures which are prepared in stiff plastic condition and are usually delivered in form of blocks wrapped in polythene. At the place of application, the blocks are sliced into small pieces and then rammed or poured into place with a pneumatic rammer.
- Ramming Refractories: The ramming mixtures are consists of carefully graded particles which are very similar to plastic refractories though are much stiffer mixes. The final product is delivered usually in dry form in which a small amount of water is added just before the application. Other ramming mixes in wet form is also available which can be applied immediately upon opening. A pneumatic rammer is usually employed for the application.

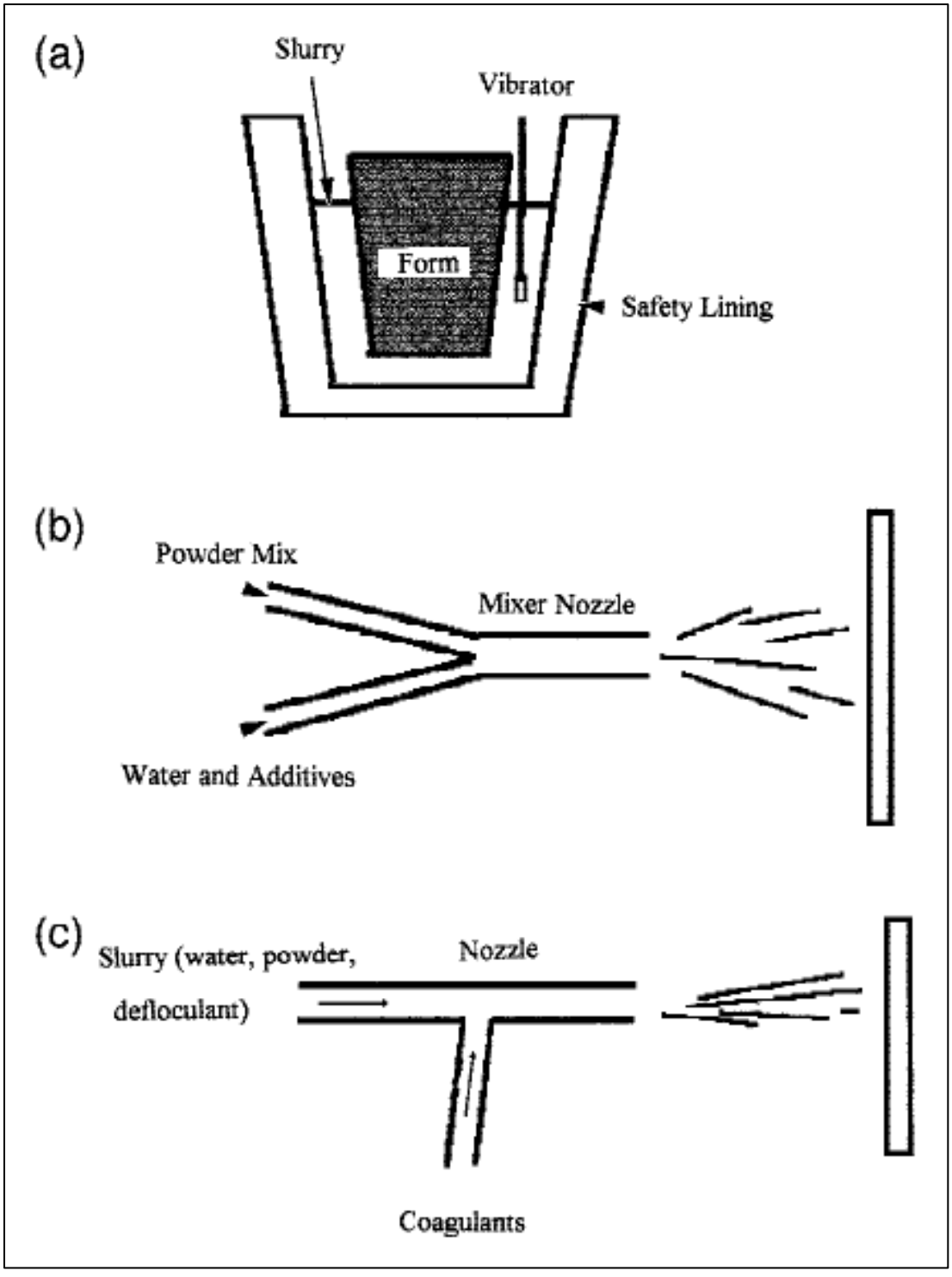

Figure 1.1: Schematic of some monolithic installation procedures: (a) vibration casting, (b) dry gunning and (c) wet gunning (or shotcreting) [1.5]

- Gunning Mixes: These are heat setting granular refractory materials which are sprayed on the application area using a variety of air placement guns and are generally used for patching and maintenance works inside kilns and furnaces.
- Fettling Mixes: These are also consists of granular refractory components, similar to gunning mixes, but they are applied by shoveling.
- Patching Refractories: The patching refractories are similar to plastic refractories but they have very soft plasticity which allows them to be pound into the place.
- Coating Refractories: They are generally used as protection for refractory linings against any chemical attack. They are fairly thin layers, normally used to cover the working surface of a refractory lining
- Refractory Mortars: The constituents are finely grounded refractory materials which form a paste when mixed with water. Normally applied by troweling for laying and bonding shaped refractories.
- Insulating Castables: These are specialized monolithic refractories which are used on the cold face of applications. There are made from lightweight aggregate materials such as vermiculite, perlite, extend-o-spheres, bubble alumina and expanded clay. Their main function is to provide thermal insulation. They are typically of low density and low thermal conductivity. Insulating refractories have an inferior mechanical strength to that of conventional castables.

1.6 Constituents of refractory castables

Among the various unshaped refractories, castables lead in all the areas of research, development, manufacturing and application. The various constituents of refractory castables are refractory aggregates, finer matrix components, binders and admixtures (additives). The different components used vary in proportion in each castable composition to obtain the desired properties essentially required for the intended application. The strength development mainly depends on the interaction between the non-continuous aggregates and the continuous bonding/matrix phase. Thus the type of binder and its properties mainly decide the strength of monolithic refractories. The main purpose of the binder is to bind or hold the various refractory grains and fines together

in the green state. At higher temperature, the binders dehydrate or decompose and strength developed from sintering in the composition. Thus variation in binder affects the bonding character and its mechanism which result in different properties and affect the applications of monolithic refractories [1.13].

Commonly used binder is high alumina cement, wherein presence of CaO affects the hot properties due to the formation of CaO containing low melting phases. Further development was initially guided by reduction of cement content, thereby improving the hot properties and later by cement free compositions. The various cement free compositions contain binders like monoaluminum phosphate, sodium silicate, resins, ρ-alumina, colloidal silica, etc. [1.14-1.18].

The bonding mechanism and kinetics can also be altered by use of additives or fine reactive powders. The right choice of additives also allows moderating the effect of temperature, especially at low temperature [1.19, 1.20]. Table 1.1 shows different additives used castables and their main function. However, before to use them, it is necessary to take into account that they can induce several effects (deflocculation, pH change, kinetic modification, etc.) and thus their effect can be different depending on the bonding system and the presence of other additives or ultrafine particles.

Table 1.1: Description and function of different additives [1.15]

1	Boric acid	Retarder (extends the working time)
2	Lithium carbonate	Setting accelerator
3	Citric acid or citrates	Retarder
4	Phosphate + silica fume	Retarder
5	Sodium carbonate	Flocculating agent
6	Calcium carbonate	Flocculating agent
7	Sodium tripolyphosphate	Retarder
8	Aluminum lactate	Retarder
9	Silicofluoric soda	Retarder
10	Hydrated lime	Flocculating agent
11	Calcium chloride	Flocculating agent
12	Aluminum sulphate	Accelerating agent (free cement)

1.7 Bonding systems in refractory castables

Different types of bond phases are used in refractories to hold the aggregates / grains together and to enable to fabricate large shapes. Accordingly, the refractories are also termed as "chemical bonded", ''carbon bonded,'' ''silicate bonded,'' ''phosphate bonded,'' ''cement bonded,'' etc. Till about 20th century, the common bonding in refractories was the natural silicate/aluminosilicate one, formed due to the vitrification of the reactants in presence of silica, present as a component or impurity. During 20th century, synthetic bonds were started by fine additions of bonding phase or by additions of cementitious and glassy bonding materials. The significant achievement in bond systems in the last century was the development of various bonding materials used in unshaped refractories, especially for the castables that are formed and shaped in-situ.

The bonding agents used in monolithic refractories can be classified according to the bonding methods as hydraulic, chemical, coagulation, etc. Calcium aluminate cement is the most commonly used hydraulic binder. The alumina content of CA Cement ranges from 40 to 80%. The higher the alumina content, the higher the refractoriness achieved. Monocalcium aluminate ($CaO.Al_2O_3$) is the main phase responsible for the specific properties of the cement [1.15, 1.21]. Another hydraulic binder is the rho-alumina, a transitory alumina phase, which can be used without calcia and with a small silica content provides high refractoriness and corrosion resistance. The hydraulic behavior allows it to work like a binder at room temperature through the formation of a gel. Chemical binders like phosphoric acid, phosphates and silicates promote bonding by the formation of new products or by polymerization reaction between the binder and the refractory material (oxide aggregates) or between the binder and the hardener. The coagulation binders include ultrafine oxide particles, colloids like silica sol, alumina sol, etc. Colloidal silica, when mixed with refractory aggregates, gels around the refractory particles on drying and forms a skeleton which holds the particles together at green stage.

1.8 Colloidal binders: silica Sol

Among the available colloidal systems, only silica sol is commercially exploited as a binder for refractory systems. The factor which favors its use as a binder is its high stability, higher solid

content; also the possibility of mullite formation at low temperature in high alumina systems favors its wide application. But the presence of free silica in the system can promote the appearance of a vitreous phase and thus decrease in refractoriness [1.15], especially critical in alkali containing system, restricted its use for high temperature applications.

1.9 New bonding systems

Among the available bonding system for monolithic refractories, each has its own limitations and drawbacks. Conventional castables contain 15%–20% calcium aluminate cement. The presence of the associated CaO in the cement binder is detrimental to the refractory, as it acts as a flux for aluminate–silicate bonds and forms relatively low-melting phases, such as gehlenite (C_2AS) and anorthite (CAS_2) and reduces hot strength [1.5]. LCC and ULCC developed with low CaO content results in an increase of service temperature of the castables. However the system still contains some CaO, thus high temperature structural strength and other high temperature properties are lowered. Cement-free binder like hydratable alumina (rho-alumina) has the problem of explosive spalling during firing due to the formation of very less permeable structure. Chemical binders have the disadvantage of introducing impurities and must be aged before use. It also leads to the release of detrimental gases like SO_2 and P_2O_5 during service condition which corrodes the equipment and also pollutes the environment.

Other colloidal systems, like alumina, mullite or spinel sol, have been also tried in refractory systems. Uses of ultrafine oxide powders as additives, obtained from the sol-gel route, have been reported to improve the refractory properties. But the use of these colloidal systems as a binder for the refractory system has been reported by few only due to various processing difficulties such as lower solid content leading to insignificant binding, poor stability of sol, high water requirement during processing, etc.

1.10 Application areas

The last two decades have seen significant improvements in monolithic refractories, especially in castable refractories in terms of bonding systems, as well as the use of refractory grains and additives. The development of LCC and ULCC has broadened castable refractory uses where

conventional castables were not suitable for the application. The properties of refractory castables vary as per the chemical constitution, and also depend on the PSD employed. Thus, there is flexibility to adjust the properties of castables as per the requirement of the application area by mere changing the chemical composition and PSD. Classified into various categories, their application area is defined by properties based on their chemical constitution. Table 1.2 shows the application areas of various cement bonded castable compositions whereas, in Table 1.3, the application areas where colloidal silica bonded compositions are applied are given. Figure 1.2 shows some of the application areas where castables are used.

Table 1.2: Application areas of cement bonded castables [1.22, 1.23]

Type of cement castable	**Application area**
Conventional cement castables: General purpose dense castables:	Boiler, chimney, foundry ladle, annealing furnace, heat treatment furnaces and various general purpose applications.
Conventional cement castables: High strength dense castables:	Repair/ free board area of steel ladle, ABC/ DSC section of DRI unit, pelletizing furnace, incinerators, skid pipes, soaking pit cover, meal chute/feed pipe/roof of pre-calciner unit of cement rotary kiln, hot metal mixer, aluminum melting furnace.
Low cement castable:	tundish permanent lining, DRI kiln lining, tip casting, inlet cone and burner pipe of cement rotary kiln, cement kiln cooler section, lower side walls of aluminum melting and holding furnace, incinerator lining. cement kiln, DRI kiln, incinerators, tundish, ladle, alumina kiln, lances, rotary kiln nose rings, striker pads, launders, snorkel of RH unit
Low cement Basic castable:	ladle repair and degasser units,
Low cement Self-flow castable:	Precast-prefired shapes as steel ladle seating blocks and housing blocks, EAF delta and launder, RH degasser units.
Low cement High alumina spinel castable:	EAF delta in-situ casting, RH degasser units, EAF launder, steel ladle working lining and impact area, tundish dams and weirs.
Ultra-Low cement Tabular alumina castable:	Critical areas in fertilizer, petroleum refinery, Carbon black industry and FCC units.
Insulation castable:	fired heaters in refineries, ABC of DRI unit, catalytic reformer ring, carbon black industry, duct lining in refineries H_2 furnace back up lining, heaters, stacks, duct in petroleum application, petroleum reformer, DRI kiln heaters

Table 1.3: Application areas of colloidal silica bonded castables [1.24]

Area	**Application**
Coke ovens	Repair materials for roof, sidewalls, and floor, door plugs
Glass tank furnace	Roof and dog house
Blast furnace	Lower and upper stack, BF cast-house trough, iron and slag runners
Foundry	Cupola well, iron well, slag runners, stirrer beams, ladles,
Reheat furnace	Sub-hearth and roof of pusher type, walking beam and rotary hearth furnace
Pre-cast shapes	Turbo-stops, baffles, dams and weirs, electric furnace deltas, steel ladle covers, BF trough skimmers.
Rotary and shaft kiln	Lining of shaft kilns,
Aluminum furnaces	Lining metal contact areas, belly band and upper side walls for aluminum melting, holding and casting furnaces

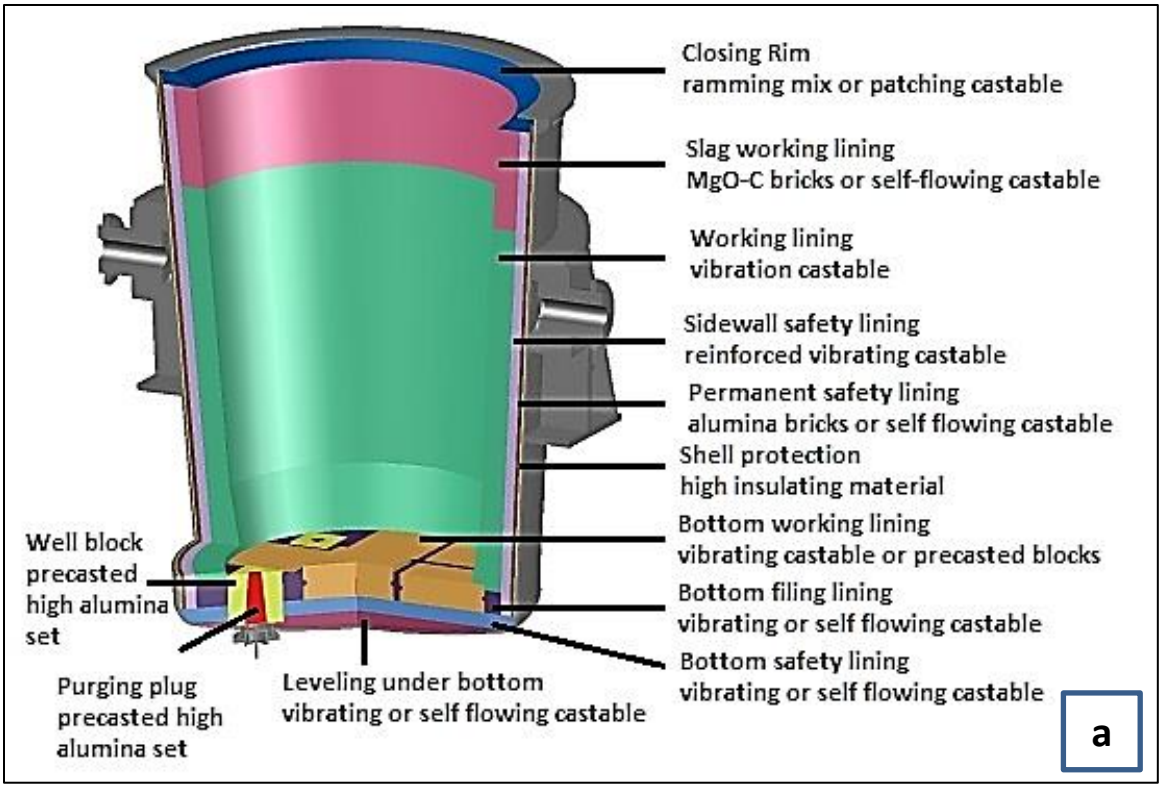
Closing Rim
ramming mix or patching castable
Slag working lining
MgO-C bricks or self-flowing castable
Working lining
vibration castable
Sidewall safety lining
reinforced vibrating castable
Permanent safety lining
alumina bricks or self flowing castable
Shell protection
high insulating material
Bottom working lining
vibrating castable or precasted blocks
Bottom filing lining
vibrating or self flowing castable
Bottom safety lining
vibrating or self flowing castable
Well block
precasted
high alumina
set
Purging plug
precasted high
alumina set
Leveling under bottom
vibrating or self flowing castable
a

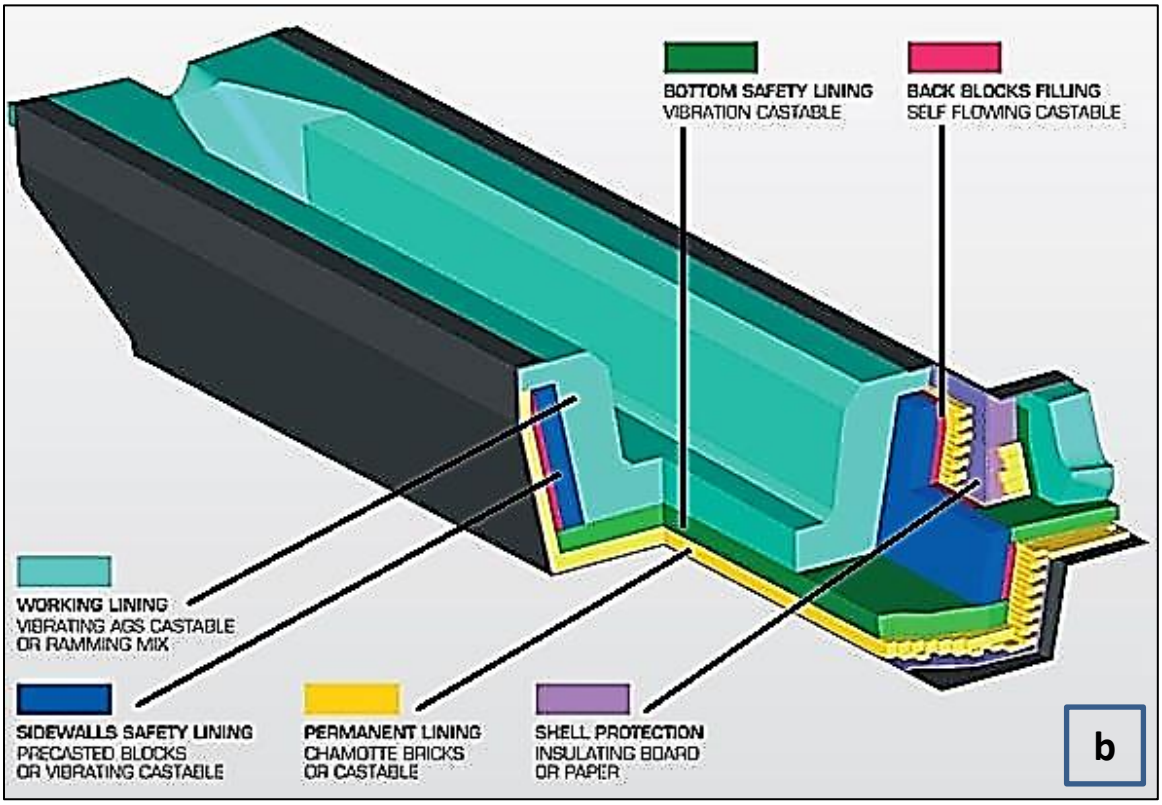
BOTTOM SAFETY LINING
VIBRATION CASTABLE
BACK BLOCKS FILLING
SELF FLOWING CASTABLE
WORKING LINING
VIBRATING AGS CASTABLE
OR RAMMING MIX
SIDEWALLS SAFETY LINING
PRECASTED BLOCKS
OR VIBRATING CASTABLE
PERMANENT LINING
CHAMOTTE BRICKS
OR CASTABLE
SHELL PROTECTION
INSULATING BOARD
OR PAPER
b

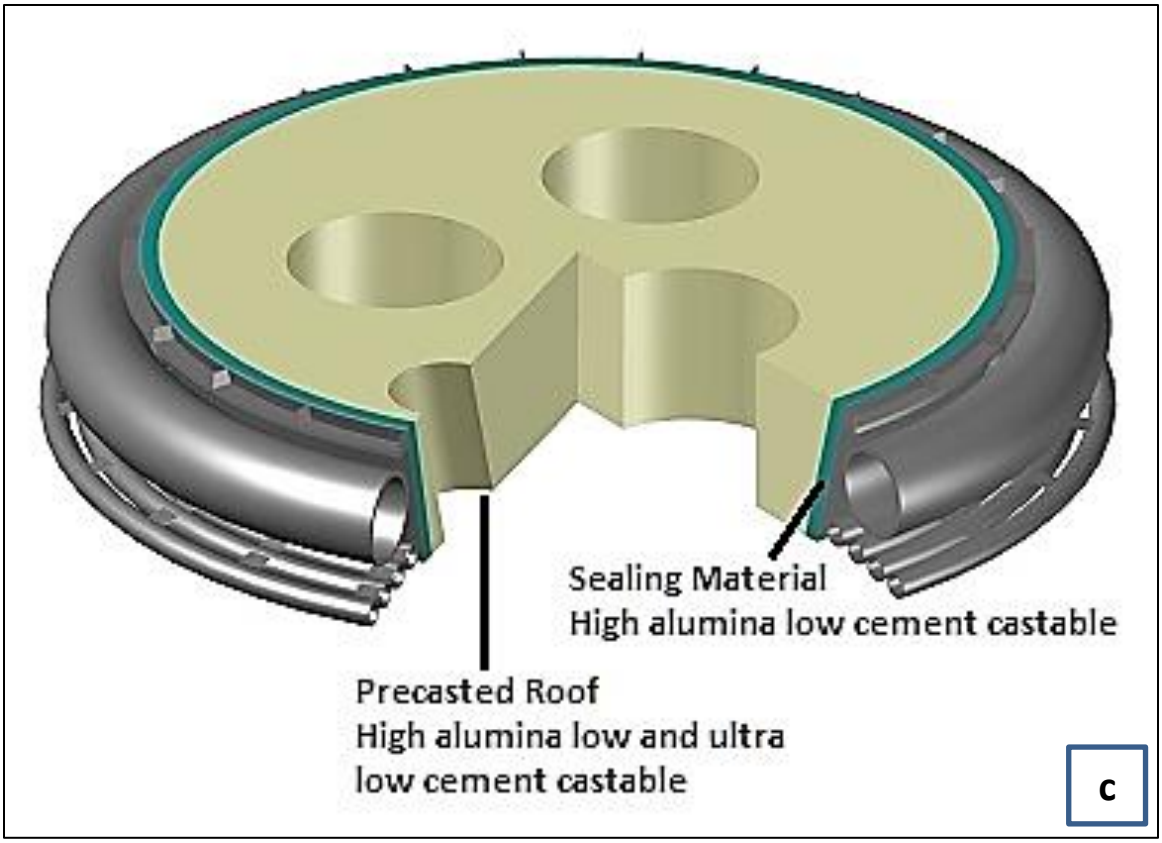

Figure 1.2: Some application areas (a) ladle, (b) cast house, and (c) roof of EAF [1.25-1.27]

Chapter 2

Literature review

The present chapter is a literature review of the refractory castables beginning with a brief introduction about the refractory materials and various properties associated with them. This is followed by the type of refractories based on different classifications. A brief description of different types of unshaped refractories is given next. The history and present perspective of various bonding systems of castables are discussed next based on the available literature. Then comes the various sol-gel based (coagulation bonding) systems; among them, silica sol is prominent and widely studied. Based on available literature, the advantages and drawbacks of silica sol are also discussed. Different processes, as per available literature, for making sols of alumina, mullite and spinel systems are described next. Also the studies on the use of these different sols in castable systems mentioned. Finally, the importance of particle size distribution and various types of distribution studied for castable systems are described.

2.1 Refractory materials:

Refractories are materials with the ability to withstand high temperature without undergoing any physical and chemical change. ASTM C71 defines refractories as - non-metallic materials having those chemical and physical properties that make them applicable for structures or as components of systems that are exposed to environments above 538^0C (1000°F) [2.1]. The sustainability of refractory materials at high temperature makes them suitable to act as heat-resisting barriers between high and low temperature zones. They are mainly used in the construction of application-specific high temperature areas/surfaces, particularly in furnaces or boilers, as they reduce the loss of heat through the structure. They are mostly used in iron and steel industries along with cement, glass, copper, aluminium and petrochemical industries and play a very crucial role in cost and quality of the products.

The operating conditions where refractories are used vary considerably, and hence a range of refractory materials with different properties are required to meet the challenge. Depending on their application, refractory materials are developed in various combinations and shapes. The physical, chemical and mineralogical characteristics of a refractory material decide the quality and its suitability for a particular application. The properties that are taken into consideration while selecting an optimum refractory lining configuration are bulk density, apparent porosity,

cold crushing strength, hot modulus of rupture, refractoriness under load, creep, thermal conductivity, thermal shock resistance, etc. [2.2-2.4].

2.2 Types of refractories

Refractories are classified on various bases like chemical composition, chemical nature or behavior, end use of refractory, methods of manufacture or in terms of physical shape. In terms of composition, they can be classified on the basis of major chemical constituent like Silica refractory, Fireclay refractories, High alumina refractories, Mullite refractories, Corundum refractories, Magnesite refractories, Dolomite refractories, Chromite refractories, Zirconia refractories, etc. [2.2-2.6].

On the basis of Chemical nature or behavior, i.e. their reaction to the type of slags, are classified as Acidic refractories e.g. Silica, Semi-silica, Aluminosilicate; Basic refractories e.g. Magnesite, Chrome-Magnesite, Magnesite-chromite, Dolomite; Neutral refractories e.g. Fireclay bricks, Chrome, Pure Alumina; and Special refractories e.g. Carbon, Silicon Carbide, Zirconia. On the basis of end use, they may be classified as Blast furnace, casting pit, etc. On basis of manufacturing method, the classification are Dry press process, fused cast, hand molded, formed (normal, fired or chemically bonded) and unformed (monolithics, plastics, ramming mass, gunning castable, and spraying, etc.)

Classification Based on physical form in which they are used is more common and are classified as shaped refractories commonly known as bricks and unshaped or monolithic refractories which are loose powdered material without any definite shape and only given shape during application. They can further be classified on the basis of application as castables, refractory mortars, ramming mass, gunning mass, plastic mass, shotcrete, etc. [2.7, 2.8].

2.3 Refractory castables

Among monolithic refractories, castables are the most important from application and market share point of view and alone have more than 40% market share [2.9]. Castables generally consist of refractory aggregates (for strength and hot properties) with varying sizes which are hold together by inorganic or organic binders.

Also known as refractory concrete, the history can be traced back to 1856 when a refractory crucible was prepared by Deville using alumina aggregate and alumina cement [2.10]. But their production was possible only after 1913 when the first industrial production of calcium aluminate (CA) cement took place. First references for a commercial refractory concrete reported being consists of bauxite and cement fondu based compositions around 1922 [2.11, 2.12]. During the 1930s, the use of refractory and insulating concretes were expanded everywhere. But the major development took place only after the Second World War. By the 1960s castables based on high purity calcium aluminate (CA) cement and high purity aggregates were common [2.13]. These were relatively simple compositions and comprising of refractory aggregates and cement with cement contents typically greater than 15%.

The presence of high CaO causes the formation of low melting phases like $CaO.Al_2O_3.2SiO_2$ (CAS_2) and $2CaO.Al_2O_3.SiO_2$ (C_2AS), on reaction with silica and alumina present in the matrix. Thus these castables have remarkably low refractoriness and other high temperature properties. From the late 1970s, the manufacturers started developing castables with lower cement content to reduce the amount of CaO [2.14, 2.15]. The aim was to develop castables with better hot properties and corrosion resistance. Reducing the cement content also helps in decreasing the water demand which favors low porosity after drying, resulting in better mechanical properties of the castables. The trend is now on development of low cement (1.0<CaO<2.5%), ultra-low cement (0.2<CaO<1.0%) and even cement free castables (bonding agents other than cement such as chemical, sol-gel, etc.). This development has greatly improved the hot properties and performance of refractory castables [2.16-2.19].

2.4 Bonding mechanism in castables

Shaped refractories like conventional bricks are machined pressed, wherein, the compaction at high pressure imparts the initial green strength to the bricks. In contrast unshaped refractories, like castables, are loose mixture composed of refractory aggregates of varying sizes and are given shape only during application by bonding together by a continuous bonding phase. The degree of interaction between the two determines the strength and other castable properties. Thus the type of binder and its properties are an important factor in deciding the strength of refractory castables. A slight variation in the properties of binder affects the bonding character and the

bonding mechanism which result in different properties and affects the applications of castable refractories. The main purpose of the binder is to bind or hold the materials together in the green state. At higher temperature, the binders then either dehydrate or decompose and finally sinter leaving behind only the refractory material. The bonding agents can be broadly classified under three different bonding mechanisms, as hydraulic, chemical, and coagulation bonding [2.9, 2.18].

2.4.1 Hydraulic bonding: This group of binders includes calcium aluminate (CA) cement, hydratable alumina (HA) and silicate cement. Hydraulic bonding occurs when the binder reacts with water at room temperature leading to hydrate formation which is responsible for the strength development at green stage. All the hydraulic binders take some time to finish the hydraulic reactions and therefore, must be allowed some time for setting and hardening.

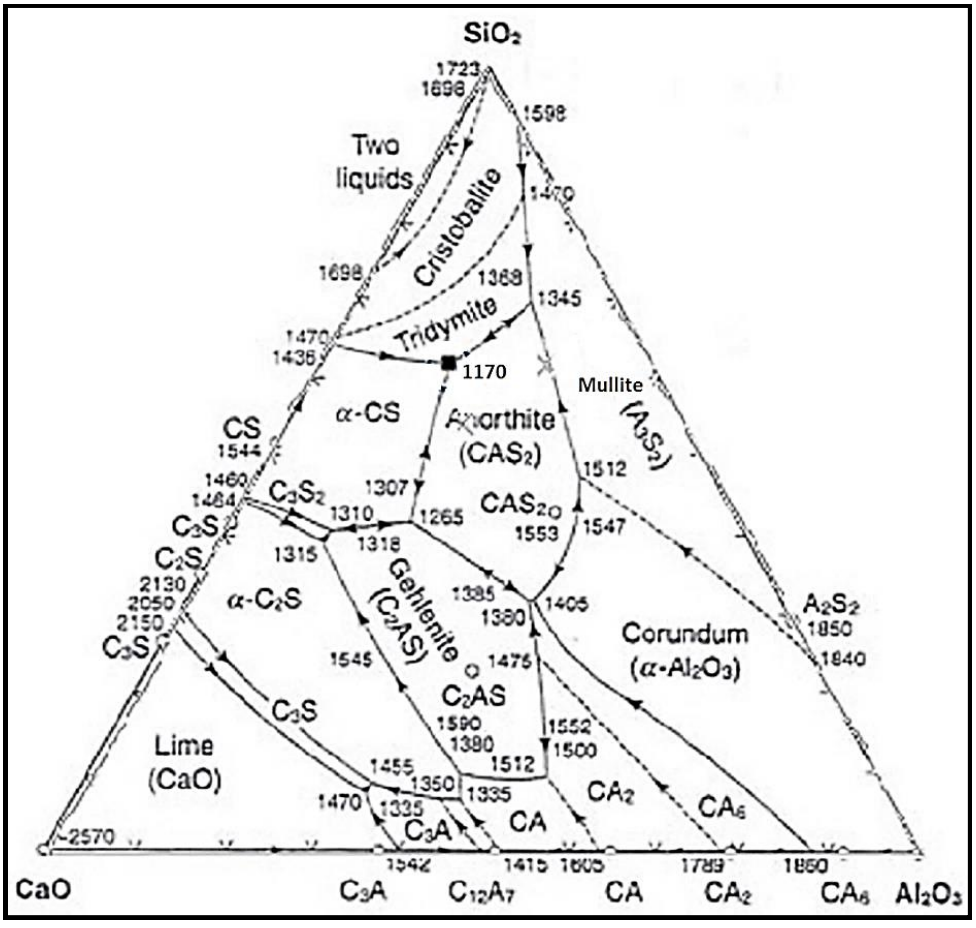

Figure 2.1: Ternary phase diagram of calcia, alumina, and silica system [2.22].

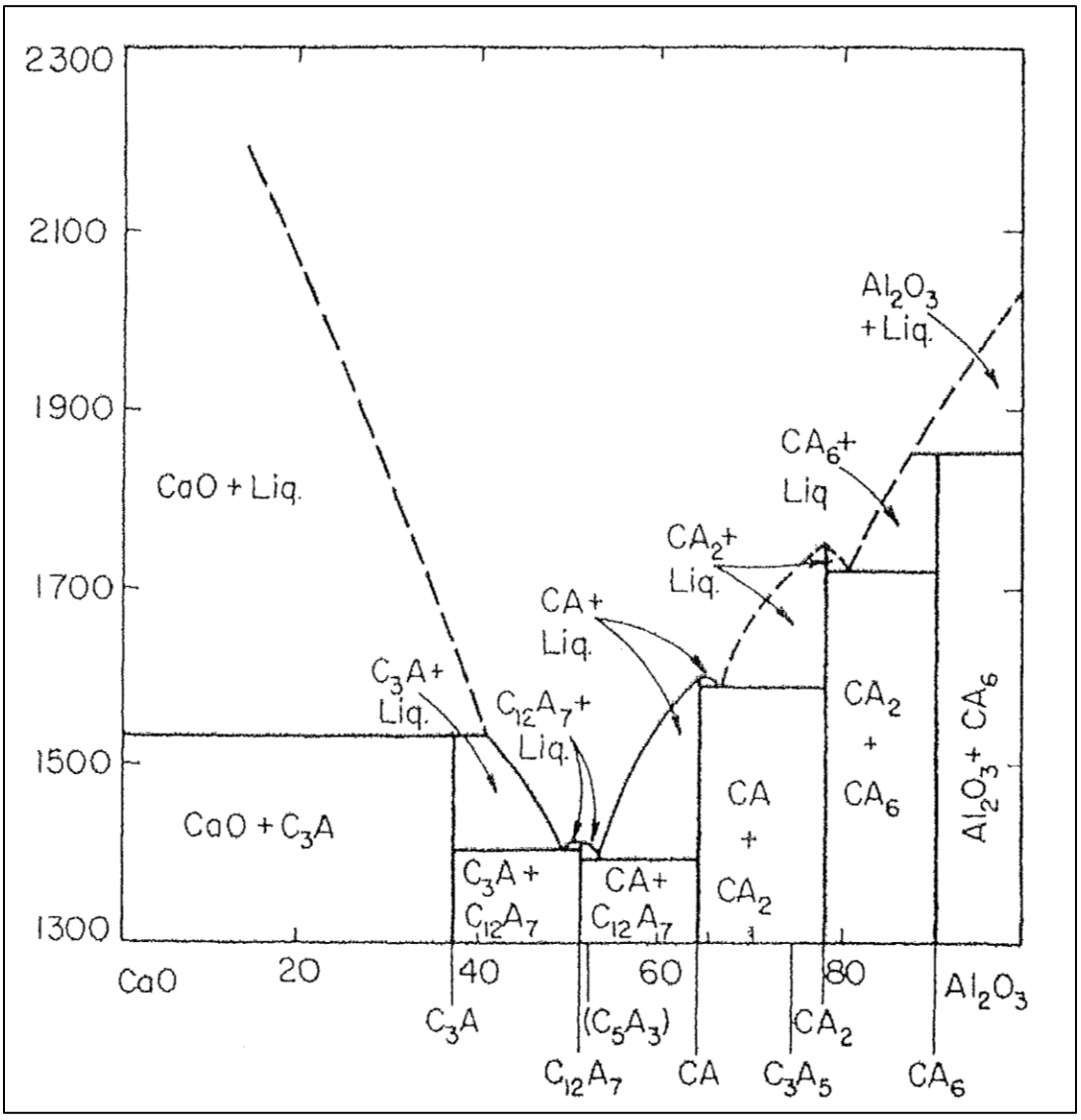

Figure 2.2: Binary phase diagram of calcia and alumina system [2.23]. (C=CaO; A= Al_2O_3)

2.4.1.1 Calcium aluminate (CA) cement: Commonly used binder for castables is CA cement which is a hydraulic binder. The initial green strength is provided by coagulation- a crystallization network results from the formation of $CaO.Al_2O_3.10H_2O$ (CAH_{10}), $2CaO.Al_2O_3.8H_2O$ (C_2AH_8), $3CaO.Al_2O_3.6H_2O$ (C_3AH_6) crystals and alumina gel $Al_2O_3.3H_2O$ (AH_3) by means of hydraulic reactions. The following reaction takes place [2.19, 2.20].

$CA + 10H \rightarrow CAH_{10}$ (<20°C)

$2CA + 11H \rightarrow C_2AH_8 + AH_3$ (20-35°C)

$3CA + 12H \rightarrow C_3AH_6 + 2AH_3$ (>35°C)

(where, C=CaO; A= Al_2O_3 and H=H_2O)

These hydrates upon heating lose water of hydration which results in spalling of the castables leading to falling in strength upto 800-900^{0}C. On further heating, recrystallization produces a frame-work of sintered material at a temperature much lower than that which would have been required to sinter the anhydrous calcium aluminate powder, increasing strength at high temperature.

But the presence of CaO in cement affects the hot properties, due to the formation of liquid phases around 1600^{0}C such as binary phases like $12CaO.7Al_2O_3$ ($C_{12}A_7$), $3CaO.Al_2O_3$ (C_3A), $CaO.SiO_2$ (CS) and $2CaO.SiO_2$ (C_2S) and ternary phases like $2CaO.Al_2O_3.SiO_2$ (C_2AS), $CaO.Al_2O_3.2SiO_2$ (CAS_2), $CaO.Al_2O_3.SiO_2$ (CAS) and $3CaO.Al_2O_3.3SiO_2$ (C_3AS_3), thus limiting its use in high temperature applications [2.20, 2.21]. The phase diagrams of $CaO-Al_2O_3-SiO_2$ [2.22] and $CaO-Al_2O_3$ [2.23] systems are shown in figure 2.1 and 2.2 respectively.

2.4.1.2 Hydratable alumina (HA): It is a transition alumina, also known as ρ-Al_2O_3, having specific crystallinity containing over 90% alumina with a LoI of 6-9% and low sodium levels. It forms $Al_2O_3.3H_2O$ (AH_3) and $Al_2O_3.H_2O$ (AH) gel in combination with water as per reaction below which upon heating dehydrate and eventually form ceramic bonds [2.17, 2.24, 2.25].

ρ-$Al_2O_3 + 3\ H_2O \rightarrow Al_2O_3.3H_2O$ (high temperature curing) [2.9]

ρ-$Al_2O_3 + 1..2\ H_2O \rightarrow Al_2O_3.(1..2)H_2O$ (room temperature curing) [2.9]

Lower porosities are achieved in the samples as a consequence of ultrafine pore structure resulted from hydratable alumina. The HA bonded products thus have improved corrosion resistance to liquids and gases. The compact and close bonded matrix without any low melting phase formation at higher temperatures leads to increase in hot strength, volume stability, higher thermal conductivities and densities with limited cracking. Hydratable alumina in combination with silica fume promotes the formation of mullite, a highly refractory material which provides improved hot strengths and excellent thermal shock resistance [2.26]. Like all bonding systems, Hydratable Alumina also has their own advantages and drawbacks. Curing for HA bonded

samples must be done above 18^0C for better strength development [2.27]. It has also been found that adding a minute amount of CA cement is advantageous in controlling the cold set [2.28, 2.29].

Similar to other systems, there are specific tradeoffs here too. The advantages with respect to a cement free system when HAs are used as bonding agents are mitigated by the tendency of explosive spalling during drying. In silica fume containing system, the permeability values obtained are very low and thus attention is required during the firing schedule as typical dry out schedule for cement is not suitable [2.30-2.32].

Comparing to cement bonded system, HAs require longer mixing time and requirement for water is also high due to the high specific surface area of the binder [2.33, 2.34]. Thus they have limited application to areas where the cement removal could be beneficial and where drying out can be controlled tightly, like in precast [2.35].

2.4.2 Chemical bonding: Bonding which is based on some chemical reactions; generally occurring at ambient conditions or little high temperatures, involving the constituents phases of the refractory are termed as chemical bonding. The binders of this group include phosphoric acid or phosphates (monoaluminum phosphate, alkali or alkaline phosphates), sodium or potassium silicates, etc. The bond is formed by new products formation or by polymerization of binder and refractory aggregates (oxide aggregates) or between the binder and a hardener.

2.4.2.1 Phosphate binders: Refractory compositions with phosphate binders are well known for their excellent resistance to most molten metals and slags, and compositions are available in various grades which are generally installed by casting, ramming or gunning. The first significant review on phosphate bonded refractory compositions can be dated back to 1950 [2.36]. These refractory compositions are generally mixtures comprising of refractory aggregates and some phosphate binder which have the ability to harden at low temperatures. The phosphate binder systems are developed mainly in two ways: by a reaction between an active component of the refractory body and orthophosphoric acid or by direct addition of a binder prepared previously, like, monoaluminum phosphate [2.37].

According to Lyons at al [2.38], the bonding action of the phosphoric acid in alumina based refractory compositions is due to the formation of Al $(H_2PO_4)_3$. With time and increase in temperature, Al $(H_2PO_4)_3$ undergoes several transformations producing $Al(PO_3)_3$ at 400-500^oC, $AlPO_4$ at 1300-1500^oC and finally alumina and releasing P_2O_5 above 1700^oC [2.39].

Mono-aluminum-phosphate is the most often applied phosphate binder in the refractory industry used either in liquid or spray-dried form. Sometimes an additional setting agent is needed to have desired setting properties at ambient temperature. An alkali- or alkali earth metal oxide component (M_xO) like MgO are mostly used as setting agents. The dehydro-polymerization reaction given below between aluminum phosphate and magnesium oxide brings the green strength at room temperature [2.9].

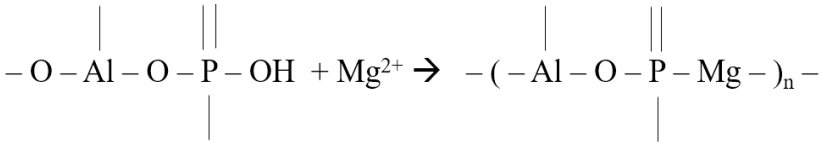

The strong hygroscopic nature of spray dried mono-aluminum phosphate results in poor shelf life when used as an additive in a single component material system. Other dry mono-phosphate binders like mono-magnesium phosphate are non-hygroscopic in nature, but due to non-solubility in water, the strength obtained is often low at the higher water additions during vibration casting.

2.4.2.2 Silicate binders: silicates are mostly used as a binder in air setting mortars and provide excellent workability and strength. Both wet and dry types of mortars are available. Sodium silicate is used as a binder in the formation of certain air setting plastics [2.40, 2.41].

The alkali metal silicates are generally used as refractory binders in combination with several other additives such as strengthening agents, components to provide hydration resistance, and plasticizers. Boric acid or B_2O_3-producing compounds such as $Na_2B_4O_7$ (sodium borate) and other similar inorganic salts are commonly used with alkali silicate bonding agents. Na_2SiF_6 (sodium fluorosilicate) in combination with water glass is used frequently in castable refractory compositions [2.42].

The setting mechanism of silicate binders is a gelification process in acidic condition. In natural condition, acid is provided by dissolution of carbon dioxide from the air. Some compounds such as sodium fluoride, aluminum polyphosphate, calcium silicate, etc. are known to act as setting agents [2.43]. For e.g. Sodium silicate ($Na_2O.nSiO_2.aq$) in presence of setting accelerator like sodium fluorosilicate (Na_2SiF_6), results in bond formation as per the reactions below.

$2(Na_2O.nSiO_2.aq) + Na_2SiF_6 \rightarrow (2n+1)\ SiO_2.aq + mH2O + 6NaF$ [2.9] or,

$2Na_2SiO_3 + Na_2SiF_6 + 6H_2O \rightarrow 6NaF + 3Si(OH)_4$ [2.44]

The resulting aqueous sol ($SiO_2.nH_2O$ or $Si(OH)_4$) produces a strong bond by forming a network structure of siloxane (-Si-O-Si-) after dehydration. However, it is found that the sodium silicate bond reacts rapidly with molten aluminum, resulting in deep joint penetration [2.41].

2.4.3 Coagulation bonding: The binders which work by coagulation binding are fine clay powder, ultrafine oxide powder, silica sol, alumina sol, etc. The close contact of fine particles in a colloidal suspension by means of Van der Waal's forces results in coagulation of the particles. The addition of a coagulator increases the coagulation activity.

According to DLVO theory, when the colloidal particles approach each other due to the attractive Van der Wall's forces, a repulsive force comes into action due to the overlap of electrostatic double layers present on each particle. The particles can coagulate, only if the repulsive force resulting from the overlap of double layers is reduced. This is generally done by addition of electrolytes (contra ions) to the colloidal solution, which enters the dispersion layer of the electrostatic double layers, making it thinner due to electric neutralization, thus reducing the repulsive forces. When the dispersion layer is compressed due to electric neutralization, it overlaps the dense layer making the potential zero. At zero potential, also known as the iso-electric point, the colloidal particles coagulate rapidly [2.9]. The coagulation binders are mainly used in refractory castables, but also in ramming materials and refractory coatings. The development of refractory castables has been summarized in Table 2.1 with their year of development,

Table 2.1: Development of refractory castables [2.45]

Bonding mechanism	1920s	1930-40s	1950s	1960s	1970s	1980s	1990s	2000s	2010s
Hydraulic bonding	Traditional cement bonded castables [high SiO_2,high $CaO + H_2O$]								
				Pure CA cement castables [high $CA + H_2O$]					
						High purity cement castables [Low $CA + H_2O$] rho-Alumina bonded castables [ρ-Al_2O_3 + uf powders + H_2O]			
Chemical bonding			Water glass bonded castables [$Na_2O.nSiO_2$+ Na_2SiF_6] Phosphate bonded castables [H_3PO_4 or $Al(H_2PO_4)_3$ + MgO or CA]						
				Sulphate, chloride bonded castables [$Al_2(SO_4)_3$ + CA, $MgCl_2$ or $MgSO_4$]					
				Polyphosphate bonded castables [$Na_5P_3O_{10}$ or $(NaPO_3)_6$ + MgO, CaO or CA]					
						Resin bonded castables [Phenolic resin, etc.] Vinyl polymers, pitch, dextrin.			
Hydraulic and coagulation bonding					Low cement castables [CA +clay or uf SiO_2 +H_2O]				
Coagulation bonding					Clay bonded castables [Ca- or Na-clay + CA + deflocculants]				
						Ultra-low cement castables [ultra-fine powders + CA] Cement free castables [ultra-fine powders + electrolyte] Sol gel bonded castables [silica sol + electrolyte]			

The advancements in nanotechnology in last two decades could also benefit the refractory industry if explored properly [2.46-2.48]. Literature shows that utilization of nano powders and colloidal suspensions in refractory castables has increased in recent years, mainly to improve the bonding and densification in castables at lower sintering temperatures [2.49-2.53]. But the agglomeration of nano powder particles (due to its high reactivity owing to a high surface area) results in poor dispersion in the matrix and thus possesses a challenge to use these as additives [2.53, 2.54]. Only if the agglomeration problem is kept under control, use of nano particle addition could improve the castable properties. Another limitation which hinders the use of nano powders as additives is the availability and the cost of available nano powder products. Nano particles containing colloidal suspensions (colloidal binders) are better alternative and are preferred [2.53].

Every bonding system has its own advantages and drawbacks and is used according to the requirements. As already mentioned, cement castables have the problem of low melting phase formation due to the presence of CaO. Also, the water requirement is high which leads to porosity and ultimately poor strength of the castables. High porosity also decreases the corrosion resistance of the castables. Likewise in chemical bonding, the decomposition and release of detrimental gases like P_2O_5 and SO_2 from the binders during service condition corrode the equipment and instrumentation and also pollutes the environment. Most of these chemical binders, when used, must be aged, so are not convenient for application. Also, the introduction of impurities such as Na_2O and K_2O from silicate binders lowers the hot properties of the refractory castables. In contrast, the binders used in coagulation binding may be the ultrafine powders or colloids with a composition similar to that of castables. Thus the advantage is high refractoriness and an increase in high temperature structural strength as there is a complete absence of low melting phases. Additionally, water requirement is also low, which decreases porosity in castables and increases corrosion resistance against high temperature melts [2.9, 2.45, 2.49].

2.5 Sol-Gel bonding in castables - Colloidal binders

A colloid or sol is a stable dispersion of particles in water wherein particles are small enough for gravity to make them settle. Particle size typically ranges from 1 to 1000 nanometers [2.55]. The name sol-gel derives from the fact that micro particles or molecules in a solution (sols)

agglomerate which under controlled conditions eventually link together to form a coherent network (gel) [2.56].

Initially, this technique was used for producing ceramic powders which provide better homogeneity in ceramic products at a relatively low temperature in comparison to solid state synthesis. But soon it was employed in refractory castables as a bonding system. The sol-gel technique involves the formation of a 3-dimensional polymeric network (gel) of colloidal particles that surrounds the refractory aggregates giving strength at the green stage on drying. At later stage of subsequent heating to high temperature, the gel bonding is subsequently replaced by ceramic bonding through sintering providing much greater strength than what at the green stage [2.57, 2.58]. The various advantages associated with sol-gel bonded castables are less mixing time, cohesive and self-flowing nature, easier installation as no vibration works, shorter drying time and reduced drying effects due to less moisture content, better corrosion resistance (absence of CaO), better oxidation resistance, better refractoriness, longer lining life and larger self-life as no hydratable phase is present [2.16].

Colloidal (sol-gel) binders, similar to any other bonding system, have their own advantages and drawbacks. Unlike CA cement or hydratable alumina, where consolidation mechanism resulted in hydrated phase generation, the bonding action of colloidal binders is based on gelation (coagulation) of the colloidal particles, which leads to a high permeable and porous structure. Technically this can be advantageous as the composition can be safely and quickly dried; reducing the risk of explosive spalling and thus the overall processing time is reduced [2.49].

Another advantage of colloidal binders, compared to CA cement based castables, is their volumetric stability at high temperature. At high temperatures, above 1100^0C, CA cement reacts with fine alumina in the matrix and produces CA_2 and CA_6 phases, which results in a theoretical volumetric change of +13.6 and +3.01%., respectively [2.59]. This volumetric expansion at high temperature needs to be addressed carefully in order to avoid any crack formation in the material system. In contrast, colloidal binders have higher volumetric stability after firing. Though colloidal silica in alumina system results in mullite formation which shows a similar expansion behavior [2.60], the particles nano dimension balances the overall expansion of the material

system [2.54]. Furthermore, the higher specific surface area of the nano binders improves the castables sinterability.

2.6 Silica sol: The only commercially used colloidal binder

Although various colloidal systems are available but the one which is widely and commercially exploited is silica sol. Silica sols are stable water-based colloidal suspensions, containing nanometric spherical amorphous silica particles up to 50 wt%, with the balance being water, thus, water is indirectly added to the system when silica sols are used as the binder. Silica sols are anionic which are generally stabilized by sodium or ammonium to a pH of 9-11 [2.35].

The factor which favors its wide application is the possibility of mullite formation at low temperature when used in high alumina systems. The other factors are its higher stability and its high solid content But the fact that free silica can still be present in the final product and can thus affect the hot properties of the castables has restricted/limited, its use in various high temperature applications mainly above 1600^0C [2.45, 2.50, 2.61-2.63]. Figure 2.3 shows the phase diagram in the Al_2O_3-SiO2 system, showing the liquid phase formation above 1595^{o}C in the system.

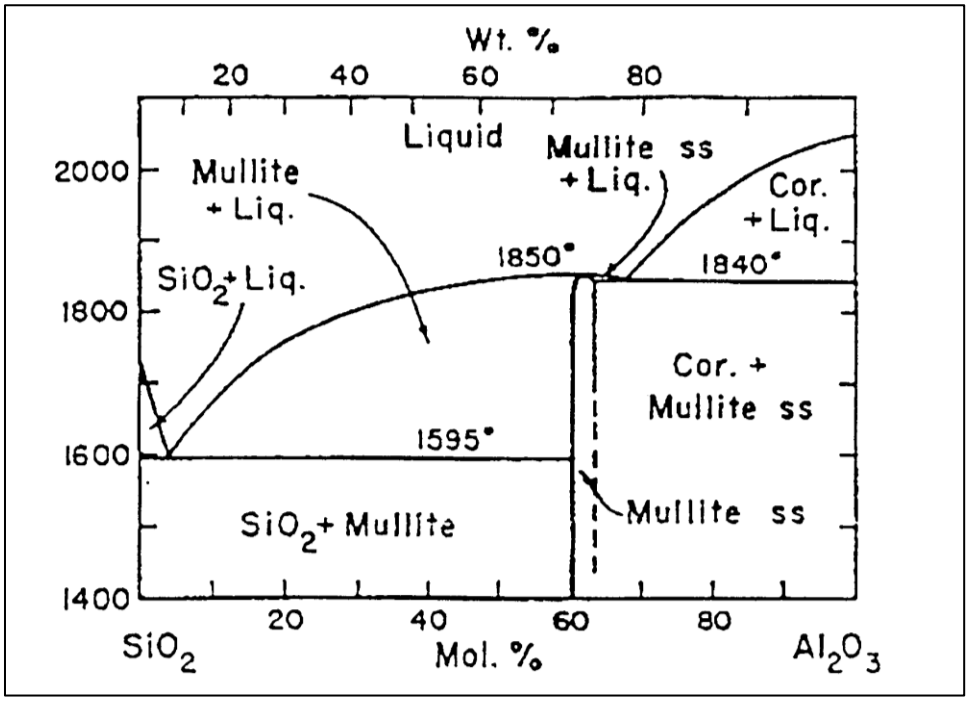

Figure 2.3: Binary phase diagram of alumina and silica system [2.64]

The mechanism of bonding of silica sol is gelation of colloidal particles. In combination with other solid particles, the colloidal silica particles linked together in branched chains, forming a 3-dimensional skeleton in which the solid particles are entrapped. Gelation can be induced by removal of water (drying) during which hydroxyl groups (Si-OH) present on the silica particle surface generate siloxane bonds (Si-O-Si) resulting in a three-dimensional network via the expulsion of water Gelation can also be brought by pH variation, or by addition of some suitable gelling agents (salt, oxide or organic solvent) [2.65]. The addition of CaO or MgO can also induce a cold setting mechanism via destabilization of the sol. For example MgO addition results in $Mg(OH)_2$ formation through the removal of hydrogen from hydroxyl (SiOH) groups which promote siloxane (Si-O-Si) formation [2.66].

The use of colloidal silica as a bonding system means that the final product is always going to have some amount of free silica which makes them acidic in nature and thus, their application is restricted in basic environments such as in numerous steel plant applications, where silica presence is not desirable [2.50]. This could be advantageous for some other applications, most probably in the area of acid resistant refractories [2.35]. But in certain applications, the presence of silica, even in compound form, is undesirable, like a very basic environment. So silica sol bonded castables are not advantageous in such applications.

The drawback of silica sol led researchers to focus their attention on other sol systems likes alumina, spinel, mullite, etc. which have high temperature sustainability. These sols can result in a very high pure castable system, nullify any chance of liquid phase formation and result in excellent strength and corrosion resistance at high temperatures. Literature study shows that not much work has been done on other sol systems by using them as a binder for refractory castables [2.45]. The reason behind this is that other sol systems have many processing difficulties such as low solid content, high water requirement during processing, low flowability, and workability.

2.7 Alumina sol

Alumina is one of the most chemically stable oxides, also known for its excellent strength, hardness, and spalling resistance. It shows high resistance for oxidizing and reducing atmosphere and is extensively used in many heat processing industries. The melting point of alumina is about

2050°C which is much greater than that of silica (m.p. 1730°C). Also, the bulk density, strength, and other refractory/physical properties are quite superior to that of silica. Thus alumina is one of the best alternatives of silica to be used as a refractory material. Though there are various synthesis methods reported for alumina synthesis, sol–gel method is one of the most promising and is widely investigated processing route because it produces solid particles with high purity and high specific surface area [2.67].

2.7.1 Alumina sol making:

There are two technical routes generally used to synthesize alumina sols. One is the polymerization process and the other is the peptization process. The polymerization process involves the hydrolysis and polycondensation reaction of precursor molecules (alkoxide precursors) in an organic solvent medium in the presence of very little water. In the peptization process, precursor molecules are allowed to undergo sufficient hydrolysis in the water medium, and then the formed hydroxide precipitates are peptized into colloidal particles [2.68]. The various sol making processes, mentioned in literature, based on use of organic (alkoxides) and inorganic (salts) precursors are as follows:

2.7.1.1. Alumina sol from alkoxide precursors:

The two most used alkoxides found in the literature are aluminum sec-butoxide, $Al(OC_4H_9)_3$ (ASB) and aluminum isopropoxide, $Al(OC_3H_7)_3$ (AIP). Dong Jin Suh et al. [1997] reported a sol-gel process to produce high surface area alumina aerogels using ASB as the precursor for alumina sol preparation [2.69]. K. R. Han, et al. [2000] reported a method to prepare almost-spherical sub-micrometer sized a-alumina via surface modification of g-alumina with an alumina sol prepared via the hydrolysis of ASB with formic acid [2.70]. Jing Chengbin, et al. [2006] reported an alumina sol using ASB and water with ethyl acetoacetate (EAcAc) as the stabilizing agent. EAcAc reacted with the hydroxyl (Al-OH) groups present on the surface of the Al_2O_3 particle and not directly with the precursor molecules. A surface modification layer formed around the colloidal particles sufficiently capped the surface hydroxyl (Al-OH) groups of the Al_2O_3 particle and the growth of the colloidal particles was effectively prevented [2.68].

Nursel Dilsiz, et al. [2002] reported a sol-gel process for producing low density alumina microspheres by using aluminum alkoxides and aluminum monohydrate (boehmite) as two different alumina precursors. Hydrolysis of aluminum alkoxides produces aluminum monohydrate which is peptized at 80 C by adding HNO_3 to get a stable sol. Similarly, boehmite sol from aluminum monohydrate was prepared by dispersing the powder in distilled water followed by HNO_3 (70 %) addition under stirring to get the stable sol [2.71]. S. Zhang, et al. [2003] studied the water wettability and oxidation resistance of graphite using the sol-gel coating of alumina sol prepared from hydration of AIP [2.72]. J. Chandradass, et al. [2006] reported alumina fibres prepared by sol-gel process. The alumina sol was prepared by mixing AIP in distilled water and refluxed in the presence of acid catalyst [2.73]. Suat Yilmaz, et al. [2008] obtained boehmite sol by hydrolyzing and peptizing the alkoxide AIP with 10 % dilute HCl and used it for coating of graphite flakes to improve its oxidation resistance [2.74]. Fatemeh Mirjalili, et al. [2011] reported a sol-gel synthesis of nano alpha alumina particles using AIP and aluminum nitrate nonahydrate (ANN) as raw materials and investigated the effect of stirring time on the synthesis [2.75].

2.7.1.2. Alumina sol using inorganic precursors:

The two most used inorganics precursors found in literature are nitrate and chloride salts of aluminum: aluminum nitrate nonahydrate, $Al(NO_3)_3.9H_2O$ (ANN) and aluminum chloride hexahydrate, $AlCl_3.6H_2O$ (ACH**)**: Toshio Maki et al. [1988] reported a sol-gel method for synthesis of alumina fibers using ACH as the alumina source and observed that the shape of particles are related to the rheological property and fiber drawing behavior of the sols [2.76]. R. Venkatesh, et al. [1999] reported the fabrication of high alumina fibre mats directly during synthesis from alumina sol prepared by minor modification of the well-known oxychloride route using ACH, aluminium metal powder, and colloidal silica sol as the starting materials [2.77]. M. Chatterjee, et al. [2002] reported a polycrystalline, high-alumina fibre mats for application as high-temperature thermal insulation materials, fabricated in situ by a single-step sol-gel spinning technique using ACH, aluminum metal powder and a colloidal silica sol as the starting materials [2.78]. A. Sedaghat, et al. [2006] reported a method for preparation of alumina mat using the sol-gel centrifugal spinning route with ACH, aluminum metal powder, and colloidal silica in aqueous solution as the precursor material [2.79]. M. Shojaie-Bahaabad, et al. [2008] reported an

aqueous sol-gel method for economical synthesis of nano alumina powder using ACH and Al powder as raw materials [2.67]. Pavel V. Krivoshapkin, et al. [2013] proposed a new technique for producing nano scale alumina fibers by obtaining gel-like disperse system from sol synthesized using ACH as the alumina source, formaldehyde, and aqueous ammonia as precipitating agent [2.80].

E. Ponthieu, et al. (1992) prepared ultrafine alumina powders using ANN, ammonia, and various surfactants through a combined sol-gel and emulsion technique. The system described is satisfactory for the production of micrometer-sized alumina powders if the removal of water from the precipitation medium and the washing procedure are carefully carried out. The nature of the surfactant is of primary importance because it conditions the character of the emulsion and its stability [2.81]. Edisson Morgado, et al. [1997] investigated the synthesis of microcrystalline boehmite by aging amorphous precursors derived from base hydrolysis of ANN solutions at 85^0C. The susceptibility of the resultant boehmite gels to form a colloidal dispersion by reaction with dilute nitric acid, i.e., their peptizability, was determined based on their particle size [2.82]. Nan Yao, et al. [2001] reported a process for alumina sol preparation using ANN as the alumina source, ammonium hydroxide as the precipitating agent and nitric acid as peptizing agent and study the effect of ultrasound as a function of time on the pH of the sol [2.83].

Maria I. F. Macedo, et al. [2004] reported the gamma alumina synthesis by sol-gel route with ANN and urea as the starting materials. The controlled hydrolysis of the aluminum ions resulted in the formation of nanoparticles of aluminum hydroxide. The resulting sol coalesced and became a transparent gel network composed of colloidal particles of $Al(OH)_3$ and a solution containing the remaining urea and the aluminum polycation, yielded γ -alumina with heating [2.84]. M. R. Karim, et al. [2011] reported a sol-gel synthesis of y-alumina using ANN and urea as the starting materials. The controlled hydrolysis by urea in aqueous media resulted in sol comprising aluminum hydroxide particles which coalesced and became a transparent gel. The gel was dried at 280°C to eliminate the remaining urea and nitrate and resulted in porous, amorphous γ-alumina powder [2.85]. Jiang Li, et al. [2006] reported the synthesis of ultrafine α-Al_2O**3** through a simple aqueous sol–gel method based on the in situ generation of water-soluble metal complexes with ANN and citric acid as raw materials [2.86]. A. Rajaeiyan et al. [2013] reported a sol-gel method based on the Pechini process to synthesize different phases of alumina

nanoparticles using a polymeric precursor with ANN and two different complexing agents, urea and citric acid [2.87].

Bimal P. Singh, et al. [2002] studied the stability of concentrated aqueous colloidal alumina powder suspensions with and without dispersant (albumin and dibasic ammonium citrate (DAC)) by measuring surface charge at different solid loading and pH values [2.88]. In their further study [2005], they reported that alumina particles were found to be optimally dispersed at pH around 3 to 7.8 without a dispersant and at pH 8.5 and beyond with dispersant. It is concluded that the degree of dispersion and hence the stability of alumina suspensions in aqueous media could be controlled by pH variation and optimum dispersant dosage [2.89]. L. Chera, et al. [2007] also studied the effect of various dispersants on the stability of aqueous suspensions of nano-sized alumina particles [2.90]. M. Thiruchitrambalam, et al. [2004] also reported the sol-gel processing of nano alumina through hydrolysis of aluminum metal to get the stable boehmite sol [2.91].

2.7.2 Alumina sol in castables:

Though many literatures are available for alumina sol making, the use of this sol as a binder for refractory castables are mentioned by few authors only. The advantage of alumina sol is its purity. Since no any other phase is present, so the chance of any low melting phase formation in high alumina system is negligible. As a result, there is an increase in hot properties as well as corrosion resistance of the refractory material. In spite of this advantage, not much work has been reported on the use of alumina sol due to various processing difficulties such as high water requirement during processing, low flowability, low solid content, poor stability of sol and poor workability [2.52, 2.53]. For lower solid contents, binding properties are insignificant whereas high water requirement during mixing for sols with higher solid contents deteriorates the mechanical properties [2.63, 2.92]. Some of the literature reporting the use of alumina sol as a binder is mentioned in next section.

S. Mukhopadhyaya and coworkers [2000] has reported the synthesis of alumina sol from two different precursors and its use as a binder together with cement in a refractory castable. They found that the sol prepared from aluminum nitrate precursor shows better properties than the one prepared with aluminum chloride but not at par when compared to conventional cement bonded

ones and stress on further experiments [2.93]. They also found that simple tapping technique could be cost effective and heat treatment of the sol before using results in an activated sol with increased solid content which further improves the physical properties of the castables [2.94]. They further studied [2001] the effect of alumina sol as a binder in cement-free castable composition and found that physical properties of sol bonded compositions are superior to cement bonded compositions. Though the green strength of sol bonded compositions is negligible, the strength increases abruptly above 900^{o}C [2.95]. They also [2003] reported a comparative study of alumina and silica sols in ultra-low cement castables and found that better homogeneity and control of microstructure are possible with the alumina sol binder and superior strength at elevated temperature were observed though the green strength is low due to lower solid content [2.96].

Ersan Yilmaz et al. [2010] investigated the effect of boehmite sol coated graphite on slag corrosion resistance of low-cement alumina castables and found an increase in oxidation resistance as well as slag-refractory resistance is greatly increased at elevated temperatures [2.97]. Han et al. [2011] in their patent works [2.92, 2.98] reported the use of alumina sol as a binder for refractory castables. They used alumina (boehmite) sol as a binder with alumina and silicon carbide refractory grains along with some organic binders. Mariana A. L. Braulio, et al. [2012] reported a comparative study between colloidal alumina and calcium aluminate cement as a binder for refractory castables and found that colloidal binders coupled with sintering additives can provide low temperature densification. Remarkable results for thermal shock, erosion, hot mechanical strength, and refractoriness were obtained [2.99].

2.8 Mullite sol:

Mullite is an aluminosilicate ($3Al_2O_3.2SiO_2$) with large technological applications due to its excellent properties like low thermal expansion, high thermal stability, low thermal conductivity, good mechanical strength, better creep resistance and better resistance to chemical corrosion [2.100, 2.101]. The sol-gel route is one of the most widely used synthesis methods for generation of mullite products with high purity and homogeneity. The hydrolysis and condensation of precursors in a sol-gel process are influenced by many factors such as pH, water content, organic

and inorganic additives, precursor materials, etc. These in turn, determines the final product properties [2.102].

The mechanism of mullite formation reaction varies with the alumina and silica precursors and the synthesis method employed [2.60]. Mullite formation from chemically synthesized precursors generally takes place in a temperature range of 850-1350^{o}C. The degree of chemical homogeneity is an important factor in determining the reaction mechanism and consequently the temperature of crystallization. The temperature of mullite crystallization is low, when the precursors have a higher degree of homogeneity [2.102, 2.103].

2.8.1 Mullite sol making:

The sol-gel process is a wet chemical route that offers homogenous distribution of the precursor materials. This high degree of homogeneity resulted in mullite formation at a relatively lower temperature (1000-1350^{o}C) when compared to traditional methods like solid state reaction of powder mixture (1500-1700^{o}C) [2.104-2.107]. Various aluminum and silicon sources have been used as precursors for mullite synthesis. Generally, the precursor is some inorganic salts or some organic compounds like metal alkoxide. For silica, alkoxides are mostly used as precursors; the two being most commonly used are tetraethyl orthosilicate (TEOS) and the tetramethyl orthosilicate (TMOS) [2.108]. TEOS was first utilized by Roy [1956] as silica source and aluminum nitrate nonahydrate (ANN) as alumina source for mullite synthesis [2.109]. Since then, both TEOS and ANN have been widely used as precursors for the synthesis of mullite by the sol-gel process [2.110] Silicic acid or the aqueous suspension of silica is another silica source that has been used as the precursor for mullite synthesis. The synthesis route that uses silicic acid is economical as compared to that which uses TEOS as silica source [2.111].

The choice of precursor materials have a strong impact on the various steps of the sol-gel process and finally on the properties of the final product. Fujio Mizukami et al. [1997] studied the effect of two different alumina sources, ANN or dibutoxy ethylacetoacetatoaluminum ($Al(OBu)_2(Ac(AcEt))$ on mullite formation with TEOS as the silica source and found that formation is much easier from ANN than ($Al(OBu)_2(Ac(AcEt)$ [2.112]. Vol'khin et al. [2000] also studied the effect of different alumina precursors, γ-AlO(OH) sol, and $Al(NO_3)_3$, on mullite formation with silica nanoparticles as silica source and found that mullite formation is lower in

the case of ANN due to a greater degree of hydroxide particle aggregation reducing the reactivity [2.113]. The control of hydrolysis and condensation reaction rates of mullite precursors is a bigger challenge of the sol-gel process, where the reactivity difference of the metal alkoxide precursors makes it difficult to control the composition and homogeneity of the materials leading to phase segregation [2.114]. The replacement of more reactive alkoxide by some hydrated salt, promote the hydrolysis of the less reactive alkoxide through the water molecules of the salt, resulting in a homogenous copolymerization of mullite precursors. The pH of the starting solution also influences the sol-gel process. At higher pH, the particle size increases while in acidic condition, the formation of smaller particles is favored [2.65].

On the basis of the degree of homogeneity present in the gel, it can be termed as the monophasic gel when the mixing of aluminum and silicon atoms takes place at the atomic level and diphasic gel when the degree of homogeneity is at nano scale [2.101, 2.115, 2.116]. There is a third type called hybrids gel which is a combination of monophasic and diphasic precursors [2.117, 2.118].

2.8.1.1 Monophasic gel

As mention above, when the mixing of the aluminum and silicon sources takes place at the atomic level in the precursor solution, the colloidal sol and thus the gel formed from it is termed as the monophasic gel. On crystallization, a stable form of orthorhombic mullite is formed at 980^{o}C, without formation of any intermediate phases [2.60, 2.106, 2.119]. They can be obtained by slow hydrolysis using TEOS, ANN, and ethanol or by using AIP with ANN in aqueous solution [2.120-2.122].

Synthesis of monophasic gel from aluminum Sulphate hydrate and silica sol was studied by Chakravorty [1993], showing the formation of tetragonal mullite at 980^{o}C [2.123]. He also studied the effect of the pH on the formation of mullite and shows that pH between 3 and 4.5 favors the formation of monophasic precursors, with mullite crystallization temperature at 980^{o}C. In a highly acidic (pH<1) or basic (pH~14) medium, diphasic precursors are formed with mullite crystallization at higher temperatures. Ban et al. reported [1996] mullite formation at 450 C (small amount) from precursors prepared with ANN, AIP, and TEOS [2.119]. The pre-calcination of precursors at 250^{0}C for 16 h result in dehydration and decomposition of part of nitrate and alkoxyl groups, creating regions with a slightly different chemical composition within

the precursor. Thus, the energetically active interfaces between these regions act as nucleation sites. Voll et al. [1998] synthesized monophasic gels with aluminum sec-butoxide and TEOS in isopropanol as starting materials and suggested a mechanism of monophasic precursor dehydration [2.124]. Sola et al [2005] in his study on monophasic gels observed an increase in the intensity of FTIR bands with temperature, at 1160 and 1130 cm^{-1} related to Si-O stretching, showing the enrichment of crystallized mullite with silica [2.125]. Leivo et al. [2006], also showed the formation of tetragonal mullite below 1000^0C, as the only crystalline phase without formation of any intermediate phases, using AIP with ANN as the aluminum source [2.120].

Effect of additives on monophasic gels was also reported by some authors [2.112, 2.126, 2.127]. Jaymes et al. [1996] studied the effect of urea on the synthesis of mullite monophasic gels from ANN and silicic acid [2.126]. The slow formation of ammonia from urea when the solution is heated at 80-100^{o}C, serves two purposes, first, promote the polycondensation of silicic acid into silica gel by raising the pH, and second, the hydrolysis and polycondensation of aluminum. Simendi and Radonji [2005] studied the effect of fluorine acid addition to mullite sol synthesis from ANN and TEOS and found that there is a decrease in the mullite crystallization temperature from 980 to 890^{o}C [2.127]. The fluoride ion breaks the oxygen bonds in mullite gel structure and increasing the homogeneity of the precursors to the molecular level. Bagchi, et al. [2009], reported a sol-gel synthesis of nanocrystalline mullite using ANN, AIP and TEOS with copper sulfate as a dopant and found that a well-crystallized mullite phase was obtained at 600 and 750^{o}C for the copper-doped samples [2.128].

2.8.1.2 Diphasic gel

Diphasic gels are formed when the homogeneity scale of aluminum and silicon is between 1 and 100 nm. Hoffman et al. in 1984 initiated the synthesis of mullite diphasic gels using boehmite sol and silica sol as starting materials [2.129]. Wei et al. in 1988 showed that mullite crystallization from diphasic gels takes place around 1200^0C, through the reaction given below:

$$3\ \delta\text{-}Al_2O_3 + 2\ SiO_2\ (\text{amorphous}) = 3Al_2O_3.2SiO_2\ (\text{mullite})$$

The Wei's study [2.115] resulted in a model for the crystallization process based on the formation of a mullite interface between the alumina and silica grains, and the growth

mechanism was controlled by diffusion of silicon and aluminum in this interface. Vollet et al. [1998] investigated phase transition sequence in diphasic gels synthesized from a colloidal boehmite sol and TEOS solution [2.130]. The gel XRD pattern was found to be compatible with a diphasic system, composed of an amorphous silica phase, and a colloidal crystalline phase of boehmite. The formation of alumina intermediate phases was followed by mullite formation at 1300^{o}C. Beran et al. [2000] investigated the dehydration and structural development of monophasic and diphasic mullite precursors prepared from ASB and TEOS as starting materials and isopropanol for monophasic and isopropyl alcohol and water in basic pH as a solvent for the diphasic precursor [2.131]. Padmaja, et al. [2001] reported an FTIR analysis of mullite sol prepared from boehmite sol and TEOS and found that the synthesized sol has diphasic nature since the spectra show Si–O–Si and Al–O–Al linkages in the gel stage as well as at 200^{o}C and there is no band corresponding to Si–O–Al linkage indicating the inhomogeneity and diphasic nature of the precursor [2.132]. Emilija Tkalcec, et al [2003], studied the crystallization kinetics of mullite formation in diphasic gels containing alumina in different crystalline form and particle size and TEOS-derived amorphous silica and found that the process is fastest in the precursor with the smallest particle size of alumina, and the slowest in the sample with boehmite-derived alumina [2.133].

The precursor pH also has a strong influence on the phase formation at different temperatures as well as the on the morphology of the formed mullite. Huang et al. [1997] reported the effect of pH variation on mullite synthesis from diphasic gels prepared from ACH, TEOS, and Water [2.134]. For acidic precursors, mullite formation takes place at 1200^{o}C, while for basic, the formation occurs at 1350 C. Anil Kumar, et al. [1997], reported the effect of pH on the formation characteristics of sol-gel derived mullite prepared by reacting boehmite sol and TEOS in a stoichiometric ratio and found that pH of the precursor at the time of gelation can highly influence the gelation characteristics, mullite formation, and microstructural features [2.135]. Jae-Ean Lee et al. [2002] studied the pH effect on samples prepared from ANN and colloidal silica and reported needle-like mullite crystals for pH less than 2 while rod-like or granular mullite for pH greater than 8. For acidic precursors, the mullite crystallization temperature was about 1200 C while for basic precursors it was above 1200^{o}C. Furthermore; the acidic precursors generate transparent gels due to very small size of the particles in acidic samples, while the gel appears to be opaque for basic samples [2.136]. Osawa et al. [2005] also studied the effect of pH

on the formation of mullite from alumina and silica sols with a stoichiometric composition and with silica excess. They reported that pH did not influence the mullite formation for precursors with silica excess, while precursors with the stoichiometric composition are affected by the pH variation [2.137].

Thim and co-authors, [2001] studied the effect of urea on mullite formation from ANN and silica sol [2.138]. Further studies by Campos et al. [2002] on precursors synthesized with silicic acid, ANN and urea (urea/Al^{3+} equal to 3/1) show mullite crystallization through the spinel type aluminosilicate formation, at a temperature close to 1200ºC [2.139]. In another work [2009] using similar samples, polymeric and colloidal sol were synthesized using different molar ratios of urea and Al^{3+}. It was reported that the effect of urea on mullite crystallization is positive for the colloidal precursor, while a negative effect is found for the polymeric precursor. Furthermore, the amount of mullite formed increases with urea content and crystallization takes place at 1100ºC for the colloidal gels. It was reported that the participation of urea in the hydrolysis and condensation steps, avoiding intense phase segregation, is the reason for the positive effect of urea on colloidal gels [2.140]. Campos et al. [2008] studied the effect of citric acid on mullite formation from ANN and silicic acid using different molar ratios of citric acid and Al3+ and reported that citric acid has a positive effect on mullite crystallization [2.141].

Anil Kumar, et al. [1997] reported the effect of seeding on the formation of sol-gel derived mullite. Mullite precursor was prepared from a mixture of particulate boehmite sol and TEOS and seeded with submicron size α-$A1_2O_3$, γ-$A1_2O_3$ and mullite and found that the seeded fine mullite particles have shown excellent influence in the early ceramic phase formation as well as densification [2.142]. Hong and Messing [1999] studied the doping effect of boria on mullite formation from diphasic gels prepared from boehmite and silica and reported that crystallization temperature reduced to 1260ºC for doped samples from 1345ºC for the non-doped samples. The temperature reduction is due to the enhanced densification and formation of fine grain microstructure in the doped samples [2.143]. Roy, et al. [2010] studied the effect of Cr_2O_3 on the mullitization of diphasic Al_2O_3-SiO_2 gel synthesized from ANN and liquid sodium silicate and found that more than 7% more mullite has been formed with the addition of maximum 3% additive only. Using the additive, the maximum reduction in apparent porosity was about 30% and maximum improvement in density in the sintered compacts was about 14% [2.144].

2.8.1.3 Hybrid gel

The concept of the hybrid gel was first introduced in 1989 by Huling and Messing [2.117] as a mixture of polymeric and colloidal sols. They synthesized the hybrid gel by mixing a colloidal boehmite-silica sol and a polymeric aluminum nitrate-TEOS sol. The polymeric part of the hybrid gel crystallizes mullite first which acts as nuclei for nucleation of the colloidal component. In 2003, Zhao et al. [2.118], reported a hybrid gel consists of a relatively small amount of monophasic gel in a diphasic gel matrix synthesized from AlOOH and SiO_2. The mullite crystallization takes place above 1250^{o}C, showing that the crystallization mechanism was controlled by the diphasic component, which is in higher proportion.

2.8.2 Mullite sol in castables:

Use of mullite precursors as additives have been reported to improve the castable properties but the use of precursor sol as a binder has been reported by few only. Mukhopadhyaya and coworkers use mullite sol along with CA cement and micro silica showed [2.145] microstructures are associated with pore formation, crack generation due to volume mismatch and excessive grain growth. Mullite sol, even in combination with alumina cement, also reported [2.146] to produce inferior properties, both at ambient and elevated temperatures, compared to that of the only cement and silica sol bonded compositions. The mullite (silica-alumina) sol bonding agent prepared by the sol- gel route from ethyl silicate and aluminum isopropanol reported [2.147] to produce improved properties in corundum based refractory castables compared to conventional cement bonded castables.

B. Mandal, R. Sarkar, P.K. Daspoddar studied the effect of three different mullite precursors on the properties of low-cement high alumina castables. The precursors were prepared from $Al(OH)_3$ and silica sol, with variation in the calcination temperature of $Al(OH)_3$. They found that there was no strength degradation for the castable at the intermediate temperature from the decomposition of cement hydrates due to the formation of mullite bond phase from the precursor material in the castable matrix, which improves bonding in the castable and compensates the strength deterioration [2.148].

2.9 Spinel sol:

Mg-Al spinel ($MgAl_2O_4$) is an ideal refractory material with a rare combination of physical, chemical and thermo-mechanical properties. The use of Mg-Al spinel as refractory aggregates has been also been reported [2.149] to improve the performance of refractory castables mainly by the enhancing hot strength, thermal shock resistance, and corrosion resistance. These advantages of spinel have encouraged developing spinel sol and using the same in high alumina composition as sole binder.

2.9.1 Spinel sol making: For Mg-Al Spinel sol synthesis, different aluminum and magnesium sources have been used for the spinel precursor synthesis. Generally, the precursor employed is an inorganic metal salt (nitrate, chloride, acetate, etc.) or an organic precursor such as a metal alkoxide. As in mullite sol synthesis, which is classified on the basis of nature of gel precursors as monophasic and diphasic, no such classification for spinel sol is found in the literature. The available literature on the spinel sol making thus can be broadly classified on the use of starting alumina and magnesia precursors as both the precursors inorganic, both organic and one organic and other inorganic.

2.9.1.1 Spinel sol making with both precursors inorganic:

Pasquier, et al. [1991] reported a Mg-Al spinel sol synthesis utilizing boehmite sol and magnesium nitrate hexahydrate, $Mg(NO_3)_2.6H_2O$ (MNH) and boehmite sol and magnesia sol in the presence and absence of seeds and found that seeding with spinel crystallites resulted in a lower formation temperature of $MgAl_2O_4$ spinel [2.150]. Guo, et al. [2004] reported a modified sol-gel synthesis route combining gelation and coprecipitation for the synthesis of mgal2o4 spinel using stoichiometric amounts of the desired metal nitrates [2.151]. Yuan, et al. [2004] reported a novel sol-gel process for preparing $MgAl_2O_4$ spinel from magnesium and aluminum nitrates, utilizing the polysaccharide gel formed by synergistic gelation of xanthan gum and locust bean gum [2.152].

Zhang and others [2004] reported a citrate sol-gel process for nano spinel synthesis using MNH, ANN, and citric acid as starting materials. The spinel formation consists of two stages, first, the decomposition of precursor compounds to γ-Al_2O_3 and MgO, followed by the solid-state reaction

between γ-Al_2O_3 and MgO to form spinel around 600ºC [2.153]. They also investigated [2004] the effect of citric acid and pH values on the sol-gel synthesis of mgal2o4 spinel and found that the concentrations of magnesium and aluminum citrate are the major factors affecting the citrate sol–gel process [2.154]. Xiaolin, et al. [2004] reported a sol-gel synthesis of spinel using MNH, ANN, citric acid, and ammonia solution as starting materials and investigated the effects of the amount and the size of $MgAl_2O_4$ crystal seeds on the formation of $MgAl_2O_4$ spinel [2.155].

Naskar and Chatterjee, [2005] reported water-based sol-gel process for spinel synthesis using aluminum and magnesium nitrates as starting materials and compared this with a sol-emulsion-gel synthesis of spinel using a surfactant with same raw materials. They found that surfactant concentration and viscosity of the sol affects the characteristics of the derived spinel microspheres [2.156]. Saberi, et al. [2009] reported the influence of heat-treatment atmosphere in the synthesis of $MgAl_2O_4$ spinel via sol-gel citrate route using aluminum and magnesium nitrates and observed that heat treatment of precursor in argon atmosphere reduces the particle size of synthesized powder significantly [2.157]. Nassar, et al. [2014] reported a hybrid sol-gel auto combustion route for nano spinel synthesis using aluminum nitrate and magnesium nitrate with oxalic acid, urea, and citric acid as three different fuels. The organic fuels act here as a chelating agent, as well as a fuel. A pure spinel phase with average crystallite size below 100 nm was reported at 800 C using the aforementioned fuels [2.158].

Pei and co-workers [2010] reported a simple aqueous sol-gel process for spinel synthesis using citrate polymeric precursors derived from magnesium chloride, aluminium nitrate and citric acid [2.159]. N.M. Khalil, et al. [2010] reported a sol-gel process for nano spinel preparation using magnesium chloride and aluminium hydroxide (boehmite) and studied the sintering, mechanical and refractory properties of magnesium aluminate spinel, magnesia–spinel and alumina–spinel refractory bodies through addition of chromia, zirconia or their mixtures [2.160].

2.9.1.2 Spinel sol making with both precursors organic:

Varnier, et al. [1994] reported a sol-gel synthesis of spinel from a heterobimetallic magnesium aluminum n-butoxide modified by polyethylene glycol. Calcination of the precursor gel at 700°C yielded a pure $MgAI_2O_4$ spinel powder that could be hot pressed to transparency [2.161]. Julien Parmentier, et al. [1998] reported a sol-gel processing of $MgAl_2O_4$ spinel using a double

alkoxide or magnesium nitrate and ASB as raw materials and proposed that the size of the particles is related to the functionality of the inorganic polymer [2.162]. Amini, et al. [2007] reported a hydrothermal-assisted sol–gel processing of magnesium aluminate spinel using different magnesium aluminium alkoxides precursors and found that the solvent employed in hydrothermal-assisted sol–gel processing has a pronounced effect on the spinel morphology [2.163]. Liu, et al. [2010] reported a sol-gel process for nano spinel synthesis using magnesium aluminium double n-butoxide as precursors [2.164]. They also [2013] studied the effect of acetylacetone as chelating agent on $MgAl_2O_4$ spinel synthesis via the sol–gel method, using same alkoxides as precursors. The reported precursors are converted to pure spinel phase at 800^0C [2.165].

2.9.1.3 Spinel sol making with one organic precursor and other inorganic

Lepkova, et al. [1991] reported a sol-gel synthesis of spinel using MNH and ASB as the starting materials and additives like B_2O_3 and TiO_2 were included as alcoholates during the hydrolysis process to intensify the process of spinel formation [2.166]. Ye and Troczynski [2005] reported a heterogeneous sol-gel process for spinel synthesis using reactive MgO powder, AIP, isopropyl alcohol and ammonia water. The effect of high-energy milling of the precursor powder on the precursor decomposition and spinel formation was investigated and found that the milling reduces the incipient temperature of spinel formation from 900 to 800^{o}C, and that of complete spinel formation from 1280 to about 900^{o}C [2.167]. Ye, et al. [2005] reported a combination of sol-gel and precipitation process for the synthesis of $MgAl_2O_4$ spinel using magnesium acetate tetrahydrate and AIP as the starting materials [2.168]. Pacurariu, et al. [2007] reported a sol-gel synthesis of spinel from MNH and AIP and compared with two other synthesis methods: thermal conversion of Organic precursor's (based on magnesium and aluminium glyoxylate) and combustion method (redox reaction of Mg and Al nitrates with an adequate fuel). Phase analysis showed that pure spinel phase is present at 700 C and the phase crystallinity varies with the method employed [2.169].

2.9.2 Spinel sol in castables:

Use of spinel sol as a binder has also been reported by some authors in ultra-low cement compositions (containing 1.5% alumina cement) [2.145, 2.146]. The microstructure of these sol

bonded castables was reported to have pores and cracks [2.145]. Also, the developed properties were reported [2.146] to be inferior compared to that of the only cement or silica sol bonded compositions. Use of spinel sol in cement containing castable composition was reported to results in reduced density, strength values and showed a microstructure with non-uniform heterogeneous matrix and disjointed bonding having locally agglomerated particles and sporadic cracks and voids [2.146].

2.10 Particle size distribution (PSD) in castables

To make any refractory we need the constituent material in various sizes to enable a better packed and dense condition. Now for shaped refractories, PSD is planned in such a way as to achieve maximum packing density. Hence minimum void space will remain within the structure, resulting in greater compaction, densification, and strength. This densely packed condition also remains valid even after firing at elevated temperatures for the highly compact mass as sintering is higher for such a compact structure due to a reduced diffusion path and less void space [2.170].

To obtain a dense packing, different sized particles, namely, coarse, medium and fine, are used in such a way that the gap between the coarse particles is filled by the medium and that of the medium particles and coarse and medium particles by the fines. As discrete sized particles are used in this packing it is called discrete packing. As the finer sized particles are fixed in the gap of the coarser ones, the particles do not move once it has been packed. Discrete packing reduces the water demand and fired porosity value due to greater packing (larger particle contacts and fewer voids) and is also reported to impart good thermal shock resistance [2.171].

But for castables, conventional concept of highest packing does not work. Castables primarily need to flow and also require compaction for density and strength, both at ambient and elevated temperatures. It is a unique requirement compared to that of the shaped refractory and also contradictory in nature as strength develops from compaction which restricts movement due to friction. Flow is important for castables for a better installation, filling of void space, compaction and property development. Again this flowability is primarily dependent on the particle size

distribution and packing of the castable system. So, there has been always a compromise between density and strength against ease of installation for castables [2.172].

Hence, a new particle size distribution concept is required, which is called continuous particle size distribution. In this distribution, particle sizes are present in a continuous manner, not in a discrete manner. Different particle size fractions are used for such a pattern. Each size fraction has a specific maximum and minimum size value, where the maximum size of one particular fraction is the minimum size value of the earlier coarser size fraction and the minimum size is the maximum size of the next finer fraction. Thus, the whole range of particles is present within the system in a continuous manner.

Various packing models have been reported over the last century, but the models proposed by Furnas - Anderegg and Andreassen - Andersen are important. Furnas developed a mathematical relationship for two different types of grading, one based on the mixing of two, three or four size fractions which is a discrete packing model, and second based on a continuous size distribution without any gap in particle sizes. Mac-Zura et al. reported [2.173] that the discrete packing model gives better density values but with very limited workability and flow properties, whereas the continuous particle packing model resulted in improved workability at low moisture content with significant strength and compactness [2.171]. However, the Furnas model for the continuous distribution of particles is only an extension of his model for discrete particle distribution to a multicomponent system. According to Furnas, the best packing occurs when finer particles exactly fill the voids within the larger particles.

Furnas model is, however, difficult and cumbersome for practical use. Parallel to Furnas, Andreassen also worked on the same problem, but with a different approach. He proposed his model based on similarity conditions. As per Andreassen model the granulation image (particle array) surrounding each and every particle of different sizes in the distribution are similar. This arrangement of particles is the similarity condition for packing as per Andreassen. So as per continuous particle size distribution of Andreassen, particle size variations and packing arrangements will be exactly similar at any magnification in the distribution. Andreassen assumed such a similarity condition for continuous particle size distribution and proposed

[2.174-2.176] a linear equation relation CPFT (Cumulative Percent Finer Than) plot against particle size as per the equation,

$$\mathbf{CPFT = [(d/ D)^q] *100}$$

Where CPFT = cumulative passing percentage under particle size d, d =particle size, D =maximum particle size and q = distribution coefficient.

Andreassen concluded that the exponent (q) in the equation plays a vital role in defining the particles sizes. Andreassen proposed the value of the distribution coefficient to be between 0.33 and 0.5 to obtain the optimum packing density. The drawback to Andreasen's approach and equation is that he did not recognize the effect of smallest particle size [2.172, 2.177] as his model results in straight lines on log-log plots continue forever. So as per his model certain fraction of particles will be there even with extremely small values, which is practically not feasible to attain. Hence the model remained away from the actual practical conditions.

To get a solution, Dinger and Funk used both the Andreassen and the Furnas distribution and proposed a new model with the introduction of a new parameter, minimum particle size. This proposed new model is easier to use compared to that of Furnas, and is frequently termed as the 'Dinger and Funk' equation or the 'modified Andreassen'. When the models are plotted in a log-log plot produce a straight line for the Andreassen distribution and lines with downwards curvature for the modified Andreassen and the Furnas distribution. The latter two models produce similar distribution patterns. The model as proposed by Dinger and Funk is given below.

$$\mathbf{CPFT = [(d^q - d_m^q)/(D^q - d_m^q)]*100}$$

Here, CPFT: Cumulative Percent Finer Than, d: particle size, d_m: minimum particle size of the distribution, D: maximum particle size and q: the distribution coefficient.

Dinger and Funk made a comprehensive treatment of packing theories. According to computer simulations, the exponent in the equation should be 0.37 to get optimum particle packing. This is similar to the proposal of Andreassen where he had proposed that such a packing occurs when the q value is between 1/3 and 1/2. Distribution with exponents less than 0.37 approach zero porosity as the width of the distribution increases. As finer and finer particles are added to the distribution, porosity will decrease and approach zero. Hence according to the above conclusion,

it has no meaning using exponents greater than 0.37 if the objective is to create a maximum packing density.

Further work on the particle size distribution models has shown that for good flowability of the castables the distribution coefficient (q) must be between 0.2 to 0.3 [2.27]. Also, studies showed that q values close to 0.3 results in vibratable castables (requiring external energy to flow well) and lower q values (<0.25) result in castables with self-flowability (that move under their own weight) [2.172]. It has also been observed that higher q values result in higher coarser fractions and lower q values result in a greater finer fraction [2.178-2.181] Lower q value with greater extent of finer fractions increases the sphericity of the particles, resulting in better flowability of the compositions and finally producing self-flowability character. But higher finer fraction increases the surface area of the system and causes higher water demand. Thus by changing the q values, one can change the particle size distribution of the castable composition and control the flow behavior and other properties.

The most important aspect in the packing models is that they are based on the volume of the particles (involving diameters in the equations). So, whenever two or more components are present (having different specific gravity values) whilst making a castable composition, the amount of components must be converted into their volume percentages to suit the model accurately. Again, these models have been developed assuming the particles as incompressible and uncrushable spheres, but for practical situations deviations are common due to the nonsphericity (angularity) of the particles, resulting in alterations from the expected rheological behavior.

2.11 Conclusion

By going through the literature review on the various aspects of refractory castables, especially on the castable bonding systems, it can be concluded that:

1. Conventional cement binder for refractory castables has limitations for high temperature applications.
2. Other cement free compositions are also available, but each having its own advantages and drawbacks.

3. Colloidal binders result in superior properties and performance of refractory castables.
4. Among different colloidal binders, only silica sol has been commercially exploited as the binder for the refractory system.
5. Colloidal silica has limitation for high temperature application due to the formation of low melting phases and eutectics.
6. Though various processing techniques are available for other colloidal systems, their use as a binder for the refractory system is reported by few only.
7. The various processing difficulties associated with other colloidal systems, during formation and during application as a binder, have limited their commercial exploitation, unlike silica sol.
8. For sol making processes of alumina mullite and spinel, various organic and inorganic precursors are employed. Among organic precursors, various metal alkoxides are used whereas for inorganic precursors, metal salts are most employed.
9. Inorganic metallic salts are preferred over organic alkoxide precursors due to economic reasons.
10. Besides chemical composition, particle size distribution is another important factor which governs the properties and performance of refractories.

Chapter 3

Motivation and Research Objective

3.1 Motivation

- Sol-gel bonded castables have various advantages over the traditional cement bonded castables and other bonding systems.
- A lot of work has been done in the field of silica sol bonded castables, but very few literatures are available for other sol systems.
- Nearly no work has been done comparing different sol systems as a binding medium, neither used solely in a high alumina castable system.
- No literature is available for use of alumina or other sol systems in high alumina castables with varying distribution coefficient.
- No work is available for highly pure (>99 %) alumina system in castable refractory.
- All these facts are the driving force for choosing the present topic.

3.2 Research Objective…

- Synthesize different sol systems using raw materials considering ease of availability and economics.
- Characterization of these synthesized sol systems by various means to understand their phase transformation at room temperature to high temperature.
- Use of these sol systems individually as a binder to prepare cement free high pure alumina refractory castables.
- Study the effect of particle size distribution as per Dinger and Funk model on the properties of refractory castables.
- Characterization of the developed sol bonded cement free castables for their various physical, mechanical and thermo-mechanical properties.
- Comparison of the best compositions of the developed sol bonded cement free castables with commercially available silica sol and conventional cement bonded composition, processed under similar conditions, for their corrosion behavior against blast furnace slag.

Chapter 4

Experimental Work

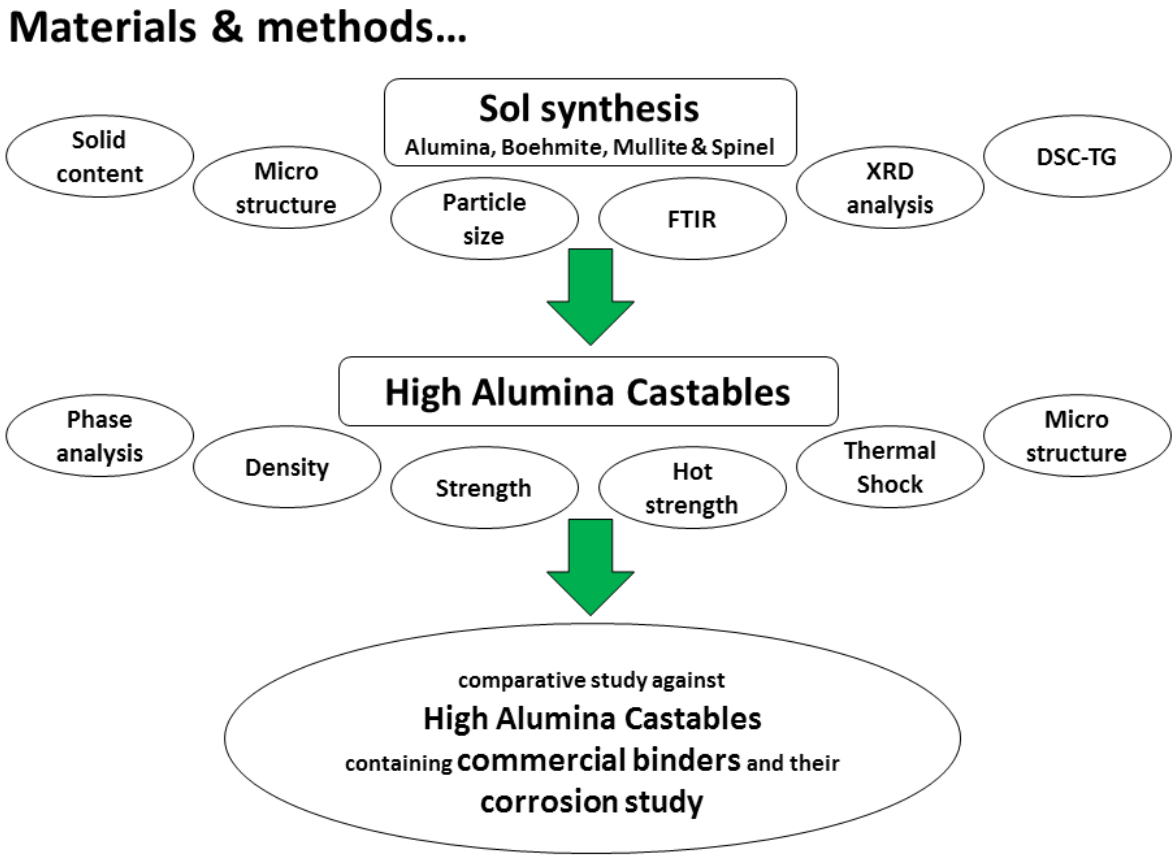

Figure 4.1: Graphical representation of experimental work

The research work consists of the preparation of different sol systems and use of these sols as a binder for the preparation of high pure alumina refractory castables (figure 4.1). Four different sol systems namely alumina, boehmite, mullite, and Mg-Al spinel are prepared and characterized for their various properties. A number of factors such as starting chemicals properties, the degree of mixing, pH, temperature and presence of impurities influence the sol-gel transformation and formation of ceramic particles after heat treatment. High pure alumina castables with varying dimensions for various property evaluations are then prepared using these sol systems as the binder. The castables are dried and fired at various temperatures and finally evaluated for its physical, mechanical and thermo-mechanical properties. The developed castables are also compared for its various properties with castables containing commercially available high alumina cement and colloidal silica as binders, prepared under similar conditions and PSD. The list of all the equipment used to carry out the experimental work is given in the last section with their specifications.

4.1 Synthesis of Alumina sol

The alumina sol is synthesized using inorganic nitrate precursor. The sol utilizes aluminum nitrate salt as the source of alumina. The raw materials required for sol making process are given in Table 4.1 below.

Table 4.1: Raw materials required for alumina sol making process.

Sol nomenclature	Raw materials used
Alumina sol	Aluminum nitrate, Ammonia, deionized water, dispersant (Darvan C)

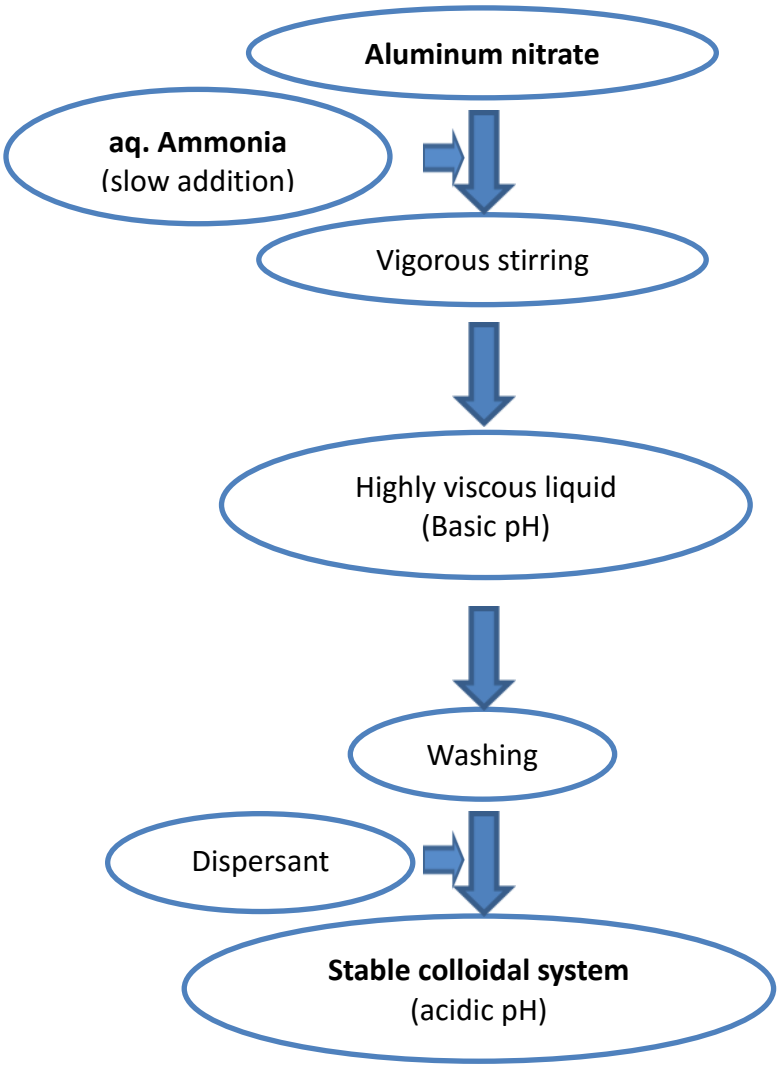

Figure 4.2: Alumina sol making process

Flow diagram for sol making process is given in Figure 4.2. For the making of alumina sol, aluminum nitrate nonahydrate (Fisher Scientific make, purity >98%) and liquor ammonia (Fisher Scientific make, 25%, sp. gr. 0.91), are used as the precursor material. First, a 1M aluminum nitrate solution is prepared by dissolving 1 Mole (375g) of aluminum nitrate in 1L deionized water. To the prepared aluminum nitrate solution (1 M), a very slow addition of liquor ammonia (Fisher Scientific, India make, 25 %, sp. gr. 0.91) under constant vigorous stirring is done (to avoid any precipitate formation) in a stoichiometric ratio (Al salt : ammonia / 1:3). A viscous liquid is formed which is washed 3-4 times to remove any unreacted precursor as well as the by-products. This is followed by addition of dispersant (ammonium polymethacrylate, 0.5%) and few drops of dilute nitric acid under constant vigorous stirring to get the stable colloidal suspension.

The reaction between the Al salt and the liquor ammonia (ammonium hydroxide) resulted in the formation of Al hydroxides. The formation of hydroxides of aluminum i.e. bayerite, $Al(OH)_3$ or boehmite, AlO(OH) depends on reaction conditions. At higher pH and lower temperature bayerite is formed and vice-versa.

4.2 Synthesis of Boehmite sol

The boehmite sol is synthesized using commercially available boehmite powder. The sol utilizes boehmite as the precursor source for alumina. The raw materials required for sol making process are given in table 4.2 below. Flow diagram for sol making process is given in Figure 4.3.

Table 4.2: Raw materials required for boehmite sol making process.

Sol nomenclature	Raw materials used
Boehmite sol	Boehmite powder, dil. nitric acid and deionized water

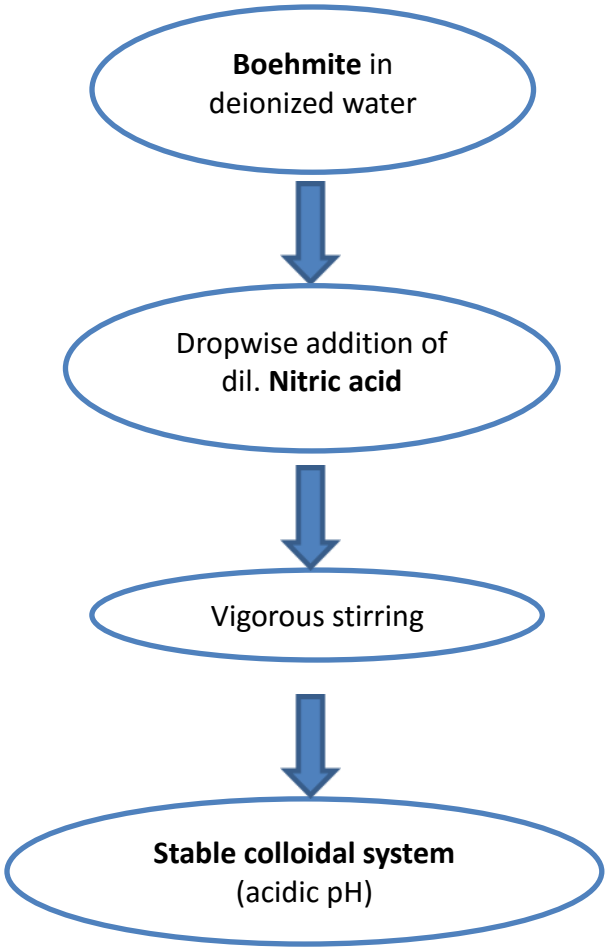

Figure 4.3: Boehmite sol making process

For making of Boehmite sol, commercially available boehmite powder (Hindalco, India) is used as the alumina precursor. The boehmite powder is added in deionized water under constant stirring with few drops of dilute nitric acid to adjust the pH for a stable suspension. The boehmite to water ratio is kept as **1:2-4**. Higher ratio leads to an unstable suspension resulting in settling of boehmite powder whereas lower ratio results in suspension with lower solid content.

4.3 Synthesis of Mullite sol

For mullite sol synthesis, again inorganic precursors are utilized. Aluminum nitrate nonahydrate is used as the source for alumina whereas commercially available silica sol as the source for silica. The raw materials required for sol making process is given in Table 4.3 below and the flow diagram for the mullite sol making process is given in Figure 4.4.

Table 4.3: Raw materials required for mullite sol making process.

Sol nomenclature	Raw materials used
Mullite sol	Aluminum nitrate, silica sol, liquor ammonia, deionized water

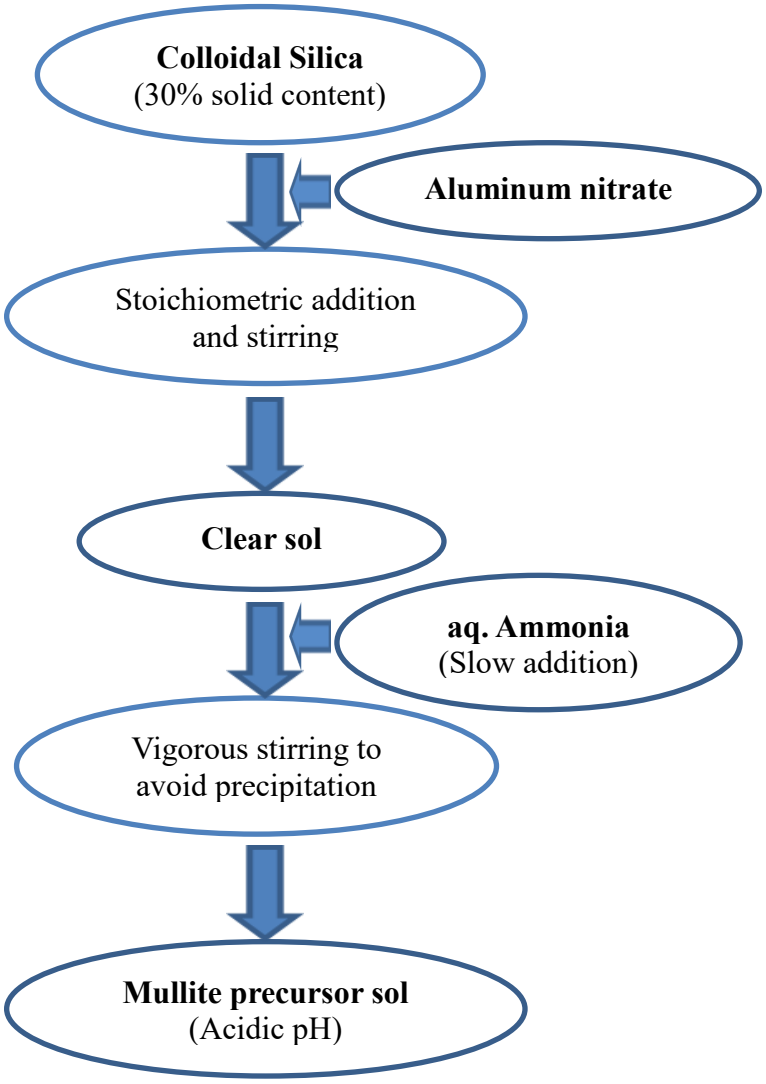

Figure 4.4: Mullite sol making process

The precursor materials used in the preparation of Mullite sol are aluminum nitrate nonahydrate (Fisher Scientific, India make, purity> 98%) as alumina source, silica sol (Dr. Khans laboratory, India make, 30% SiO_2) as silica source and ammonia solution (Fisher Scientific, India make, 25%, sp. gr. 0.91). Aluminum nitrate in a stoichiometric ratio to silica content of silica sol (Alumina: Silica / 3:2) is dissolved in silica sol under stirring and then liquor ammonia in stoichiometry to alumina source is slowly added to the solution under constant vigorous stirring

to avoid any precipitate formation. Addition of ammonia is found to increase the pH and viscosity of the colloidal solution. The suspension is stirred for about 5-6 hours and a clear stable mullite precursor sol is obtained.

4.4 Synthesis of Mg-Al Spinel sol

The Mg-Al spinel sol synthesis again utilizes inorganic precursors for sol making process. Aluminum nitrate is again used as the alumina source and magnesium nitrate is used as the magnesia source. The raw materials required for sol making process are given in Table 4.4 below and the flow diagram for making the spinel sol is given in Figure 4.5.

Table 4.4: Raw materials required for Spinel sol making process.

Sol nomenclature	Raw materials used
Spinel sol	Aluminum nitrate, magnesium nitrate, ammonia solution, deionized water

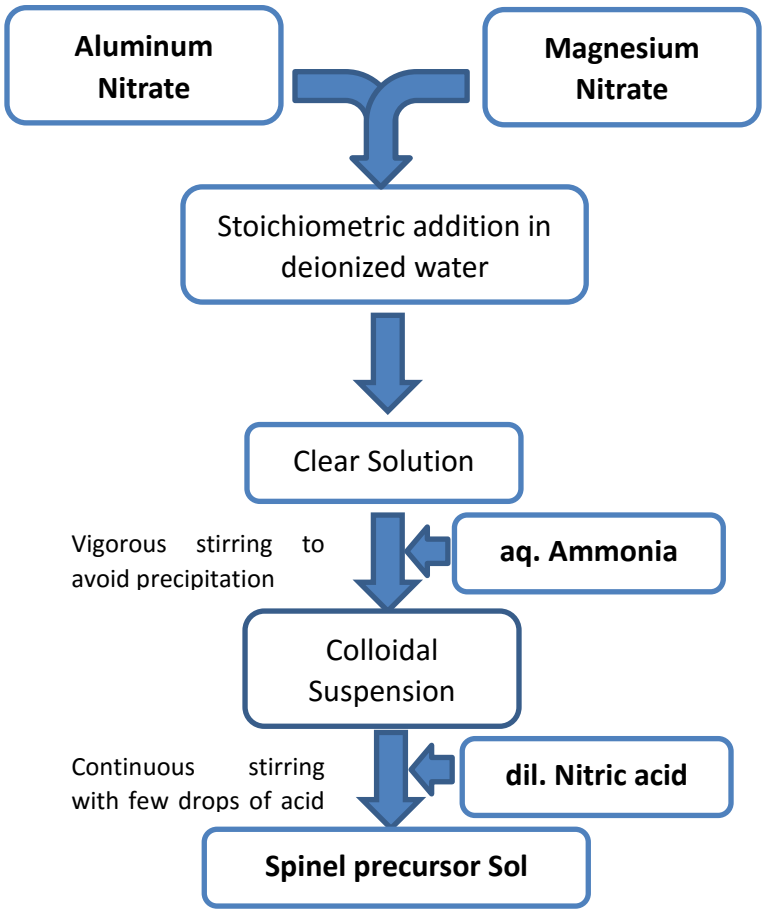

Figure 4.5: Spinel sol making process

The raw materials used in the preparation of Spinel sol are aluminum nitrate nonahydrate (Fisher Scientific, India make, purity> 98%) as alumina source and magnesium nitrate hexahydrate (Fisher Scientific, India make) as magnesia source. Alumina and magnesia precursors in stoichiometric spinel ratio (Al:Mg / 2:1) is dissolved in deionized water to get a clear solution and then liquor ammonia (Fisher Scientific, India make, 25 %, sp. gr. 0.91) in stoichiometry to alumina and magnesia source is slowly added to it with constant vigorous stirring to avoid any precipitate formation. Ammonia addition increases the viscosity and pH of the system. The whole system is stirred until a clear colloidal suspension of spinel precursor is formed with few drops of dilute nitric acid added to stabilize the colloidal system.

4.5 Characterization of synthesized sols

The synthesized sols are characterized for their various properties. The pH of the sol is measured with the help of a digital pH meter (μC pH system 361, Systronics, India) and solid content is determined by a loss on ignition (LOI) method on firing the sol in an alumina crucible at 1000^{o}C for 2 h. The particle size and its distribution in the developed sol are measured in dilute condition with the help of a particle size analyzer (Zetasizer zetameter, ZEN 3690, Malvern instruments, US make).

To identify the nature of bonding present in sol particles, Fourier transform infrared (FTIR) spectra of the powdered gel obtained from drying the sol are taken by a FTIR spectrometer (Perkin Elmer, USA). For the measurement of FTIR spectra, very thin pellets are prepared by mixing about 2 mg of the dried gel powder with 20 mg of IR grade potassium bromide, KBr salt and pressing the mixture at a pressure of 3 ton for 1 min. The wave number range used for absorption spectra measurement is 4000 cm-1 to 500 cm^{-1}.

The thermo-gravimetric (DSC-TG) analysis of the gel, obtained from drying the sol, is done in a simultaneous DSC-TG system (STA449C/4/MFC/G, Netzsch, Germany). This technique is an excellent approach for analyzing any decomposition, phase transformation or crystallization behavior in the material during heat treatment. For measurement, about 50 mg of the powdered gel obtained by drying the sol at 60^{o}C is taken and the measurements are recorded from room temperature to 1200^{o}C with a heating rate of 10^{o}C/min.

Phase identification of the powders obtained from drying the sol, calcined at different temperatures (200^0 to 1200^0C), is done by X-ray diffraction technique performed in an X-ray diffractometer (Multipurpose X-ray Diffraction System, Ultima-IV, Rigaku, Japan) using Cu Kα radiation (λ= 1.542 nm) at 35 kV and 10mA. All the samples are scanned from 10^0 to 70^0 (2θ mode, where θ is the Braggs angle) in a continuous mode at a scanning speed of 2^o/min. The peak positions and the relative intensities of the XRD patterns of the powders are compared with standard references (JCPDS files) for phase identification in the calcined powders.

Microstructural studies of the calcined powders obtained from drying the sol are investigated in a field emission scanning electron microscope (FESEM, model Nova Nano, FEI, USA, make) with EDX (energy dispersive x-ray) analysis attachment (Bruker, US make), after gold coating through a sputter coater.

4.6 Preparation of High Alumina Castable with different sol binders

For the preparation of castables, white tabular alumina (WTA) grains (Almatis, India) and white fused alumina (WFA) grains (Chinese source) of different sizes are used as aggregates and sintered alumina (Almatis, India) as fines. Two different batch compositions comprising different alumina grains and fines for the castables is formulated using Dinger & Funk model with distribution coefficient (q) values 0.23 and 0.29 and the details are given in Table 4.5. Since packing models are based on the volume of particles, so if two or more components with different specific gravity values are present, their amount should be converted to their volume percentages. In the present study, alumina is only used as aggregate materials and fines (all components are different types of alumina), hence there is no change in specific gravity of the components used. So the volume percent (or fraction) is exactly similar to that of weight percent (fraction). The CPFT values obtained from the packing model are directly used as their weight percent. The details of the physicochemical properties of the raw materials used in the preparation of the batches are provided in Table 4.6. The variation of the CPFT (cumulative percent finer than) against particle sizes for distribution coefficients 0.23 and 0.29, used in the present study is provided in figure 4.6.

Fixed amount (5 and 7/8 vol/wt%) of sol was added in two different batch compositions (distribution coefficient (q) values 0.23 and 0.29) during the processing of castables making total four batches for a single sol. Further, some amount of water was added to the mix, if required, to attain desired flow and consistency. Care has been taken to ensure that castable slurries prepared by using different sol systems should have similar flow consistency (flow value 180-200 mm). The alumina and boehmite sols are used at 8% (vol/wt) where as mullite and spinel at 7% (vol/wt). The mullite and spinel sols at 8% level are excess in amount and cause segregation. So to maintain a similar slurry rheology in different batches, mullite and spinel sols are added at 7% level.

Table 4.5: Batch composition for developed sol bonded castables on basis of q value

Components	**Size** (in mm)	**[q=0.23] Wt.%**	**[q=0.29] Wt.%**
White Tabular Alumina	3 - 2	11.07	12.70
White Tabular Alumina	2 - 1	16.69	18.56
White Fused Alumina	1 - 0.5	14.23	15.18
White Tabular Alumina	0.5 - 0.3	09.13	09.39
White Tabular Alumina	0.3 - 0.1	16.34	16.04
Alumina Fines	D_{50} = 0.0025	32.52	28.10

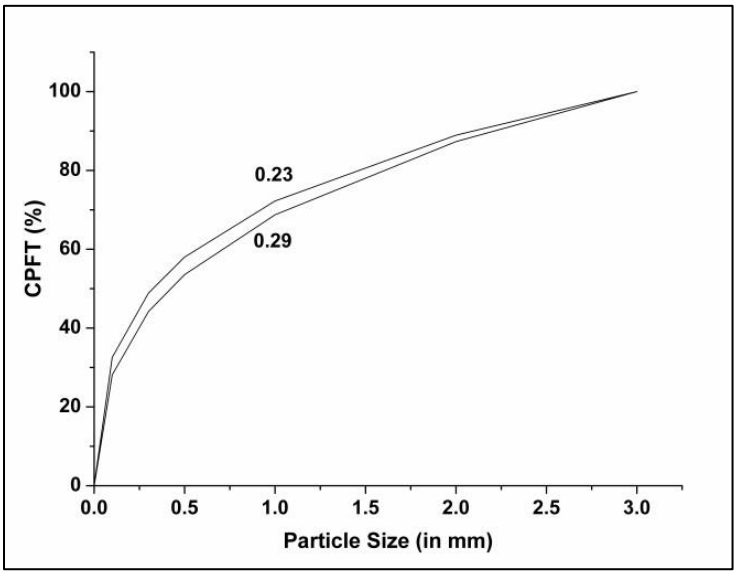

Figure 4.6: CPFT values against particle size as per Dinger and Funk model (q= 0.23 and 0.29)

Table 4.6: Physio-chemical properties of alumina grains and fines

Constituent	WTA Grain (%)	WFA Grain (%)	Alumina fines (%)
Al_2O_3	99.34	98.93	99.5
SiO_2	0.03	0.1	0.03
Fe_2O_3	0.035	0.06	0.03
TiO_2	-	Trace	Trace
CaO	-	0.1	0.02
MgO	-	-	0.01
$Na_2O + K_2O$	0.15	0.4	0.1
Particle size, µ	-	-	D_{50}=2.5
Bulk density	3.61 g/cc	3.77 g/cc	-
Apparent porosity	3.93%	1.8%	-
Sp. surface area (m^2/gm)	-	-	3.0
Phase analysis	Corundum	Corundum	Corundum

First, all the raw materials are dry mixed in a Hobart mixer (model N 50, Hobart make, OH, US). Initially, the coarser components are added and mixed and then the finer components have been added. Developed sol is added finally and the whole content is mixed thoroughly for 5-6 min. Water is added to the batch during mixing after sol addition depending on the flow consistency of the mix. The amount of water required varies with the sol and its content and addition of water is done to attain similar flow consistency for all the compositions with different sols.

On obtaining the proper flow consistency, the mixing is stopped and the mix is cast in lubricated iron molds of 50 mm cube size by simple tapping / vibration technique. These cube shapes are used for density, strength (CCS), thermal shock resistance (TSR) and corrosion resistance

measurement. For hot strength (HMOR) measurement, casing is done in a mold of size 150x25x25 mm^3. The cast specimens are allowed to be cured within the mold for one day. It is then, demolded, air dried for one day and then, again oven dried (Acmas Technocracy make, India) at 110°C for 24hrs. The dried specimens are fired at 1000^0 and 1650°C with a soaking period of 2 hours at the peak temperatures. The heating rate is kept 2^0C/min from room temperature to 400°C; 3°C/min from 400 to 1200°C; 2°C/min from 1200° to 1500°C and 1°C/min from 1500 to 1650°C. A 10 min of soaking is given at each stage, with a final soaking of 2 hour at the peak temperature. All the firings are conducted in a 1700°C programmable electric furnace (Bysakh & Co**,** India). The flow chart for castable making process is given in Figure 4.7.

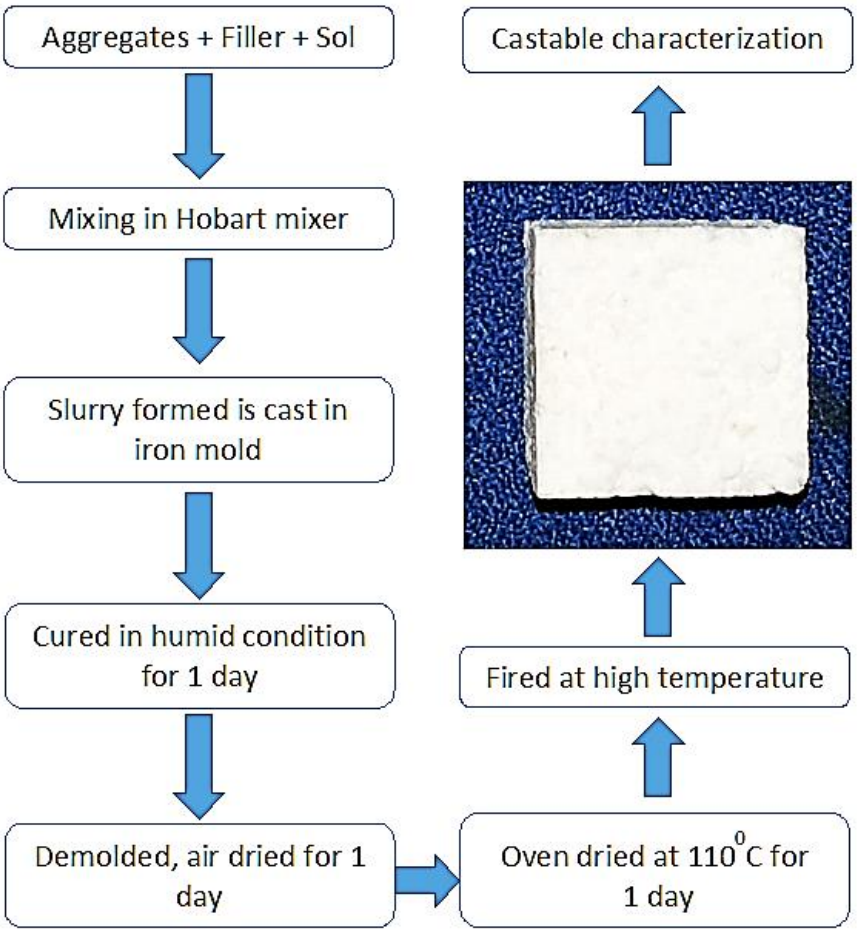

Figure 4.7: Flow chart for developed sol bonded castable making process

Both tabular alumina and fused alumina grains are used in the study to get optimized and improved properties like strength and spalling resistance from the tabular alumina grains and corrosion resistance from fused grains. Figure 4.5 shows that castable with q value 0.23 contains a higher amount of fines and so to obtain similar flow consistency (or slurry rheology) higher amount of liquid is required, that is the free water used for q=0.23 compositions, especially for 5% sol containing composition. Higher extent of fines results in the higher surface area and thus, a higher amount of liquid requirement for wetting the surface to attain proper flow consistency.

The castable samples are fired for property evaluation at a temperature of 1650^0C, much higher than any conventional castable and found that no shrinkage or deformation or any liquid phase formation occurs in the composition. This is due to higher purity and absence of any low melting phases in the system and indicates that theses sol bonded compositions are well suitable for applications at and above 1650^0C. Photographs of different fired shapes of the castables are shown in figure 4.8.

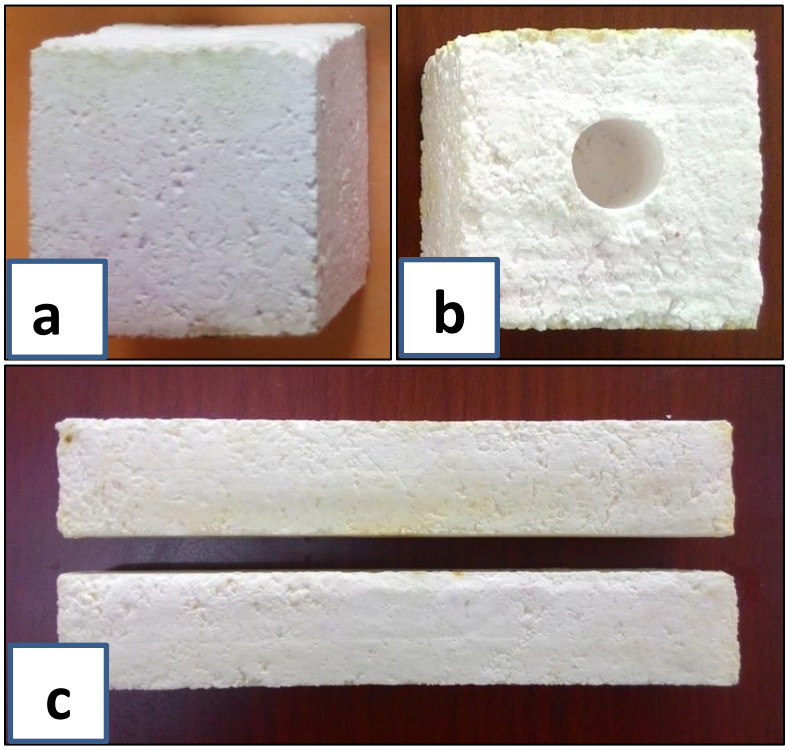

Figure 4.8: Developed castables for (a) CCS & TSR, (b) corrosion testing and (c) HMOR measurement.

4.7 Characterization of High Alumina Castable with different sol binders

Dried and fired (1000 and 1650^{o}C) castable samples are characterized by their bulk density (BD) with Archimedes immersion technique. The cold crushing strength (CCS) of the dried and fired castables is measured in a compressive testing machine (Aimil, India, make). The thermal shock resistance (spalling test) of the samples, prefired at 1650°C, is done as the retained strength after thermal shock of different thermal cycles. Each cycle is consisting of heating the samples at 1200°C for 10 min followed by quenching them in water (at room temperature) for 10 min. The residual strength (as CCS) of the samples are measured after 2, 4, 6 and 8 thermal cycles and compared with the actual strength (CCS) values of the samples.

Hot modulus of rupture (HMOR) tests is also conducted for the developed castables. Cast bar samples (150x25x25 mm^{3}) are fired at 1650^{o}C for 2 h and then used for the measurement of the hot strength after cleaning the surface. The hot modulus of rupture is evaluated in a HMoR Tester (Bysakh & Co., Kolkata, India) with alumina supporting and mullite loading rods. The bar samples are heated to 1400^{0}C at the rate of 5^{0}C/min and after 30 min of soaking at peak temperature, HMoR test is conducted on the bar samples with a loading rate of about 1.3 kg/sec.

Phase analysis of the matrix part (grains are avoided to reduce the interference of the major corundum grain phase and identify any trace phase formed) of the castables fired at 1650^{o}C is done to identify the phases developed on firing in the castable matrix. Microstructural study of the fractured surface of 1650^{o}C fired castables with gold coating is done to understand the microstructural development in the castables on firing.

For slag corrosion test, samples with a cylindrical hole (25 mm height and 15 mm diameter) are made in the middle of the cubes (50 mm) of different compositions at green stage and the holed samples are fired to 1650°C for 2 h followed by furnace cooling. The voids of the fired samples are then filled up with 3 gram of finely grounded blast furnace (BF) slag. The cubes with slag are then fired at 1500°C for 2 h and then cooled within the furnace. After normal cooling, the samples are cut along the vertical axis and the extent of slag penetration is noted. Small portion from slag corroded and non-corroded areas are further cut and taken out for the microstructural and EDX analysis. Each data represented here are an average of five individual measurements.

4.8 High Alumina Castable with traditional Cement and Silica sol for comparative study

The developed sol bonded high alumina castable compositions are parallelly compared with the conventional castable compositions with cement and silica sol bonding having similar PSD and purity, processed under similar conditions. High alumina castable with cement and silica sol bonding is prepared by using similar alumina sources as used in developed sol bonded castable compositions earlier. For cement containing castables, high alumina cement (CA-14), fume silica, ammonium polymethacrylate as deflocculant and citric acid (99.5% purity, Loba Chemie, India) as an anti-setting agent are used. For silica sol bonded castable, commercially available silica sol is used. The details of the Physico-chemical properties of the fume silica, high alumina cement, and silica sol are provided in Table 4.7.

Table 4.7: Physico-chemical properties of fume silica, cement, and silica sol.

Constituent	**Fume silica**	**HAC (CA-14)**	**Silica sol**
SiO_2 %	96.1	0.3	31.5
Al_2O_3 %	0.4	71	
Fe_2O_3 %	0.1	0.20	
CaO %	0.2	28	
MgO %	0.1	0.4	
$Na_2O + K_2O$ %	0.4	0.3	
LoI %	0.9	0.35	68.5
Sp. surface area (m^2/gm)	20	0.4	
Phase analysis	Amorphous	CA_2, CA	Amorphous

Batch composition for the castables is formulated using Dinger & Funk model with distribution coefficient (q value) 0.23. Fixed amount of 5 wt% cement and 7 vol./wt% silica sol is used individually for each composition. Cement containing composition is also added with silica fume

4 wt% as flow modifier and required amount of water is added to the composition for desired flow properties of castable. Table 4.8 shows the details of the batch compositions for cement and silica sol bonded castable compositions.

Table 4.8: Batch composition for cement and silica sol bonded castables.

Components	**Size** (in mm)	**C/23 (wt %)**	**S/23 (wt %)**
WTA	3 - 2	11.07	11.07
WTA	2 - 1	16.71	16.71
WFA	1 - 0.5	14.24	14.24
WTA	0.5 - 0.3	09.13	09.13
WTA	0.3 - 0.1	16.35	16.35
Alumina fines	D_{50} = 0.0025	23.50	32.50
Cement (HAC)		5	
Fume silica		4	
Deflocculant		0.3%	
Anti-setting agent		0.1%	
Sol (vol. /Wt.)%			7%
Water (vol. /Wt.)%		5.66%	0%

The flow chart for castable making process is given in Figure 4.9. The castable making process is similar to one mentioned in previous section except the binders used and high temperature firing. The silica sol bonded and cement bonded compositions are fired to 1600^{o}C and not to 1650^{o}C as done for developed sol bonded compositions because of glassy phase formation and deformation in the shape of castables when fired to 1650^{o}C. The presence of CaO and SiO_2 in the cement and formation of SiO_2 from silica sol in the alumina castable system leads to formation of low

melting phases and eutectics at about and below 1600°C (figure 2.1). So for these castables, the highest temperature of firing is kept at 1600°C for evaluation of refractory properties. The castables are characterized by its bulk density, CCS, HMoR, TSR and corrosion resistance. The sample preparation for all these characterizations is similar to developed sol bonded compositions. Microstructural study of the fractured surface of 1600^0C fired castables with gold coating is done to understand the microstructural development in the castables on firing.

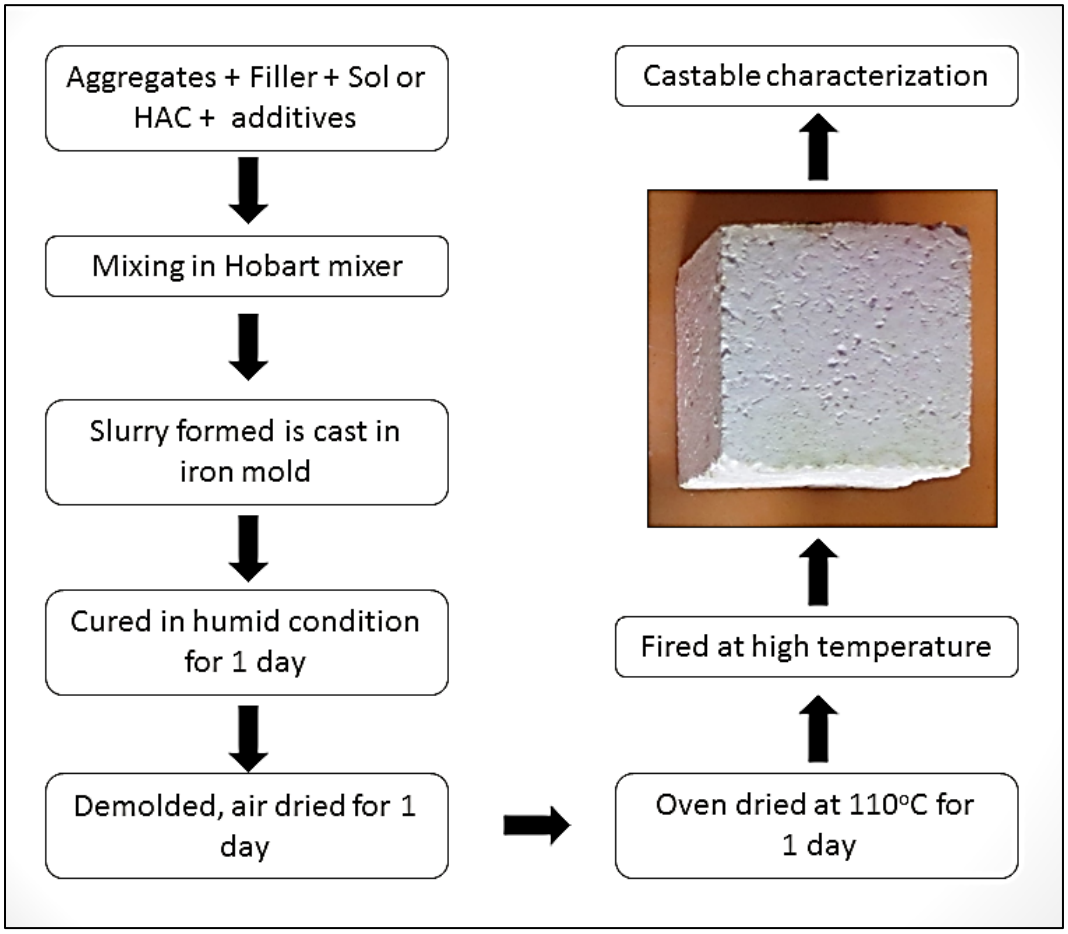

Figure 4.9: Castable making process for cement and silica sol bonded castable

4.9 List of equipment used to carry out the experiments.

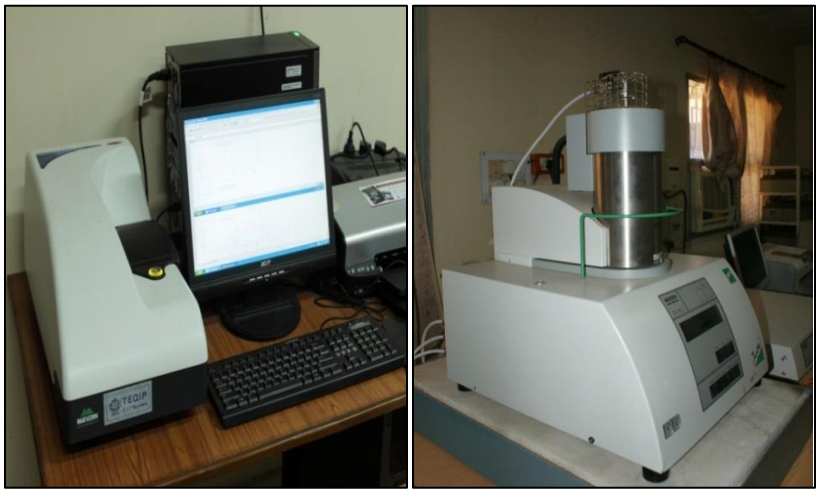

Figure 4.10: Particle size analyzer and DSC-TG system

Figure 4.11: FESEM and XRD analyzer.

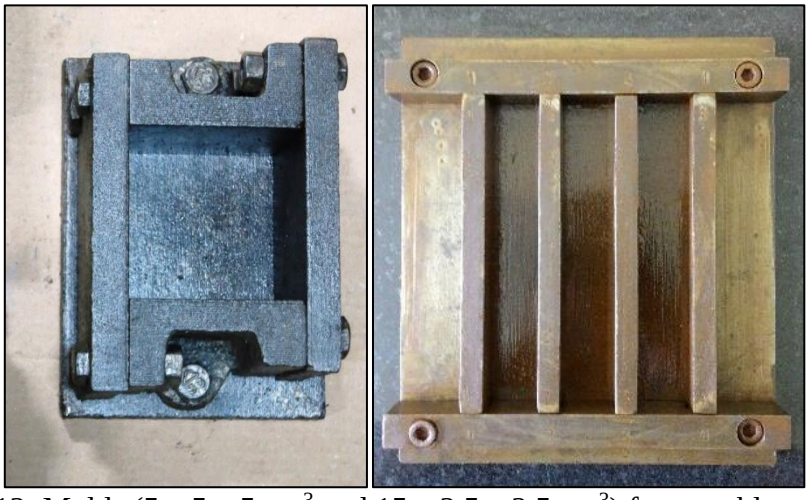

Figure 4.12: Molds (5 x 5 x 5 cm^3 and 15 x 2.5 x 2.5 cm^3) for castable processing.

Figure 4.13: Hobart mixer and Hot air oven.

Figure 4.14: Compressive testing machine and Raising Hearth furnace.

Figure 4.15: Chamber furnace and HMOR furnace

Chapter 5

Results and Discussion

This chapter deals with the results and discussion of various characterizations done on the developed sols and thereafter, the castables synthesized using these sols as a binder. The chapter is divided into 5 sections. The first section covers the various characterization results and discussion of developed alumina sol and castable prepared from this sol using it as binder; second section is about boehmite sol and castable bonded by it; the third section covers the result and discussion of mullite sol and castables prepared from it; the fourth section covers the spinel sol and castables bonded by it. The fifth and final section of this chapter deal with the comparative study of optimized batches of various developed sol bonded castables with castables bonded by commercial binders, like silica sol and high alumina cement. This section also discusses the thermal shock properties and corrosion behavior of various compositions against blast furnace slag and microstructural study of the corroded samples. Figure 5.1and 5.2 show the sol and castable sample with the characterization done for their property evaluation.

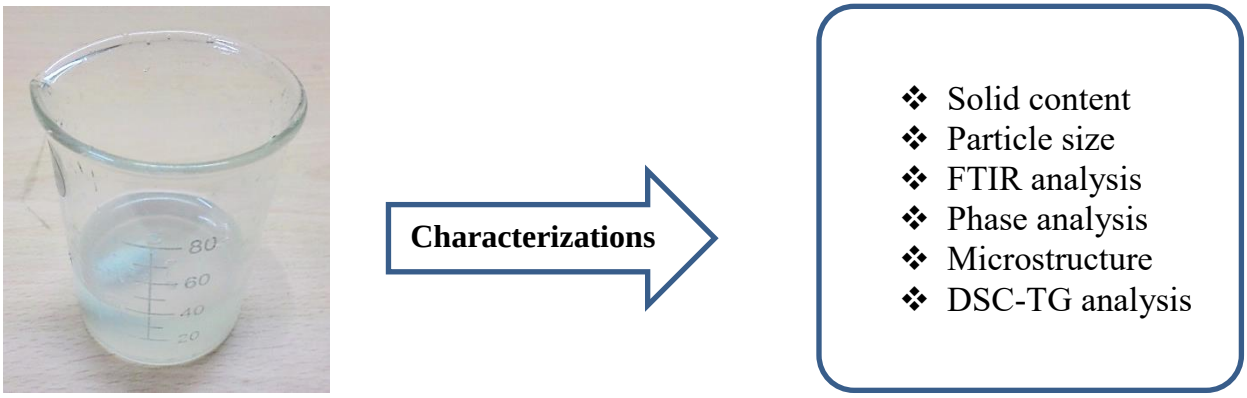

Figure 5.1: Developed sol and its various characterizations

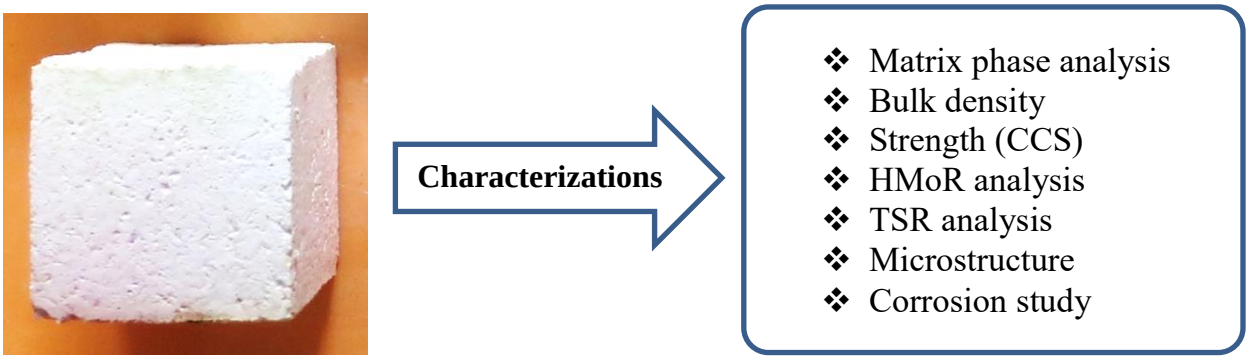

Figure 5.2: Developed sol bonded castable and its various characterizations

5.1 Alumina sol bonded high alumina castable composition:

This section covers the result and analysis of various characterizations done on synthesized alumina sol and high pure alumina castables prepared using this sol as binder. Alumina sol prepared from inorganic precursors is characterized for its solid content, particle size analysis, FTIR, phase formation on calcination, DSC-TG, etc. The sol is used as a sole binder at two different amounts in high-alumina refractory castables, with two different particle size distributions (PSDs), by varying distribution coefficients as per Dinger and Funk model. The castables are processed conventionally and characterized for various physical and mechanical properties after heat treatment at various temperatures.

5.1.1 Sol-gel characterization: The synthesized alumina sol shows stability more than a month at room temperature and gelling tendency when dried above 40^0C. Hence it undergoes gelation with time due to loss of water. The solid content of the synthesized Sol is found to be about 6 %.

5.1.1.1 P**article size analysis**: The particle size distribution (PSD) curve of the developed sol is given in figure 5.3. The PSD plot shows that all the particles are within the size range of 10-60 nm with a peak around 20 nm. The distribution for the Sol prepared from nitrate precursor also shows that major fractions of the particles are below 40 nm size

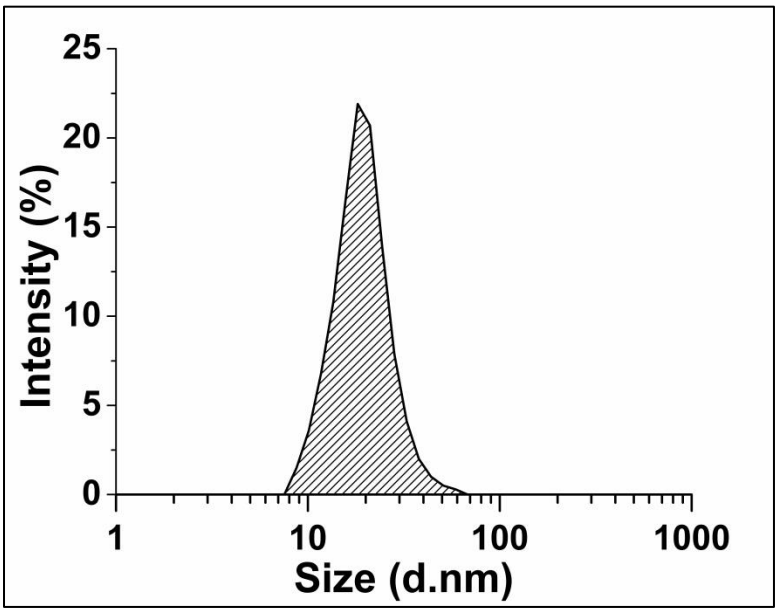

Figure 5.3: Particle size distribution in alumina sol.

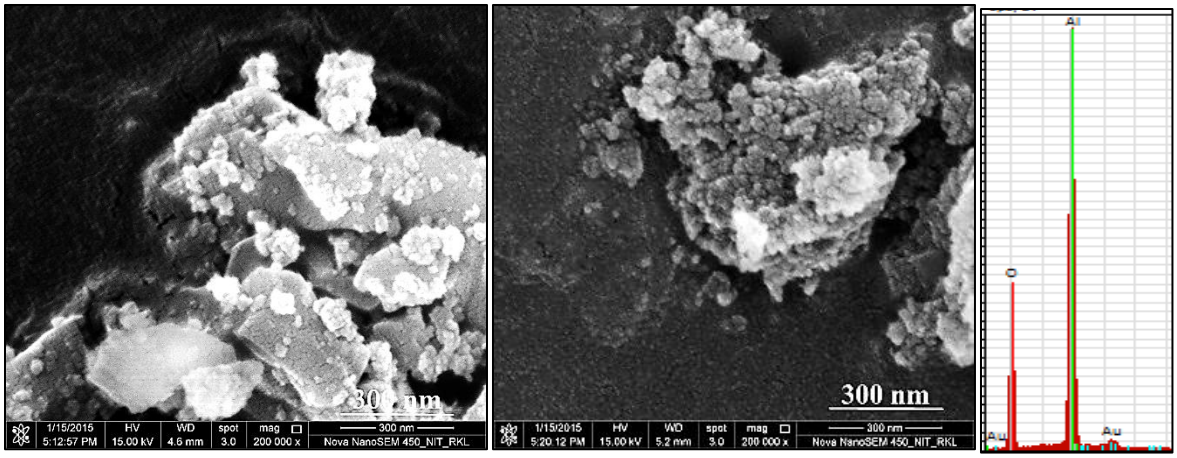

Figure 5.4: Microstructure of alumina sol powders heated at (a) 200^0C, (b) 1000^0C and (c) EDX frame analysis of 1000^0C calcined powder

5.1.1.2 Microstructural analysis: Microstructural photograph of the powder dried at 200 and calcined at 1000 C is given in figure 5.4. The microstructure of powders dried at 200^0C shows small lumps of particles highly agglomerated because of high reactivity due to its ultrafine nature. The agglomeration continues at 1000^0C. Both the microstructures confirm that particles formed after drying and calcination are having nano dimensions. Again the elemental analysis (EDX) of the particles formed after calcination at 1000C confirms the presence of only aluminum and oxygen ions (gold ions are found due to coating).

5.1.1.3 FTIR analysis: The FTIR spectrum of the dried sol powder is given in figure 5.5. The absorption bands in the ranges 500-1000 and 3200-3700 cm^{-1} in the spectrum are related to Al-O and O-H stretching vibrations respectively [5.1-5.7] The band positions at 524, 576, 607, 641,745 and 1070 cm^{-1} are related to the stretching mode of Al–O whereas the bands at 3267, 3464, 3479, 3540, 3610, 3688 cm^{-1} are related to characteristic stretching vibrations of O–H in sol [5.2-5.4] On basis of the above analysis, the FTIR spectrum indicates the presence of amorphous aluminum hydroxides in the powder obtained from sol. Meanwhile, the absorption bands present between 1500 and 1700 cm^{-1} are due to the bending moments of H_2O and the bands at 1382 and 1378 cm^{-1} are due to the characteristic stretching vibration of nitrates [5.1].

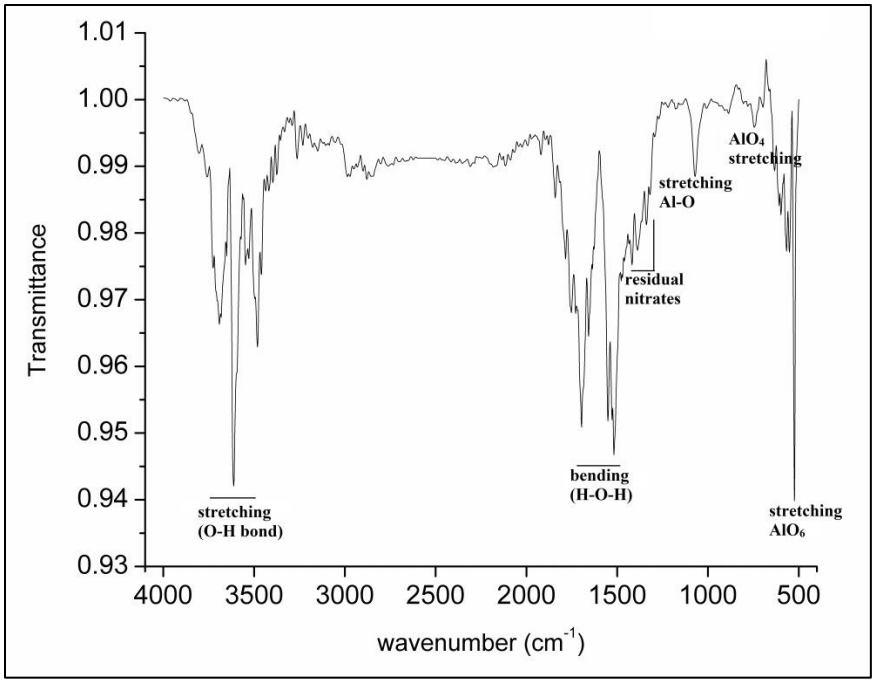

Figure 5.5: FTIR spectra of alumina sol precursor powder dried at 200^0 C

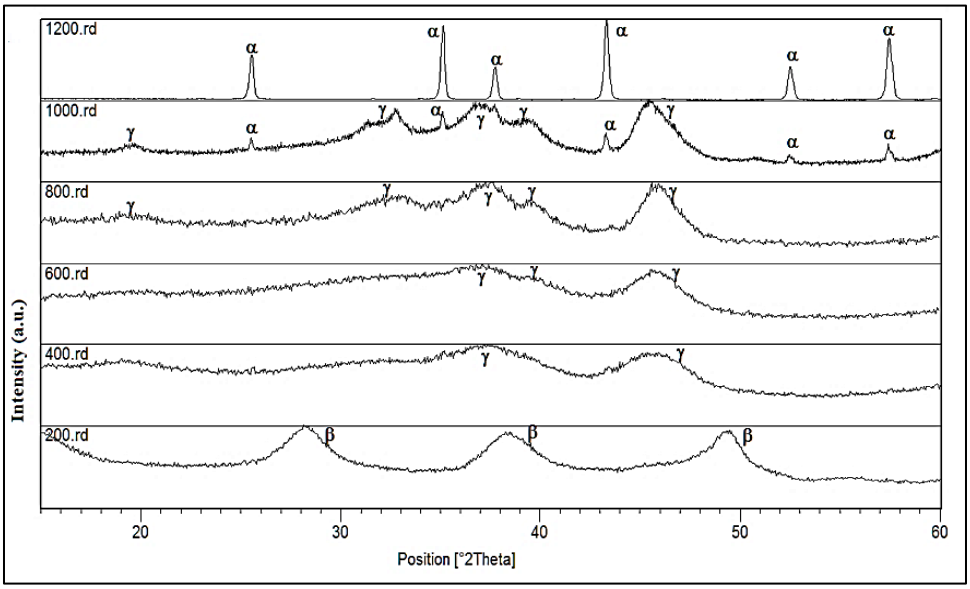

Figure 5.6: Phase analysis of the alumina sol calcined at different temperatures (α= α−alumina, γ= γ−alumina and β=boehmite).

5.1.1.4 XRD analysis: Phase analysis of powders obtained from Alumina Sol by calcination at different temperatures (200^0C-1200^0C) is shown in figure 5.6. The pattern at 200^0C shows the presence of only boehmite phase. As the calcination temperature increases to 400^0C, boehmite converts to γ-alumina. The crystallinity of γ-alumina increases up to 800^0C. The powder calcined at 1000^0C shows α-alumina phase as the prominent one though some amount of γ-alumina phase also exist. Thus it can be said that conversion of γ-alumina to α-alumina has started below 1000^0C. At 1200^0C, only the α-alumina phase was obtained.

5.1.1.5 Thermo-gravimetric (DSC-TG) analysis: The DSC-TG pattern of the dried powder obtained from Sol is given in figure 5.7. The DSC pattern shows endothermic peaks around 120^0C and 280^0C and at 600^0C which are associated with the removal of physically absorbed water, bonded OH group and conversion of boehmite to γ-alumina phase respectively. Also, a small exothermic peak at 300^oC is observed possibly due to decomposition of NH_4NO_3 which may have strongly adhered to the sol particles and might not have removed during washing [5.8]. The TG plot also shows a sharp decrease in weight on increasing temperature till about 550^0 C and beyond 600^0C there is nearly no loss. This indicates that physical and chemical bonded water are completely removed before 600^0C [5.8].

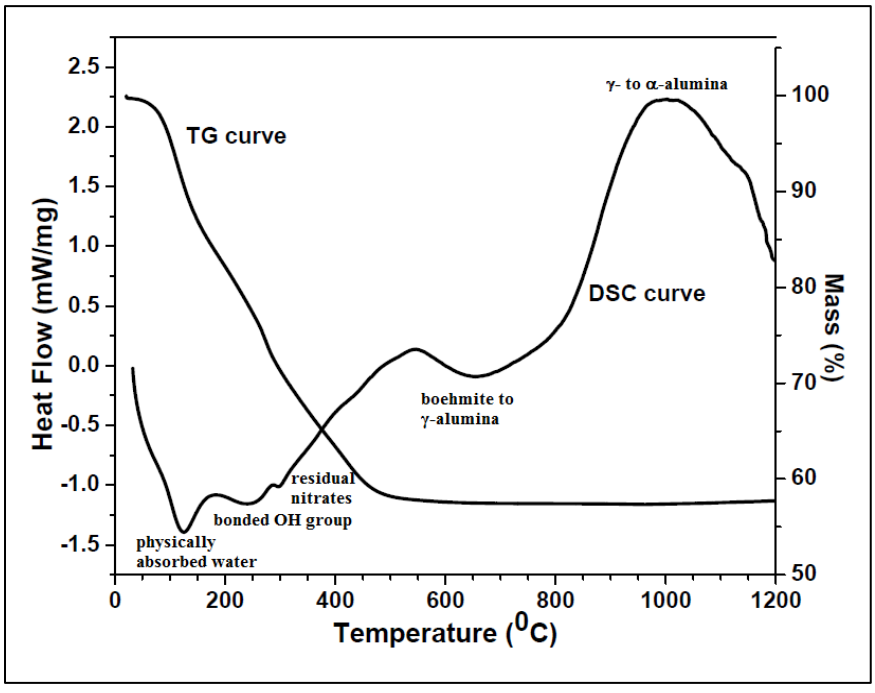

Figure 5.7: DSC-TG analysis of dried powder obtained from alumina sol

5.1.2 Castable characterization: The materials used for making high alumina castables are highly pure and alumina sol binder and the matrix phase are chemically similar. As a result, a highly pure castable system of alumina only is formed which can withstand very high temperature and would be highly corrosion resistant. This alumina sol bonded castable compositions are suitable for high temperature applications, at and above 1650^{o}C, due to the absence of any low melting phase present and formation in the system. Details of nomenclature of the batches with q values, amounts of sol used water required during processing are given in Table 5.1.

Table 5.1. Batch name and amount of alumina sol used in different batch composition

Batch name	**A/23/5**	**A/23/8**	**A/29/5**	**A/29/8**
q value	0.23	0.23	0.29	0.29
Sol [vol. /Wt.]%	5	8	5	8
Water [vol. /Wt.]%	2.66	0.66	2.5	0.5

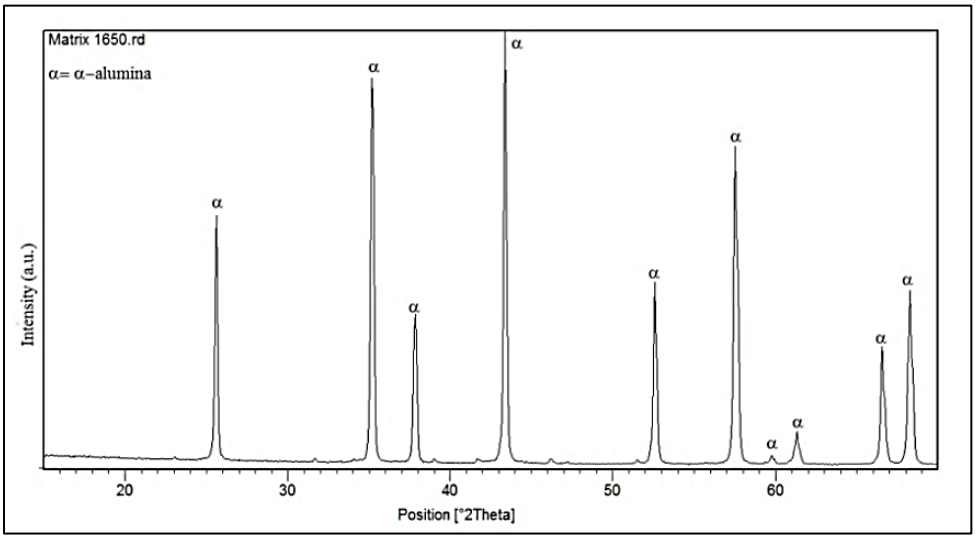

Figure 5.8: Phase analysis of the castable matrix of A/23/5 composition.

5.1.2.1 Phase analysis of the matrix: Properties of the sintered castables are dependent on the impurity phases, if any, present in the castable matrix. To understand the presence of any impurity phase in the matrix, phase analysis study of the matrix part of the sintered castables was

done by powder x-ray diffraction (XRD) technique. No phase other than corundum is observed in the 1650^{o}C sintered castable compositions, indicating high purity nature of the compositions. XRD pattern of the matrix part of the sintered A/23/5 composition is shown in figure 5.8 as a representative one.

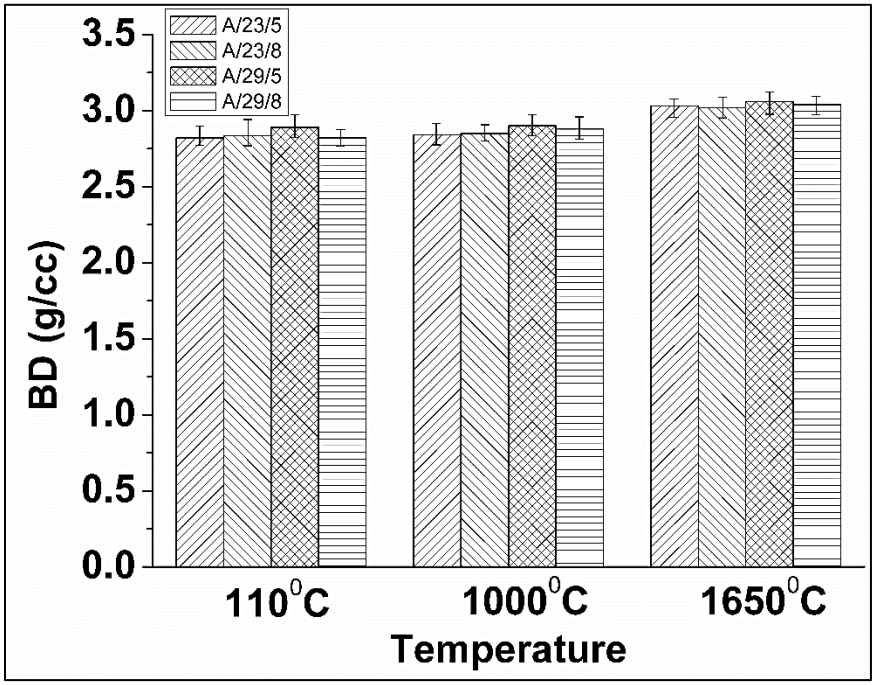

Figure 5.9: Bulk density of alumina sol bonded castable against temperature.

5.1.2.2 Bulk density (BD) study: Figure 5.9 shows the variation of density of different alumina sol bonded castable compositions at the temperature of 110, 1000 and 1650^{0}C. At higher temperature, the density obtained by castables is governed by two factors- porosity due to the removal of physically and chemically bonded water and densification due to sintering of castable components. The density values for all the castables at peak temperature lie in the range of 3.00 to 3.10 g/cc. Castables with 8% Sol has lower density values than castables containing 5% Sol. This can be attributed to the fact that solid content of sol is very less about 6 % and thus net water content is more for 8% sol bonded castables (Table 5.1). Thus higher porosity lowers the density of 8% Sol bonded castables in comparison to 5% Sol bonded castables. For all the castables, composition with q value 0.29 have higher density values due to more amount of coarser components in comparison to compositions with q value 0.23.

5.1.2.3 Cold Crushing Strength (CCS) Study: The figure 5.10 shows variation of cold compressive strength (CCS) values of developed alumina Sol bonded castable compositions against their processing temperatures. All the compositions are having very low green / dried strength, as also reported in the literature [5.8]. This may be due to the formation of weak coagulation bonding in the sol system. But after firing at the higher temperature of 1650^0C, the CCS value increases significantly. This shows that the binding strength provided by sol at the green stage is very low. Upon firing at high temperature, sol-gel bonding is replaced by ceramic bonding due to sintering of fine alumina particles formed from sol material in the matrix.

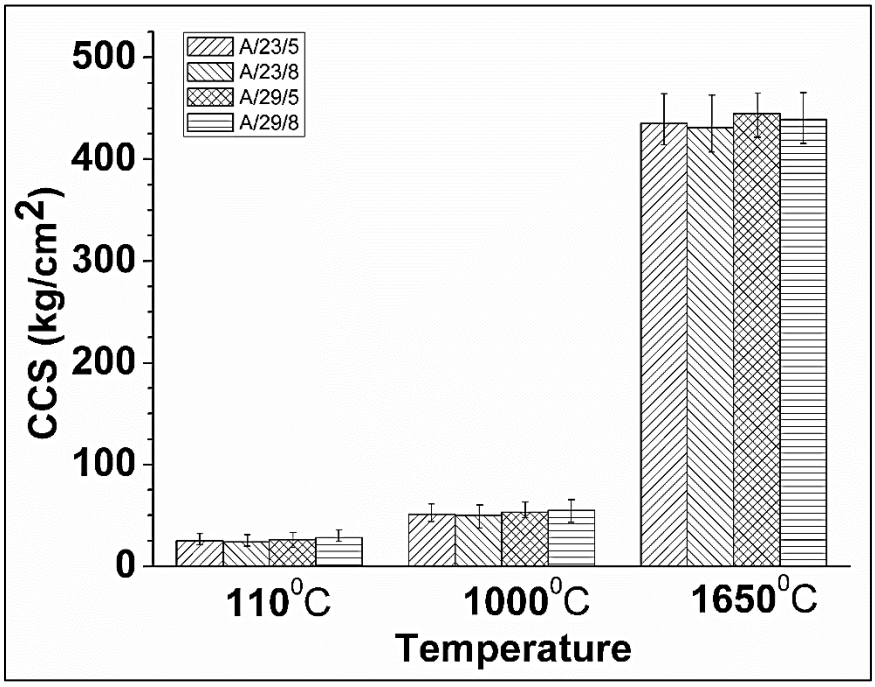

Figure 5.10: CCS of alumina sol bonded castable against temperature.

The strength of castables mainly depends on sintering between the matrix components and porosity obtained at elevated temperatures. The strength values of castables obtained are in accordance with the density values. The presence of finer particles enhances the sintering between the sol particles and the refractory aggregates. Greater sintering increases the densification which is shown in the density values also. Sintering at 1650^oC shows no deformation and liquid phase formation in the composition, which indicates that these compositions are well suitable for application at and above such temperature due to the absence of any other material in the system.

5.1.2.4 HMoR analysis: The HMoR analysis of the alumina sol bonded compositions is given in figure 5.11 below. The hot flexural strength of all the compositions is well above 100 kg/cm^2 indicating these compositions have better resistance to high temperature loading. Not much variation in hot strength values was observed among the batches with varying distribution coefficient and sol content. The high hot strength values further indicate a well compact structure within the castable without any liquid phase formation in the matrix phase, as there was no impurity in the system. High pure alumina sol as a binder in a high pure alumina matrix results in a solid state bonding and produces high hot strength properties.

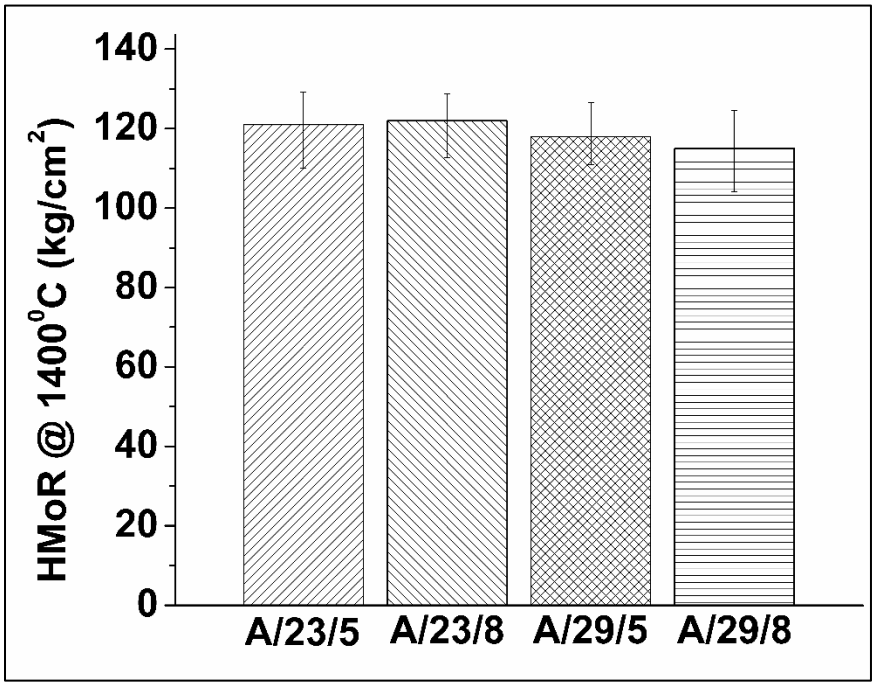

Figure 5.11: HMOR values of the alumina sol containing castables.

5.1.2.5 Microstructural analysis: The microstructure of the 1650^{o}C sintered A/23/5 batch shows (Fig 5.12) a well compact structure with nonuniform angular grains, indicating higher compaction and densification in the batch. A/23/5 batch was selected for microstructural study as a representative one. The presence of finer alumina particles might have helped in better densification. Also, the castables were prepared from only pure alumina sources and presence of no impurity phase resulted in no liquid phase as can be observed from the microstructure. In the matrix part, nonuniform grains are observed with a little amount of porosity. Also, very fine tiny particles are found in the matrix phase, which might have formed from the alumina sol. The

highly pure chemistry of the composition is also confirmed by the EDX analysis which shows the presence of only Al and O indicating that composition is only composed of alumina.

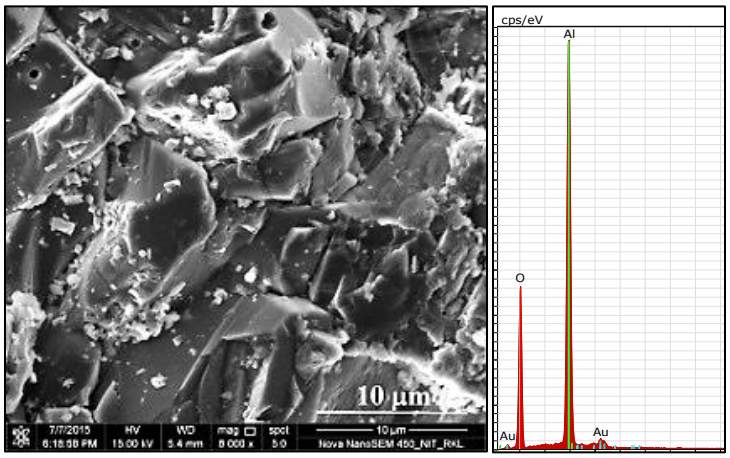

Figure 5.12. SEM photomicrograph of A/23/5 composition and EDX analysis.

5.1.3 Summary of the section:

Alumina sol prepared through Nitrate route have a solid content of ~6% and particle size is in the range of 10-60 nm with the major fraction of particles below 40 nm size. The FTIR study on the dried gel powder obtained from the sol confirms the presence of hydroxides in the dried gel powder. Phase analysis and DSC-TG of the sample shows the formation of α-alumina from the synthesized sol. The synthesized sol is solely used as the binder in no cement high alumina castables. No deformation in the castables was observed and well sintered density and strengths were obtained at 1650^{o}C. The hot flexural strength of all the compositions is well above 100 kg/cm2 indicating these compositions have better resistance to high temperature loading. The castables show higher refractoriness as there is no deformation found in castables even when fired up to 1650^{0} C. As the castable composition does not contain any low melting phases so these can be used for temperatures much greater than their conventional counterparts.

5.2 Boehmite sol bonded high alumina castable composition:

This section covers the result and analysis of various characterizations done on boehmite sol synthesized from commercially available boehmite powder and high pure alumina castables prepared using this sol as binder. Developed boehmite sol is characterized by its solid content, particle size analysis, FTIR, phase formation on calcination, DSC-TG, etc. The sol is used as a sole binder in high-alumina refractory castables, with different particle size distributions (PSDs), by varying distribution coefficients as per Dinger and Funk model. The castables are processed conventionally and characterized for various physical and mechanical properties after heat treatment at various temperatures. Reasonable strength is obtained for the sintered castables, and no impurity phase is found in the matrix phase of the castables.

5.2.1 Sol-gel characterization: The synthesized boehmite sol shows stability more than a month at room temperature and gelling tendency when dried above 40^0C. Hence it undergoes gelation with time due to loss of water. The solid content of the synthesized boehmite Sol is found to be about 17 % respectively.

5.2.1.1 Particle size analysis: The particle size distribution (PSD) curve of the boehmite sol prepared from commercially available boehmite powder is given in figure 5.13. The PSD plot shows that all the particles are within the size range of 20-400 nm with a peak around 50 nm. The distribution curve also shows that major fractions of particles are having size below 100 nm.

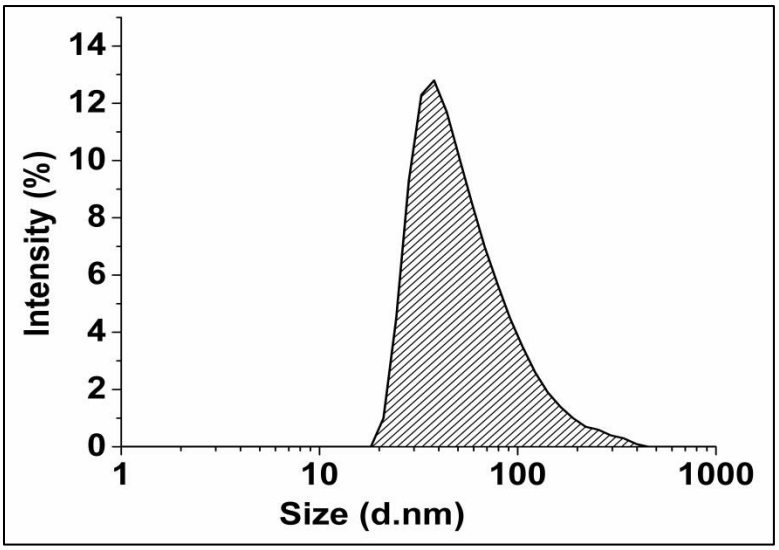

Figure 5.13: Particle size distribution in Boehmite sol.

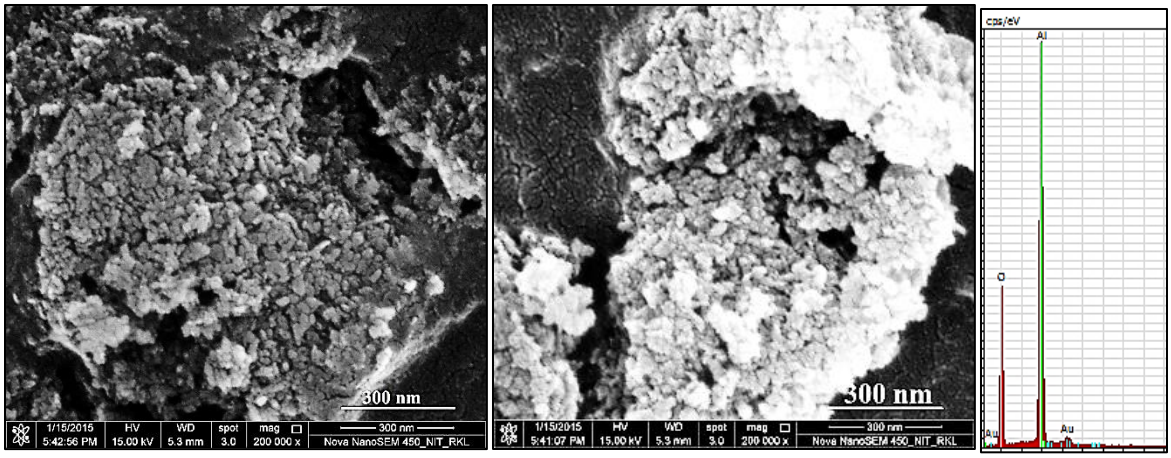

Figure 5.14: Microstructure of boehmite sol powders heated at (a) 200^0C, (b) 1000^0C and (c) EDX frame analysis of 1000^0C calcined powder

5.2.1.2 Microstructural analysis: The figure 5.14 shows the microstructural photograph of the powder obtained from boehmite sol after drying at 200ºC and calcined at 1000ºC. The microstructure in figure (a) shows agglomerated particles. Both the microstructures reveal that particles formed after drying and calcination are having nano dimensions. Again the elemental analysis (EDX) of the particles formed after calcination at 1000ºC confirms the presence of only aluminum and oxygen ions (gold ions are found due to coating).

5.2.1.3 FTIR analysis: The FTIR spectrum of the dried sol powder is given in figure 5.15. The absorption bands in the ranges 500-1000 and 3200-3700 cm^{-1} in the spectrum are related to Al-O and O-H stretching vibrations respectively [5.1-5.7]. The band positions at 520, 546,597, 741 and 1070 cm^{-1} are related to the symmetric stretching vibration of the Al-O in boehmite sol whereas the bands at 2964, 3159, 3454, 3479, 3545,3619,3688 cm^{-1} are for stretching vibrations of O-H in sol [5.2-5.4]. On basis of the above analysis, the FTIR spectrum indicates the presence of amorphous aluminum hydroxides in powders obtained from sol. Meanwhile, the absorption bands present between 1500 and 1700 cm^{-1} are due to the bending moments of H_2O and the bands at 1382 and 1378 cm^{-1} are due to the characteristic stretching vibration of nitrates [5.1].

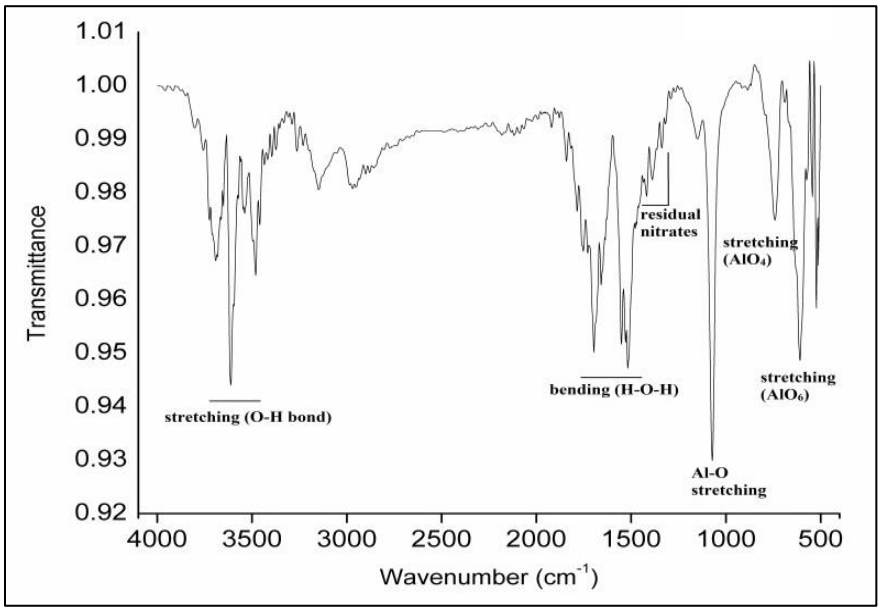

Figure 5.15: FTIR spectra of Boehmite sol precursor powder dried at 200^0 C

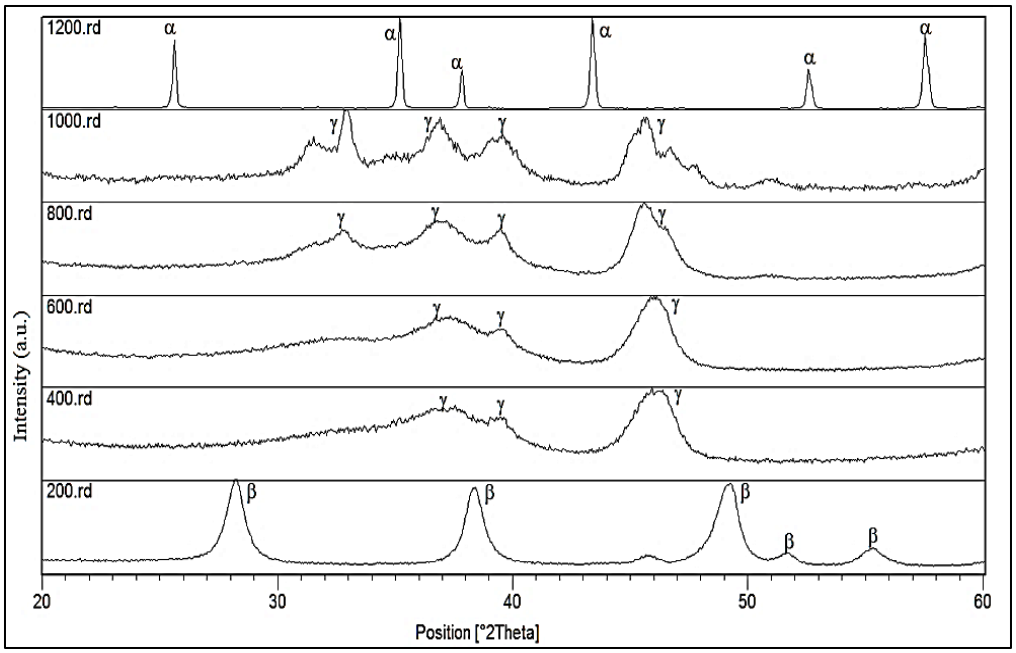

Figure 5.16: Phase analysis of boehmite sol calcined at different temperatures (α= α–alumina, γ= γ–alumina and β=boehmite).

5.2.1.4 XRD analysis: Phase analysis (figure 5.16) of calcined powders obtained from boehmite Sol by calcination at different temperatures (200^0C-1200^0C) has the similar pattern as obtained for calcined powders of alumina Sol. At 1000^0C, the pattern shows only the presence of γ-alumina. This is in contrast to the pattern obtained for calcined powder of alumina sol where the α-alumina phase is the prominent one. This can be attributed to the presence of more finer colloidal particles in alumina sol prepared from nitrate precursors as compared to boehmite Sol prepared from commercially available boehmite powder. The presence of finer particles results in phase transformation at a lower temperature. The pattern at 1200^0C shows only the α-alumina phase [5.9].

5.2.1.5 Thermo-gravimetric (DSC-TG) analysis: DSC-TG curve of dried powder obtained from boehmite Sol is given in figure 5.17. The pattern shows an endothermic peak around 100^0C due to the removal of physically absorbed water. From 400°C to 600°C, a weight loss occurs due to the conversion of boehmite into γ-alumina which corresponds to an endothermic reaction. From 1000°C to 1200°C, an exothermic reaction occurs due to the transformation of γ -alumina to α-alumina. [5.10-5.12]

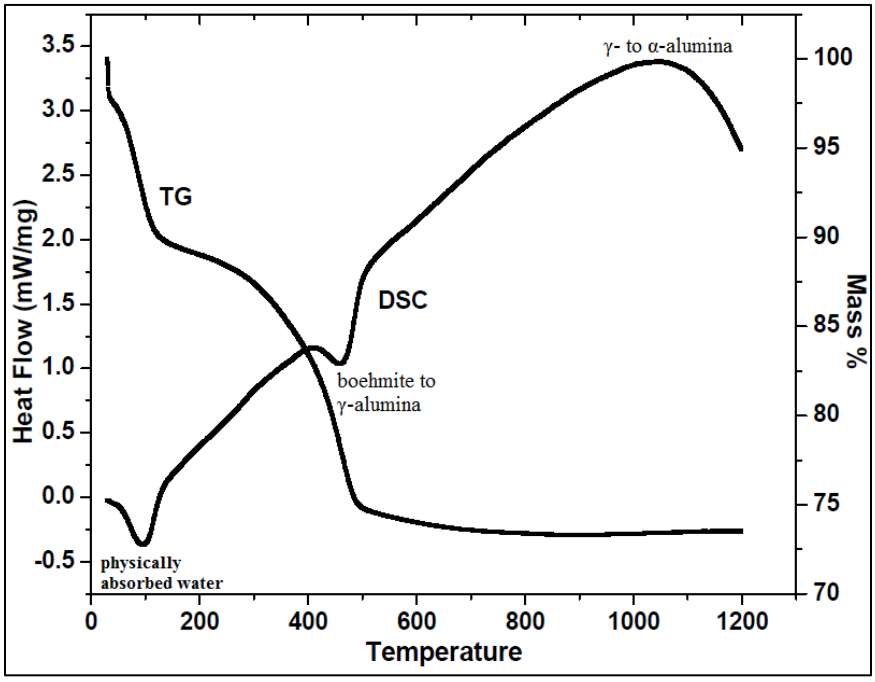

Figure 5.17: DSC-TG analysis of dried powder obtained from boehmite sol

5.2.2 Castable characterization: The materials used for making high alumina castables are highly pure and boehmite sol binder and the matrix phase are chemically similar. As a result, a highly pure castable system of alumina only is formed which can withstand very high temperature and would be highly corrosion resistant. This boehmite sol bonded castable compositions are suitable for high temperature applications, at and above 1650ºC, due to the absence of any low melting phase present and formation in the system. Details of nomenclature of the batches with q values, amounts of sol used and water required during processing are given in Table 5.2.

Table 5.2. Batch Name and amount of boehmite sol used in different batch composition

Batch name	**B/23/5**	**B/23/8**	**B/29/5**	**B/29/8**
q value	0.23	0.23	0.29	0.29
Sol [vol. /Wt.]%	5	8	5	8
Water [vol. /Wt.]%	2.5	0.0	2.0	0

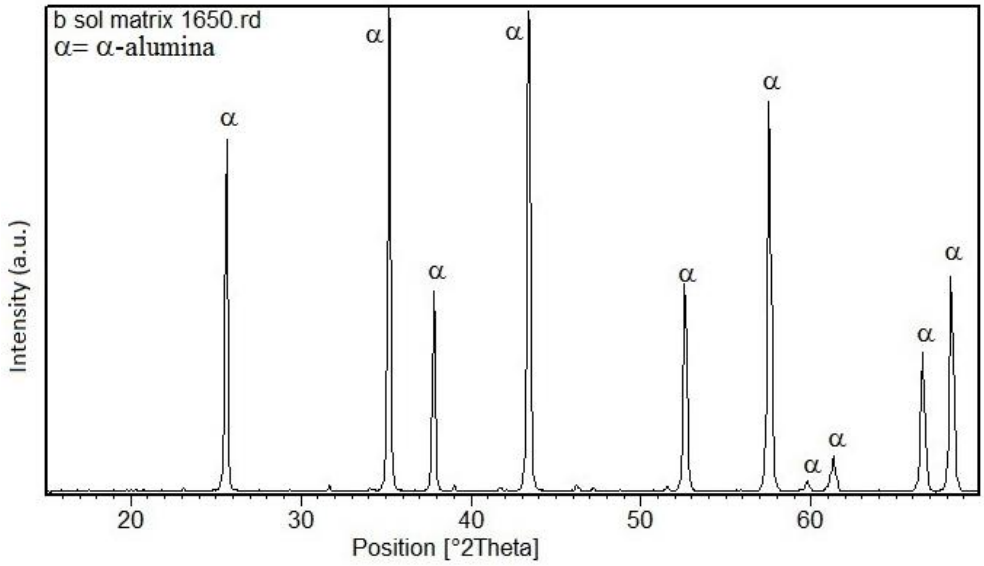

Figure 5.18: Phase analysis of the castable matrix of B/23/5 composition

5.2.2.1 Phase analysis of the matrix: Properties of the sintered castables are dependent on the impurity phases, if any, present in the castable matrix. To understand the presence of any impurity phase in the matrix, phase analysis study of the matrix part of the sintered castables was done by powder x-ray diffraction (XRD) technique. No phase other than corundum is observed in the 1650ºC sintered castable compositions, indicating high purity nature of the compositions. XRD pattern of the matrix part of the sintered B/23/5 composition is shown in figure 5.18 as a representative one.

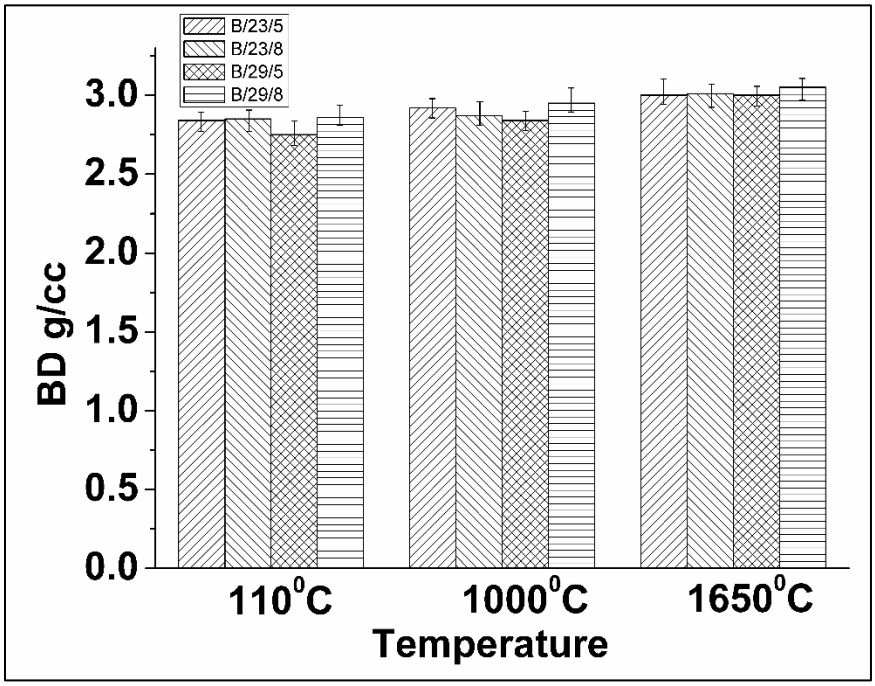

Figure 5.19. Bulk density of boehmite sol bonded castable against temperature.

5.2.2.2 Bulk density (**BD**) **study**: Figure 5.19 shows the variation of density with temperature for different Boehmite Sol bonded castable compositions. The density obtained by castables is governed by two factors: degree of bonding between different components and porosity formed due to the removal of volatile matter (here physically and chemically bonded water). Similar to developed alumina sol bonded composition, here also the density values for all the castables at peak temperature lie in the range of 3.00 to 3.10 g/cc which is considered a good value. The 8% sol bonded castables have higher density values for both the distribution coefficients which are opposite to that obtained for alumina sol bonded compositions. The net water content in 8% sol bonded castables is less in comparison to 5% sol bonded castables due to higher solid content in

boehmite Sol. Thus lower porosity and higher sintering in the 8% compositions resulted in higher bulk density. Similar to alumina compositions, here also the 0.29 batches have comparatively higher density values due to the presence of coarser particles.

5.2.2.3 Cold Crushing Strength (CCS) Study The figure 5.20 below shows the variation of cold compressive strength (CCS) values of developed boehmite Sol bonded castable compositions against their processing temperatures. All the developed compositions acquired very low green strength, similar to alumina sol bonded compositions. The weak coagulation bonding of the colloidal boehmite particles resulted in poor green strength. The strength increases significantly after firing at the peak temperature due to the replacement of weak coagulation bonding formed at the green stage by strong ceramic bonding formed at the higher temperature. The sintering of finer alumina particles formed from the sol and the finer alumina matrix resulted in densification and strength development in the castable at higher temperature

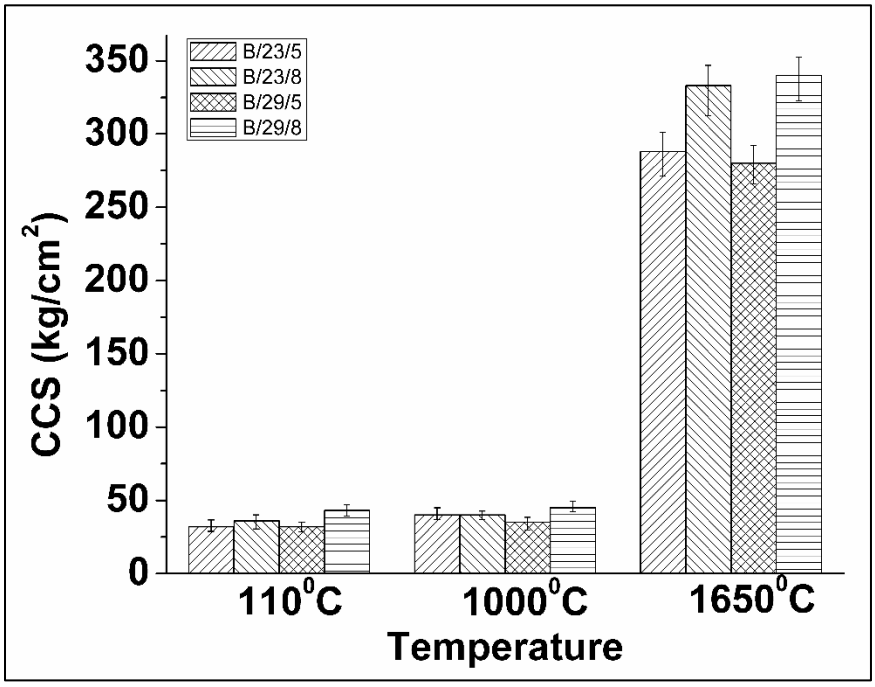

Figure 5.20. CCS of boehmite sol bonded castable against temperature.

Strength obtained by castables at higher temperatures is mainly dependent on the sintering between the finer matrix components and degree of porosity present in the castable. Finer components enhance the sintering which results in densification. This can be evident from the

strength values of 8% sol bonded composition of both distribution coefficients, which is greater than composition using 5% sol as binder. The strength values of castables compositions obtained are in accordance with their density values. Sintering of the compositions at the peak temperature of 1650^{o}C shows no sign of any deformation or liquid phase formation in the composition thus enables these compositions to be used at and above this temperature.

5.2.2.4 HMoR analysis: The flexural strength (modulus of rupture) values of the different boehmite sol bonded compositions at the temperature of 1400^{o}C are shown in the figure 5.21 below. Similar to the cold strength (CCS), the compositions with more amount of finer components showed better resistance to high temperature loading.

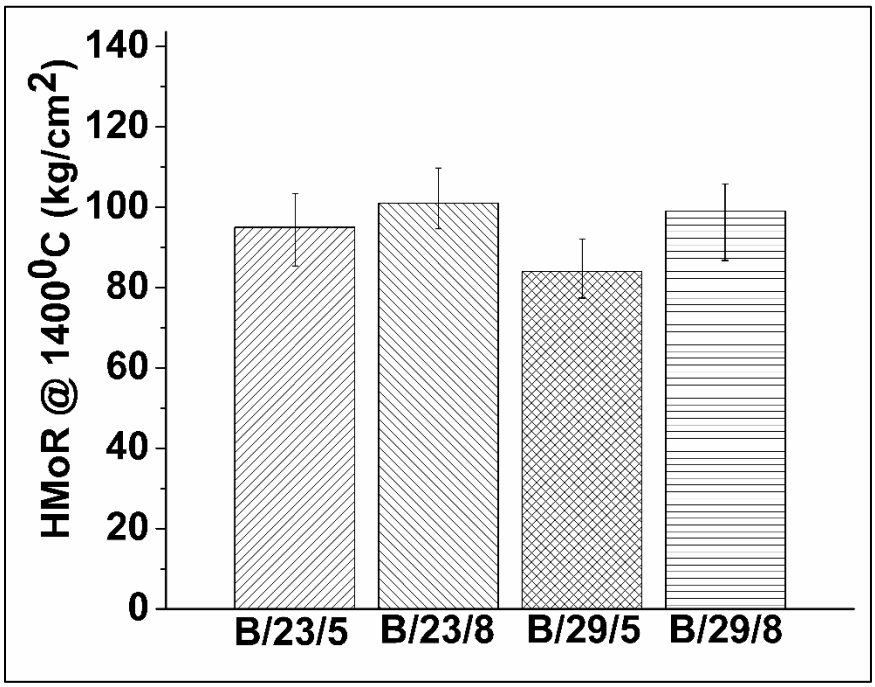

Figure 5.21. HMOR values of the boehmite sol containing castables.

5.2.2.5 Microstructural analysis: The microstructure of the B/23/5 batch sintered at 1650^{o}C is shown in figure 5.22. It shows a well compact microstructure of nonuniform angular grains, resulted from the compaction and densification of the matrix components. Batch B/23/5 was selected for microstructural study, as a representative one. The ultrafine alumina particles formed from the boehmite sol at higherr temperature increases the densification process by increasing the extent/degree of sintering in the matrix phase. Also, the castable composition possessess

highly pure chemistry composed of only alumina, wherein absence of any impurity phase resulted in microstructure without any liquid phase. This is also confirmed by the EDX analysis of the microstructure which shows the presence of only Al and O indicating that composition is only composed of alumina.

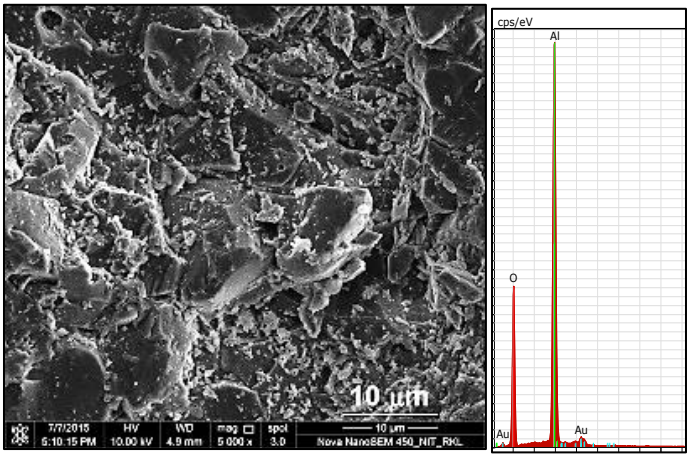

Figure 5.22 SEM photomicrograph of B/23/5 composition and EDX analysis

5.2.3 Summary of the section:

A boehmite sol is prepared using commercially available boehmite powder. The resulted Boehmite Sol have a solid content of ~17% and particle size is in range 20-400 nm with major fraction below 100 nm. The FTIR study on the dried gel powder obtained from the sol confirms the presence of hydroxides in the dried gel powder. Phase analysis and DSC-TG of the samples shows the formation of α-alumina from the boehmite sol. This sol is solely used as the binder in no cement high alumina castables. No deformation in the castables was observed and well sintered density and strengths were obtained at 1650^{o}C. The castables show higher refractoriness as there is no deformation found in castables even when fired up to 1650^{0} C. As the castable composition does not contain any low melting phases so these can be used for temperatures much greater than their conventional counterparts.

5.3 Mullite sol bonded high alumina castable composition:

This section covers the result and analysis of various characterizations done on synthesized mullite sol and high pure alumina castables prepared using this mullite sol as binder. Development of high pure alumina castable is studied by using synthesized mullite sol as the sole binder. Mullite sol is prepared by wet chemical route and is characterized by its solid content, particle size, thermal analysis, phase development with temperature, microstructure, etc. This sol is used at two different percentages in high alumina castable compositions with two different particle size distribution patterns. Conventional castable processing is done on the compositions and the characterizations are done after heat treatment at three different temperatures.

5.3.1 Sol-gel characterization: The synthesized mullite precursor sol, which appears to be nearly transparent, shows stability for more than a month at room temperature and gelling tendency when dried above 40^0C. Hence, it undergoes gelation with time and temperature due to loss of water. The average solid content of the sol was found to be about 12.5% as a loss on ignition basis after firing at 1000^0C.

5.3.1.1 Particle size analysis: The particle size distribution plot in figure 5.23 shows that all the sol particles are having nano-size dimensions and within the size range of 10-100 nm with a peak around 25 nm. The distribution shows that major fraction of sol particles is smaller than 50 nm.

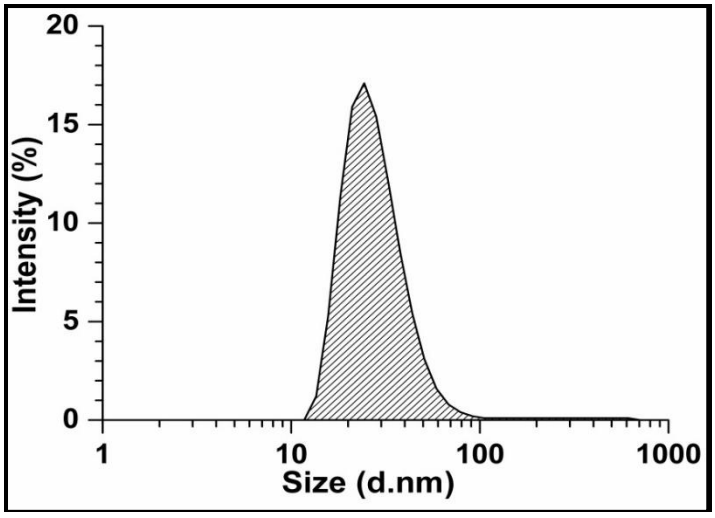

Figure 5.23: Particle size distribution in mullite sol.

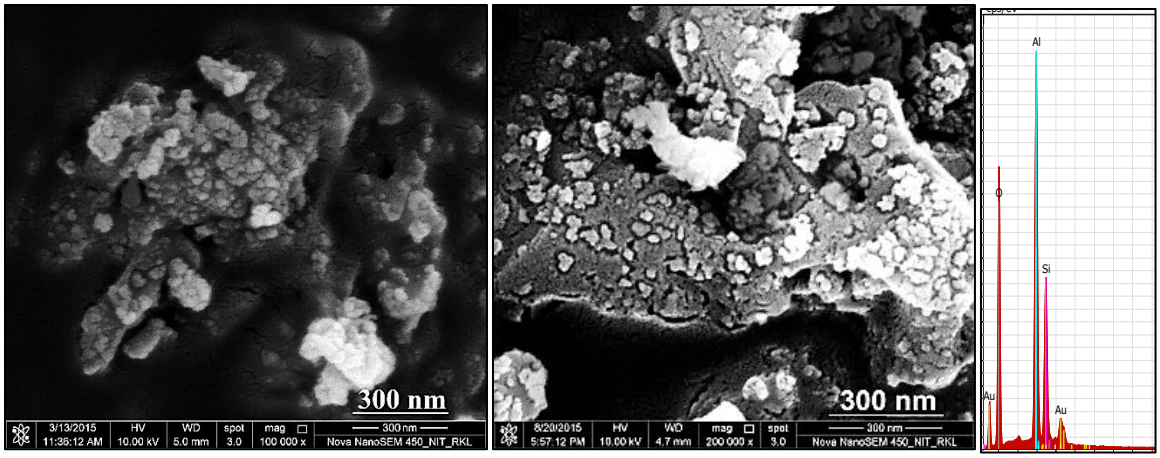

Figure 5.24: Microstructure of mullite sol powders heated at (a) 200^0C, (b) 1000^0C and (c) EDX frame analysis of 1000^0C calcined powder

5.3.1.2 Microstructural analysis: Microstructural photograph of the 200^0C and 1200^0C calcined sol powders (Figure 5.24a and b) shows small distributed and little agglomerated near spherical particles. Again the elemental analysis (EDX) on the microstructure photograph frame (frame analysis of 1200^0C calcined powder) confirms the presence of only aluminum, silicon and oxygen ions (gold ions are found due to coating) and the atomic ratio of the ions is also close to that of the mullite composition (figure 5.24c), confirming the formation of nano mullite particles in the calcined powders.

5.3.1.3 FTIR analysis: Figure 5.25 below shows the FTIR spectra of the mullite precursor dried at 200^0C in the wavenumber range 4000-400 cm^{-1}. The broad band around 3500 cm^{-1} in the spectra is due to H-O-H stretching vibrations [5.13]. Another band around 1630 cm^{-1} may be due to deformation vibrations of the molecular water [5.14-5.17]. These bands are the evidence of the molecular water present in the structure. The bands due to Si–O stretching (SiO4) modes and O–Si–O bending (SiO4) modes appeared around 1170 and 450 cm^{-1} respectively. Further bands around 850 and 550 cm^{-1} are due to stretching vibrations of the Al–O in AlO4 and AlO6 respectively and at 720 cm^{-1} is due to bending vibrations of Al-OH [5.14-5.17]. The band due to the vibrational modes of residual nitrates has also appeared near 1380 cm^{-1} [5.14].

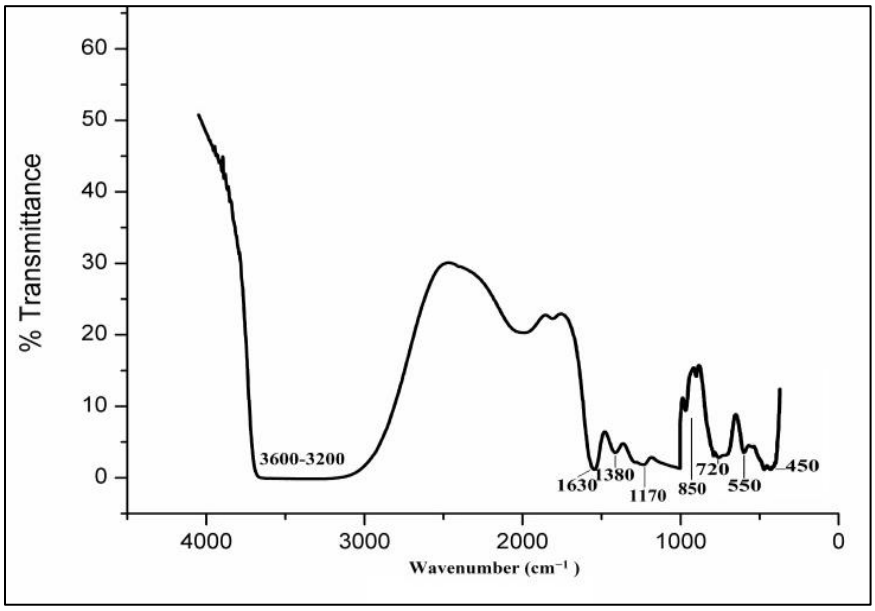

Figure 5.25: FTIR spectra of mullite sol precursor powder dried at 200^0 C

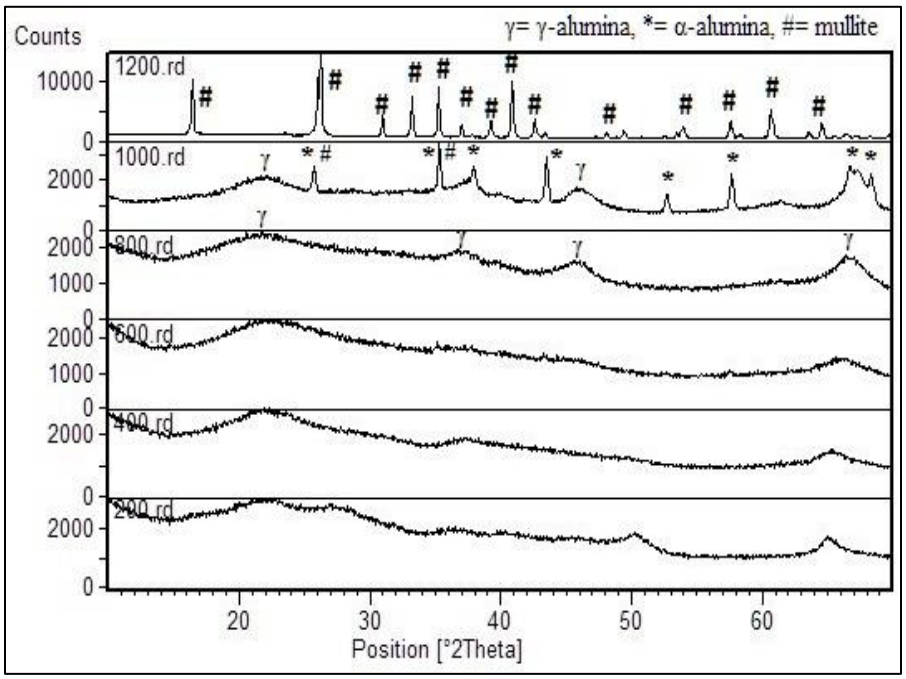

Figure 5.26: Phase analysis of mullite sol calcined at different temperatures

5.3.1.4 XRD analysis: The powder obtained after drying the mullite precursor sol is found to be amorphous in nature up to about 600^0C (figure 5.26). At 800^0C, it shows some peaks resembling that of γ- alumina. As the calcination temperature increases to 1000^0C, some crystalline phases that resembles with α-alumina along with traces of mullite and γ- alumina phase also appears. At 1200^0C, the pattern shows only the orthorhombic mullite phase. No free silica phase is observed at any temperature, which confirms that silica remains in the amorphous state throughout the calcination range [5.18] and directly reacts with alumina to form mullite from around 1000^0C. From the pattern obtained, it can be inferred that amorphous alumina precursor first transforms into γ- alumina and then crystalline to α-alumina at 1000^0C and then Si substitution in alumina lattice takes place leading to the formation of mullite as observed in the powders after calcination at 1200^0C [5.19]. JCPDS number 10.0425 for γ-alumina, 10.0173 for α-alumina and 15.0776 for mullite are used.

5.3.1.5 Thermo-gravimetric (DSC-TG) analysis: The DSC pattern of the mullite precursor gel, as shown in figure 5.27, shows endothermic peaks at 120^0-150^0C associated with mass loss in TG plot due to removal of physically absorbed water followed by another endotherm at 210^0C due to transformation of aluminum trihydrate $Al(OH)_3$ to boehmite AlO(OH) phase [5.20, 5.21]. Again a sharp exothermic peak at around 310^0C on the DSC curve with a sudden loss in mass as observed in TG curve is due to decomposition of remaining nitrates present in the sol and simultaneous slow and gradual conversion of boehmite to γ-alumina was observed as a gradual mass loss which continues upto 520^0C [5.19, 5.21, 5.22]. Nearly no mass loss was observed after this and indicates the onset of crystallization. A broad exothermic peak was observed in DSC plot around 960^0C is due to simultaneous γ- to α-alumina transition, which is also confirmed by phase analysis study. Again a diffused peak in DSC plot around 1125^0C marks the mullitization reaction between amorphous silica and alumina phases followed by crystallization of mullite phase [5.19, 5.23]. This is also supported by phase analysis study as complete mullite formation was observed at 1200^0C. Mullite formation is promoted due to the intimate mixing of the reacting components on a colloidal scale.

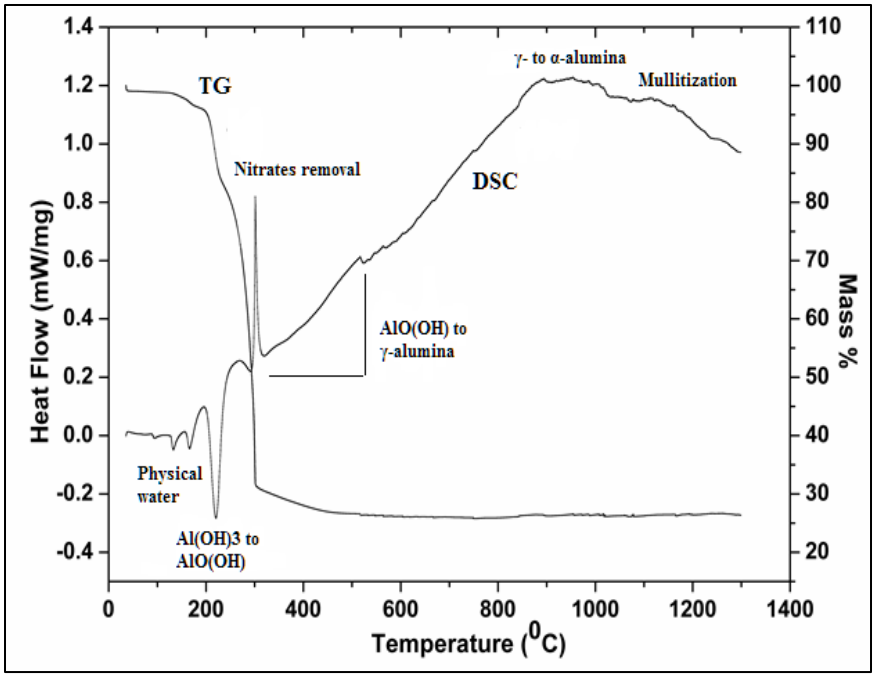

Figure 5.27: DSC-TG analysis of dried powder obtained from mullite sol

5.3.2 Castable characterization: The raw materials used for making refractory castables have highly pure chemistry. As a result, the castables developed are highly pure, consisting of alumina and mullite (from bond) only, can withstand very high temperature and would be highly corrosion resistant. Details of nomenclature of the batches with q values, amounts of sol used, are given in Table 5.3.

Table 5.3. Batch Name and amount of mullite sol used in different batch composition

Batch name	**M/23/5**	**M/23/7**	**M/29/5**	**M/29/7**
q value	0.23	0.23	0.29	0.29
Sol [vol. /Wt.]%	5	7	5	7
Water [vol. /Wt.]%	2.5	0	0.5	0

5.3.2.1 Phase analysis of the matrix: Matrix of the 1650ºC fired castables shows sharp crystallinity and consists of only corundum as major and mullite as minor phases. No other impurity phases and unreacted form of silica were detected in the study. This confirms the high purity of the compositions and absence of low melting phases too. XRD pattern of the matrix part of the sintered M/23/7 composition is shown in figure 5.28 as a representative one.

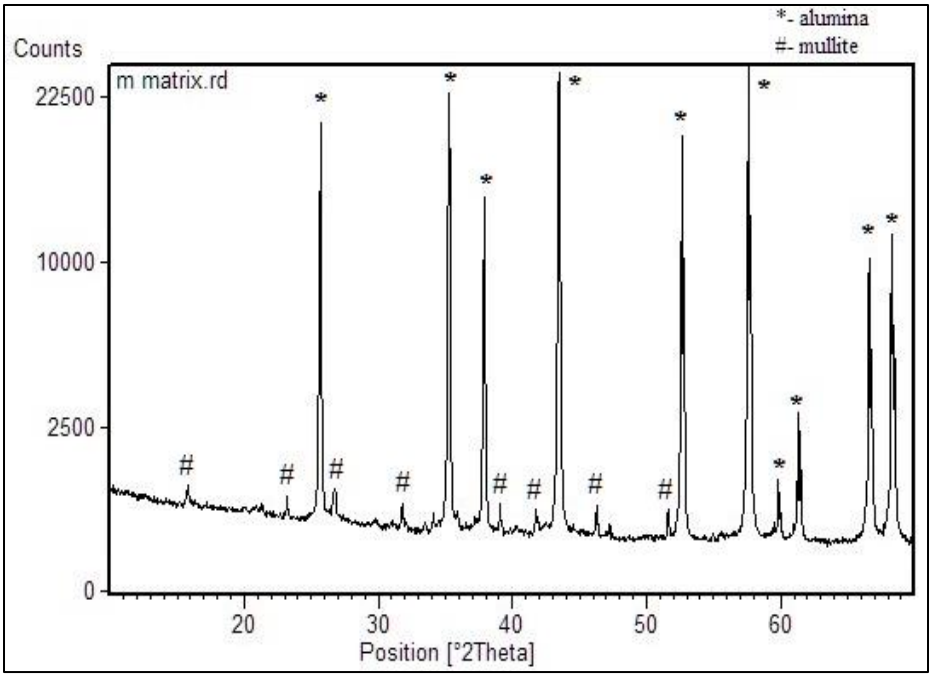

Figure 5.28: Phase analysis of the castable matrix of M/23/7 composition

5.3.2.2 Bulk density (BD) study: The density of castables increases with increase in firing temperature as shown in figure 5.29. The presence of ultrafine colloidal mullite precursor particles helps to increase the sintering of the castables at high temperatures and thus an overall increase in density; although the mullite formation is accompanied by volume expansion affecting the densification process. For all the castables, the density at the intermediate temperature of 1000^0C is little less as compared to that of the dried condition. This is mainly due to the formation of a porous structure on the removal of physically absorbed and chemically bonded water from the sol and the castable samples (also free water added). At the higher temperature of 1650^0C, the sintering is strongly promoted due to the presence of fine colloidal particles resulting in an increase in the bulk density.

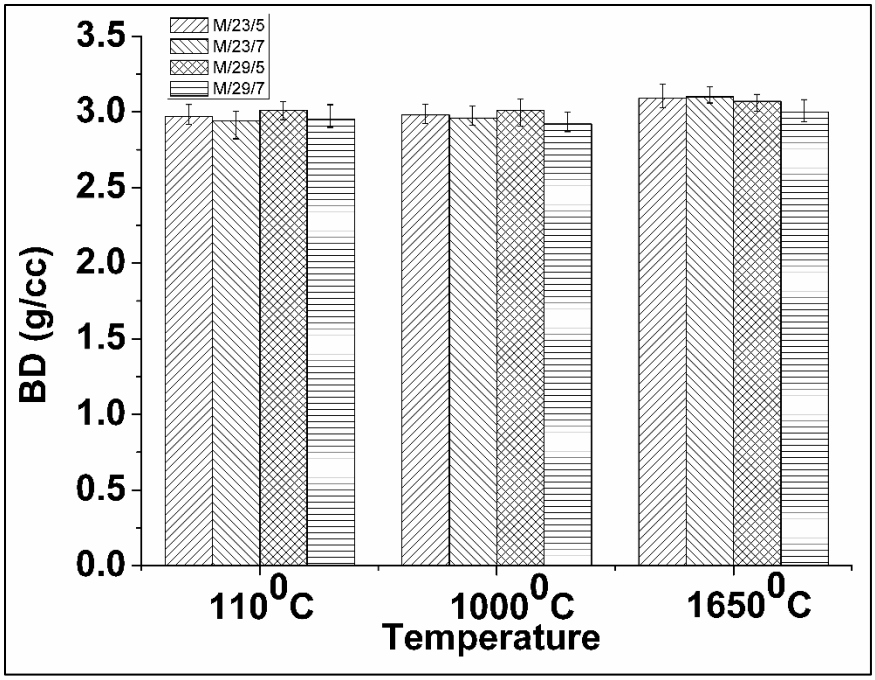

Figure 5.29: Bulk density of mullite sol bonded castable against temperature.

5.3.2.3 Cold Crushing Strength (CCS) Study: Figure 5.30 shows the variation of CCS values of different castable compositions against their processing temperatures. At dried conditions, the strength of the castable samples is lower, as the strength development is poor due to weak coagulation bonding of the gel particles. Upon firing at high temperature, sol-gel bonding is replaced by ceramic bonding, which was enhanced due to the presence of fine mullite particles. Thus, a significant increase in strength values is observed after sintering.

The batches with 7% sol content have higher CCS values compared to the batches containing 5% sol. This is due to the presence of higher amount of fine sol particles which leads to greater sintering and hence higher CCS values. The strength obtained at higher temperature is comparable to its conventional counterpart (say cement bonded ones) along with the advantage that this nano mullite bonded composition can be used at a much higher temperature than 1650^0C, where conventional bonds will fuse and are not applicable.

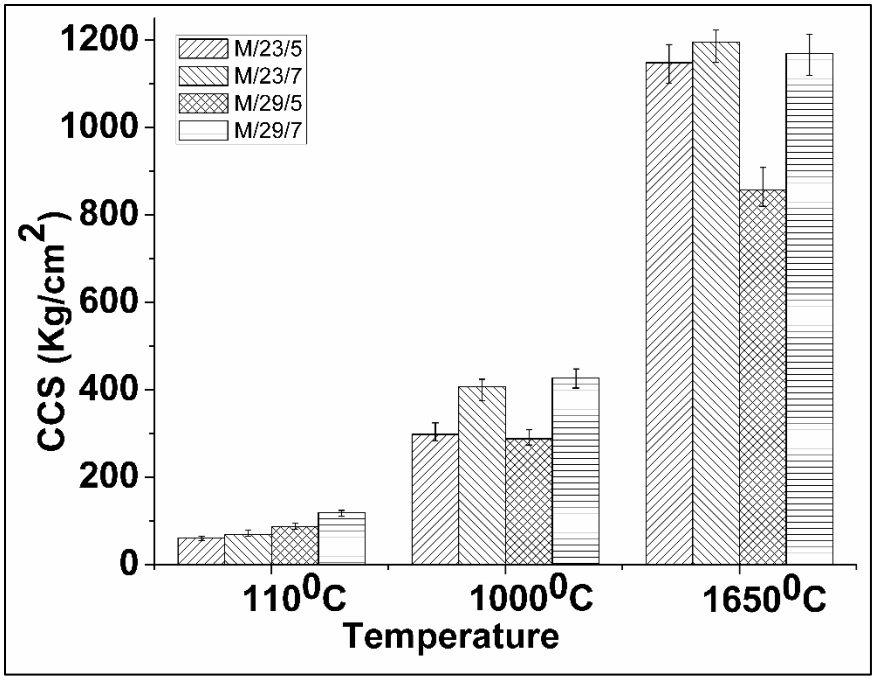

Figure 5.30: CCS of mullite sol bonded castable against temperature.

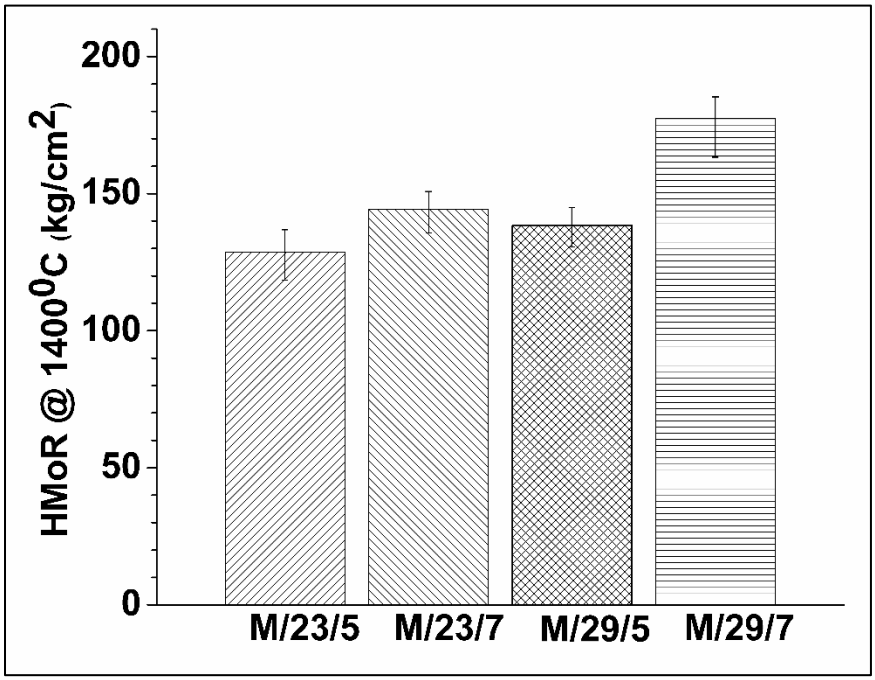

Figure 5.31: HMoR values of the mullite sol containing castables.

5.3.2.4 HMoR analysis: The figure 5.31 shows the flexural (hot modulus) behavior of the developed castables. All the batches are having HMoR values more than 100 kg/cm^2 (10 MPa) at 1400^{0}C which may be considered good for the refractory castables [5.24]. Here also the batches with 7 % sol content shows better hot modulus values because of greater sintering due to the presence of higher amount of fine sol particles, enhancing the sintering and strength development. The HMoR values are considerably high due to high purity of the compositions and no low melting compound formation in the matrix phase. Mullite sol which has converted to mullite crystals on heating results in improved sintering due to fine particles formation, but it has no low-temperature liquid formation or eutectic, thus the strength at high temperature is high.

5.3.2.5 Microstructural analysis: It is also well established that the properties of fired ceramic materials are determined not only by the phase constituents but also by the development of their microstructure, i.e. the arrangement or distribution of those phases, their relative amounts, porosity, size, shape, orientation etc. [5.25]. FESEM study of the sintered samples was done to understand the microstructural development of the castables after sintering. Highly compact grain structure with little porosity is observed, having high grain to grain contact. The presence of finer sol particles helps in better sintering and densification and results in a compact microstructure. This compact structure indicates the high strength of the sintered products. Castable composition M/23/7 fired at 1650^{0}C is shown in figure 5.32 as a representative one. The elemental mapping of the microstructural frame was done by EDAX study (frame analysis) and is shown in figure 12b. This shows a nearly homogenous distribution of Al and O ions all through the microstructural frame with a lesser extent of silicon ions. This also indicates the uniform distribution of mullite phase all through the microstructure and confirms the presence of only these three elements in the compositions and showing the purity level of the castables.

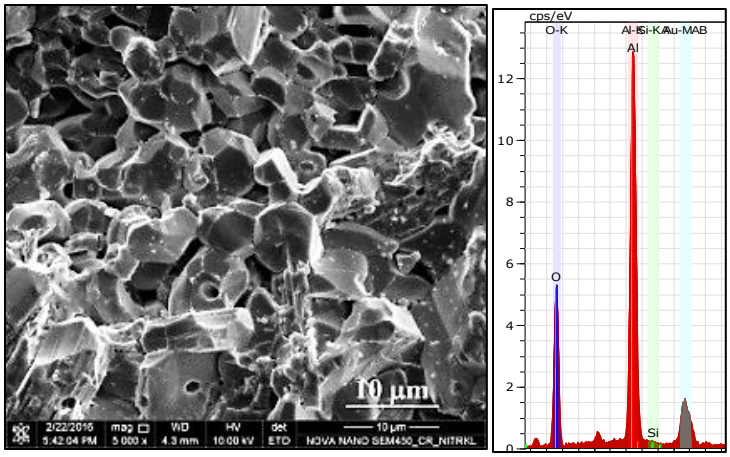

Figure 5.32: SEM photomicrograph of M/23/7 composition and EDX analysis

5.3.3 Summary of the section:

High pure alumina-based castable has been developed with only mullite sol as binder. Stable mullite sol was developed by simple wet chemical synthesis route, characterized for various properties and utilized at 5 and 7 volume to weight percent levels in the pure alumina compositions with two different particle size distributions. Conventional processing technique of the castable was used and the presence of ultrafine nano mullite precursor particles in the castable matrix leads to greater sintering among the matrix components. As a result, well sintered density and strengths were obtained at 1650^0C, which temperature is much above than any conventional castables. The absence of impurity in the castables nullifies the formation of any liquid phase, as confirmed by phase analysis study of the matrix phases. Densification, strength, hot strength, thermal shock resistance of the developed mullite sol bonded high pure alumina castable was evaluated. Superior properties for mullite sol bonded composition were obtained; thus, makes it suitable for very high temperature applications.

5.4 Spinel sol bonded high alumina castable composition:

This section covers the result and analysis of various characterizations done on synthesized spinel sol and high pure alumina castables prepared using this spinel sol as binder. A cement free high pure alumina castable composition is developed for high temperature applications using synthesized Mg-Al spinel sol as binder. The spinel sol is prepared from nitrate precursors and characterized for its pH, solid content, particle size, FTIR, thermal behavior (DSC-TG), phase formation with temperature (XRD), microstructure (FESEM), etc. High alumina castable formulations with two different particle size distributions (PSDS) are conventionally processed using the synthesized sol as a sole binder at two different amounts. Castables were characterized for various refractory properties after heat treatment at different temperatures.

5.4.1 Sol-gel characterization: The synthesized spinel precursor sol (a homogenized mixture of Al and Mg hydroxides) prepared from inorganic precursors appears to be nearly transparent and has pH in between 3-4. It shows gelation when dried above room temperature due to loss of water. The average solid content of the sol was found to be about 8 % as a loss on ignition basis after firing at 1000^0C.

5.4.1.1 Particle size analysis: From the particle size analysis, in figure 5.33, it can be observed that particles are having nano-size dimensions ranging from 10-200 nm with a peak around 40 nm. The distribution shows that major fraction of the sol particles is smaller than 100 nm.

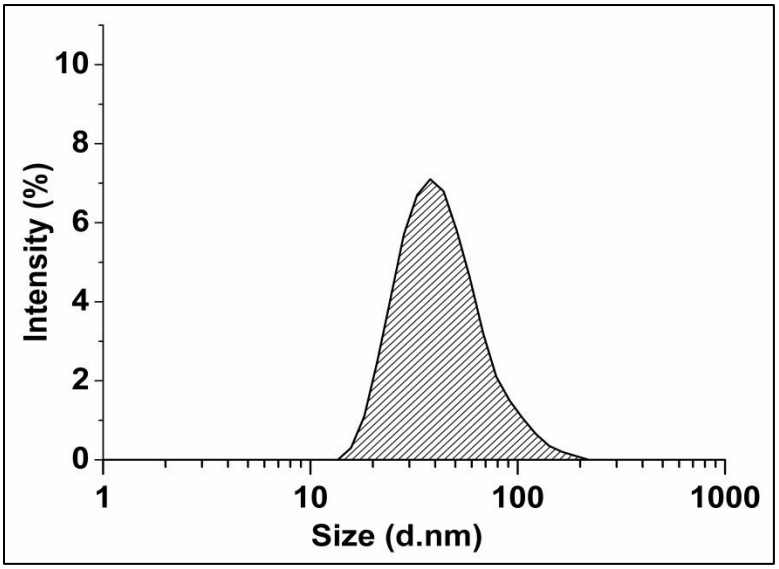

Figure 5.33: Particle size distribution in spinel sol.

5.4.1.2 Microstructural analysis: Figure 5.34 shows particle morphology of the powder obtained from calcination of sol at 200^0C and 1000^0C. The microstructure of powders dried at 200^0C revealed that the particles are highly agglomerated because of high reactivity due to its ultrafine nature. The agglomeration continues even at 1000^0C. In both the microstructures, particles are having nano dimensions. The elemental (EDX) analysis of the microstructural frame of fig 4b is given in figure 4c. EDX analysis confirms the presence of aluminum, magnesium, and oxygen (gold (Au) elemental peak is coming from the coating of the sample). The atomic ratio of these elements is close to that of spinel composition, indicating the formation of nano spinel particles in the calcined sample.

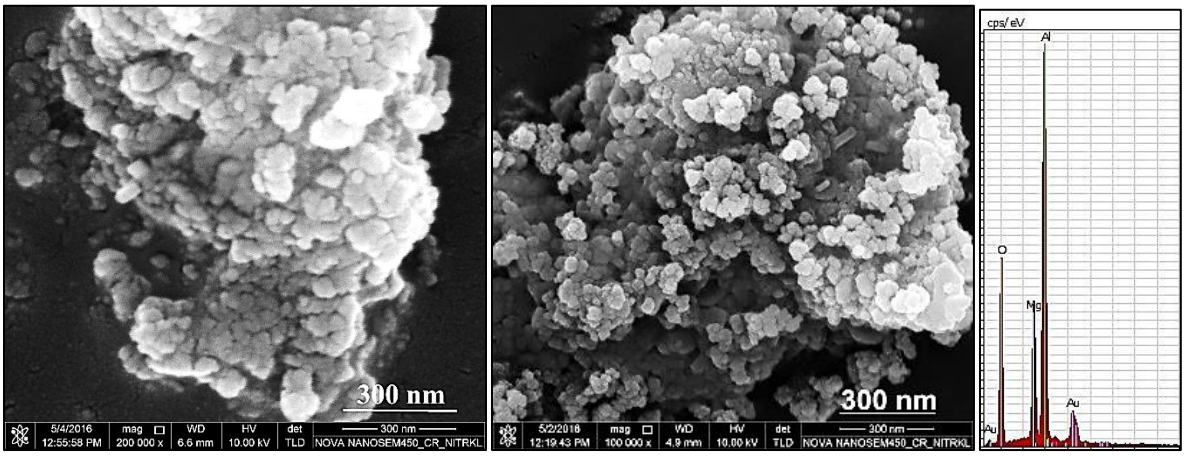

Figure 5.34: Microstructure of spinel sol powders heated at (a) 200^0C, (b) 1000^0C and (c) EDX frame analysis of 1000^0C calcined powder

5.4.1.3 FTIR analysis: Figure 5.35 shows the FTIR spectra of the spinel precursor dried at 110^0C. The IR spectrum shows that the precursor sol contains hydrates, The broad band around 3400 cm^{-1} is due to O-H stretching vibrations (symmetric and antisymmetric) [5.26-5.29] and the band at 1640 cm^{-1} appears due to deformation vibrations of the molecular water [5.27-5.30]. Both bands are the evidence of the molecular water in the structure. Further bands at 1380 cm^{-1} [5.26, 5.30] and 830 cm^{-1} [5.26] appear due to vibrational modes of nitrates. The broad band below 1000 cm^{-1} is due to M-O-M (metal oxygen metal) bond. Among these, the band appeared around 550 cm^{-1} may be associated with the vibrations of the Al–O stretching in the AlO_6 octahedral [5.26, 5.27, 5.30].

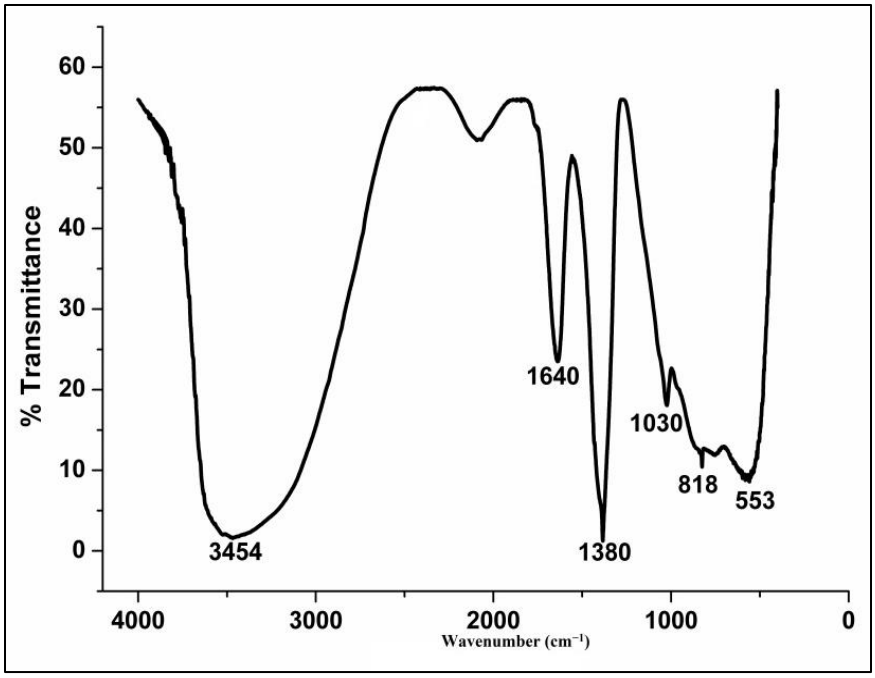

Figure 5.35: FTIR spectra of spinel sol precursor powder dried at 200^0 C

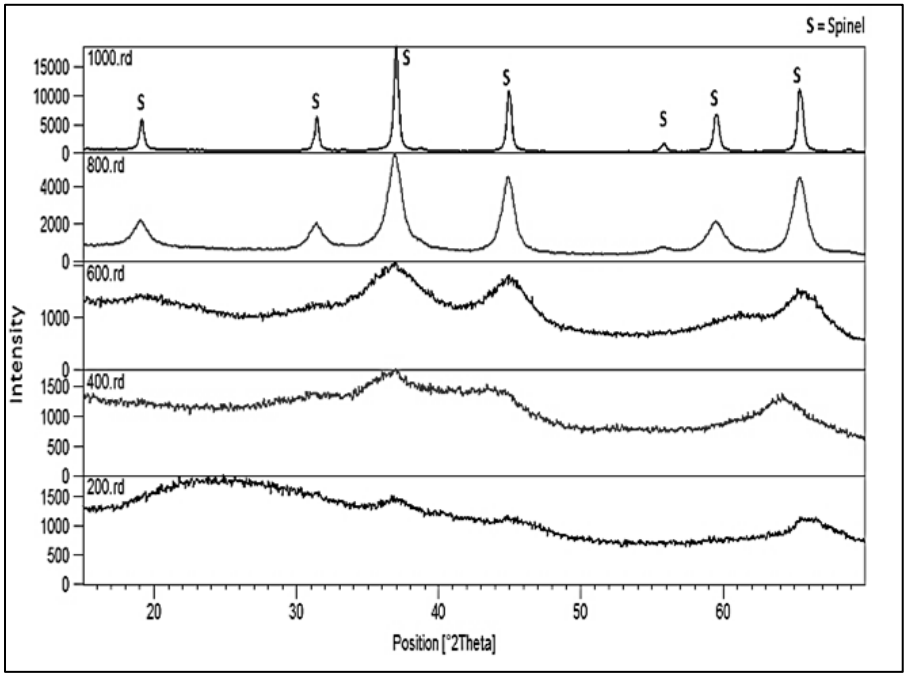

Figure 5.36: Phase analysis of spinel sol calcined at different temperatures [JCPDS-73.1959].

5.4.1.4 XRD analysis: Figure 5.36 shows the phase analysis study of the spinel precursor powders after drying and calcining at different temperatures. Sol precursor was found to be nearly amorphous after drying and poorly crystalline till about a calcination temperature of 600^0C. The initiation of spinel crystal formation was observed at about 400^0C. This may be attributed to the presence of highly reactive ultrafine nano-sized homogenously mixed particles in sol derived spinel precursor powder. The solid-state reaction for spinel formation is known to be exclusively heterogeneous in nature, in contrast, the sol–gel synthesis, involves the reaction to proceed at the atomic level. This reduces the diffusion path, increases the diffusion area of the particles and thus enhances the volume diffusion [5.31]. The nano-sized spinel precursors having high specific surface area increase the reactivity resulting in the lowering of temperature required for the spinalization reaction. The poorly crystalline spinel precursor powder transforms to well crystalline material at and above 800^0C. Further increase in calcination temperature results in confining of peak shapes and increase in intensities, indicating crystallite growth [5.32, 5.33].

5.4.1.5 Thermo-gravimetric (DSC-TG) analysis: The DSC-TG pattern of the spinel precursor gel obtained from sol dried at 110^0C is given in figure 5.37. It shows an endotherm at 150^0C [5.29, 5.34] due to the removal of physically bonded water followed by endothermic conversion of amorphous aluminum hydrate to boehmite, AlO(OH) at 220-230^0C [5.29, 5.34, 5.35], as also confirmed by the wt. loss in the TG curve at same temperature range. Another weight loss between 280 to 450^0C is probably due to gradual dehydroxylation of mixed hydroxides-AlO(OH) to γ–Al_2O_3 and $Mg(OH)_2$ to MgO [5.29, 5.34-5.36]. A sharp exothermic peak in the DSC curve around 300^0C is due to decomposition of byproduct nitrate compounds also shown by a sharp decrease in mass in the TG curve [5.26]. The absence of any significant weight-change after this indicates the onset of crystallization. The presence of homogenous ultrafine spinel precursors in the colloidal suspension results in lowering of spinel formation temperature. The broad exothermic peak around 550^0C is due to crystallization of the spinel formed between 400-500^0C from the homogenized mixture of γ–Al_2O_3 and MgO also confirmed from the phase analysis study.

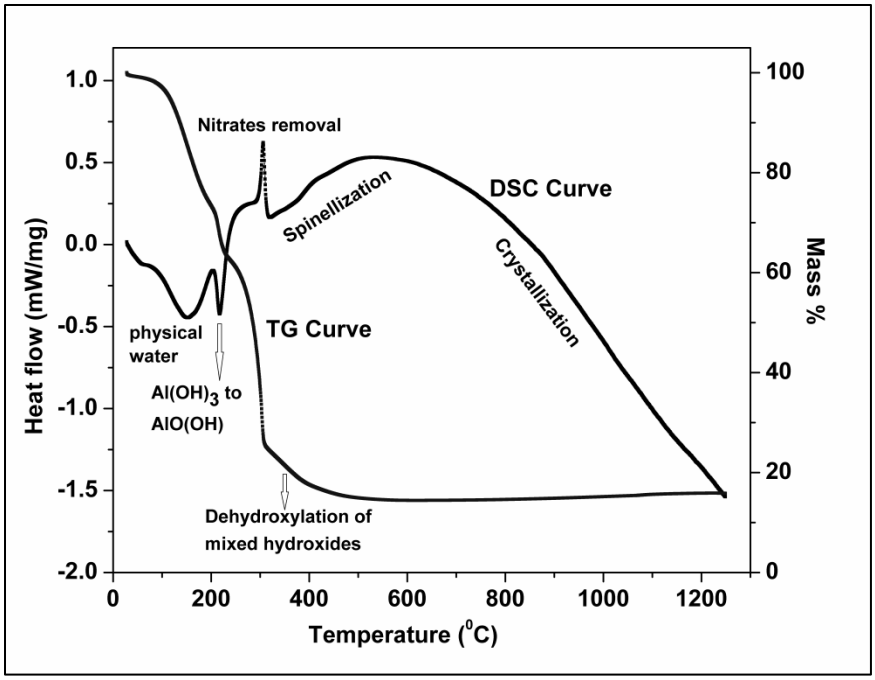

Figure 5.37: DSC-TG analysis of dried powder obtained from spinel sol

5.4.2 Castable characterization: The raw materials utilized in the making of castables are alumina grains and fines with high purity. The developed castables, as a result, only consisting of alumina as major phase and spinel (from bond) as the minor phase, are chemically high pure and can withstand very high temperatures. Details of nomenclature of the batches with q values, amounts of sol used are given in Table 5.4.

Table 5.4. Batch Name and amount of spinel sol used in different batch composition

Batch name	**S/23/5**	**S/23/7**	**S/29/5**	**S/29/7**
q value	0.23	0.23	0.29	0.29
Sol [vol. /Wt.]%	5	7	5	7
Water [vol. /Wt.]%	2.5	0	0.5	0

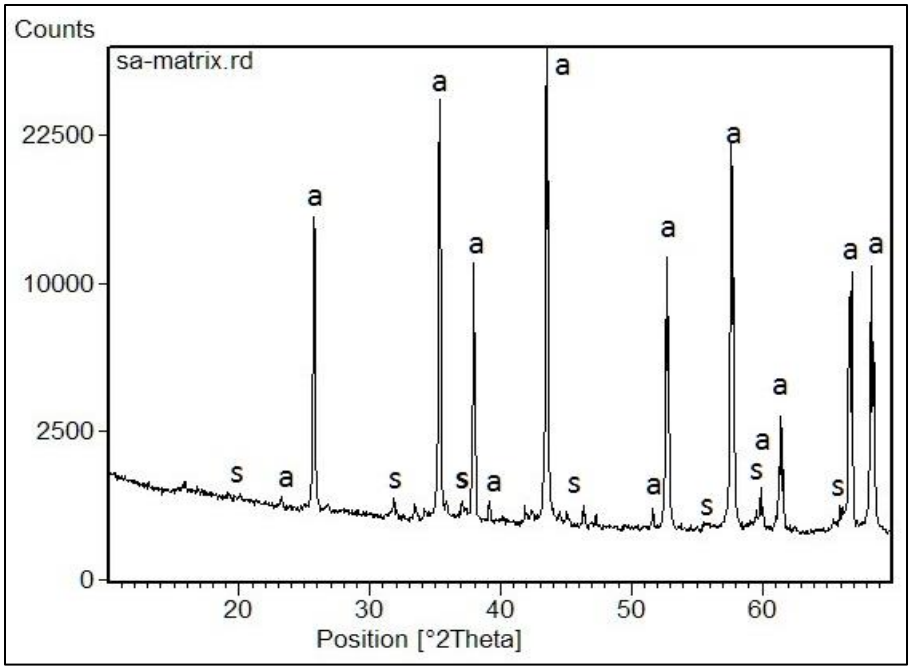

Figure 5.38: Phase analysis of the castable matrix of S/23/7 composition

5.4.2.1 Phase analysis of the matrix: The presence of any low melting impurity phase has pronounced effect on the properties and performance of refractory castables, as commonly observed for cement-containing compositions. The present castable composition is chemically high pure system and the phase analysis of the matrix part of the composition fired at 1650^0C shows sharp crystallinity with only corundum as major and spinel as minor phases. The absence of any other phase confirms the high purity of the compositions. The figure 5.38 shows the phase analysis of the matrix part of S/23/7 composition as a representative one. In the figure, 'a' = α alumina and's' = spinel phase. JCPDS no. 10.0173 for alumina phase and 73.1959 for spinel phase is used.

5.4.2.2 Bulk density (BD) study: The density versus temperature analysis of castables is shown in figure 5.39. The density of castables of S/23/7 and S/29/7 batch at all temperatures is lower than castables with 5% sol because of higher water content resulted in more porous structure when fired at higher temperatures. The density of all castables only marginally decreases at 1000^0C due to the formation of the porous structure caused by the removal of physical and chemically bonded water associated with the sol and initiation of spinel formation. But, at 1650^0C, the density increases again for all the castable compositions due to the higher extent of

sintering caused by the presence of ultrafine spinel particles which increases the sintering effect and, thus increase in density. The density values of all the castables are found to be above 3.0 g/cc level, even after marginal fall at 1000^{o}C. This indicates that the degradation of the quality of the castables at intermediate temperatures, as commonly observed for cement bonded compositions, is not prominent and the studied compositions can work better compared to the conventional cement and silica sol bonded castables.

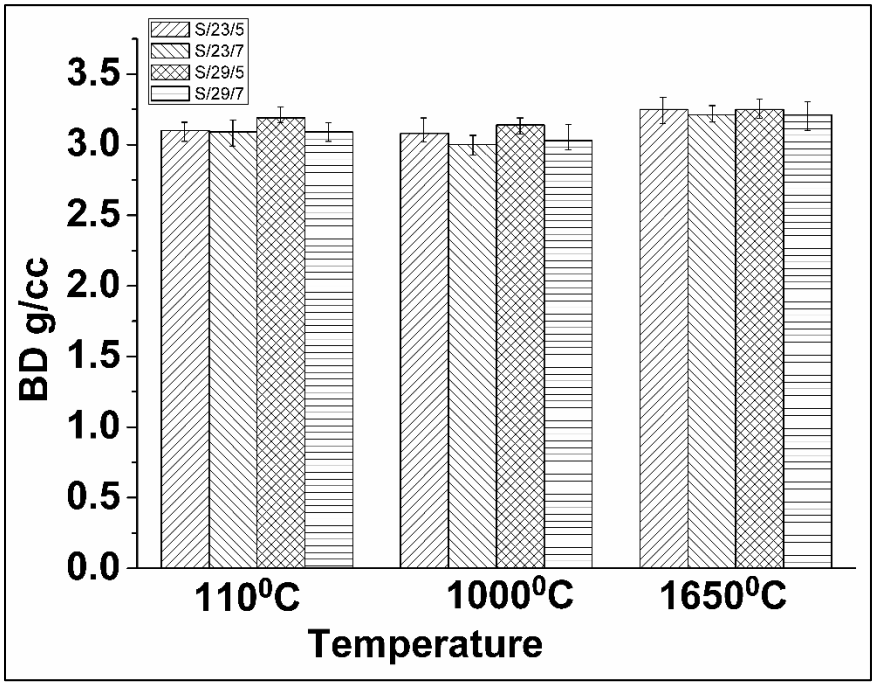

Figure 5.39: Bulk density of spinel sol bonded castable against temperature

5.4.2.3 Cold Crushing Strength (CCS) Study: The figure 5.40 shows the variation of CCS values against processing temperature of different castable compositions. At low temperatures, sol-gel bonding of the spinel bonded castable provides marginally poor strength values due to weak coagulation bond of the gel structure. This has resulted in CCS values below 100 kg/cm^2 for all the castables after drying. But with the increase in temperature, the well and uniformly distributed nano-dimensional spinel particles (as also observed in fig. 4C) initiates the sintering within the compositions, resulting in increased strength values at 1000^{o}C. Hence strength values increased at intermediate temperatures, in contrast to the decrease in conventional cement bonded compositions due to the destruction of cement hydrate bonds. At 1000^{0}C, batches having q value of 0.23, that is having the higher extent of finer fraction, initiates greater extent of

sintering and resulted in higher strength values. Further increase in temperature has caused further sintering within the matrix phase with fine alumina present causing the formation of strong ceramic bond and also within the whole castable composition, resulting in a strong increase in strength values, as observed after firing at 1650^{o}C. 7% sol containing compositions showed marginally higher strength values may be due to the presence of greater extent of bonding material and resulting in the higher amount of nano particles, causing greater bonding. Again, at 1650^{o}C, batch S/23/7 shows the highest strength values among all the compositions due to the presence of highest extent of fines in the composition (fine fraction due to lower q value and higher amount of bonding spinel phase) compared to others and hence greater sintering and better bonding. No deformation and/or any liquid phase formation is observed in any of the compositions, even when sintered at 1650^{o}C. The absence of any low melting phase thus makes these compositions well suitable for application at and above such temperature.

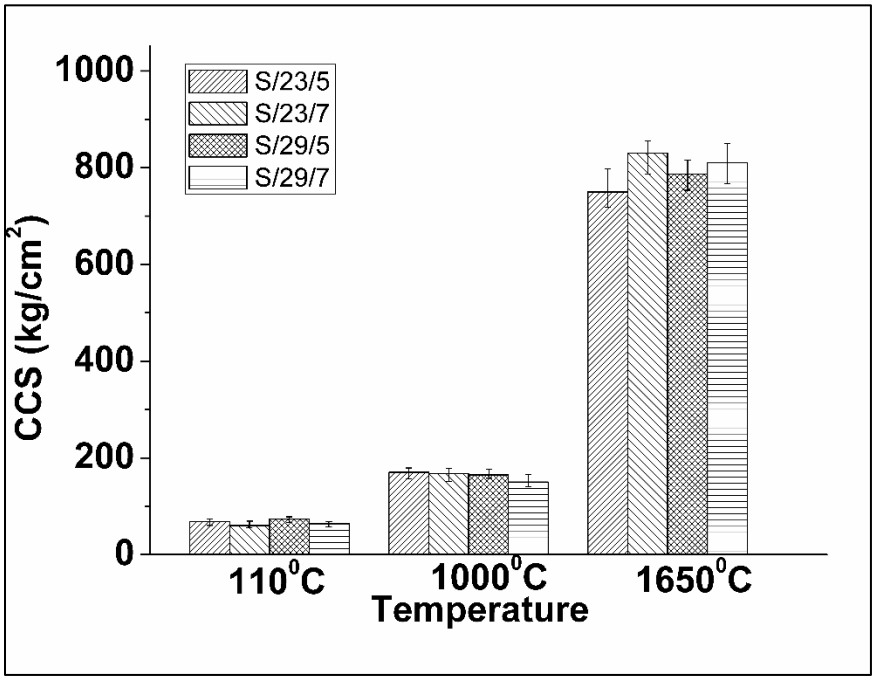

Figure 5.40: CCS of spinel sol bonded castable against temperature

5.4.2.4 HMoR analysis: Hot strength values (measured as hot MOR) of the castable compositions tested at 1400^{o}C is plotted in figure 5.41. High hot strength values of above 100 kg/cm^2 (10 MPa) at 1400^{0}C are obtained for all the compositions, which indicates a well compact structure of the castable without any liquid phase formation at high temperatures due to

high purity. 7% sol containing compositions have shown higher hot strength values, which may be associated with the greater extent of bonding material and resulting in the higher amount of nano particles, causing greater bonding within the compositions. Coarser components have better resistance to thermo-mechanical stress as can be seen that castables for batches 0.29 have higher HMoR values correspondingly. Here also the composition S/23/7 shows the highest hot strength value among all the compositions may be due to the presence of highest extent of fines and nano particles present in the composition.

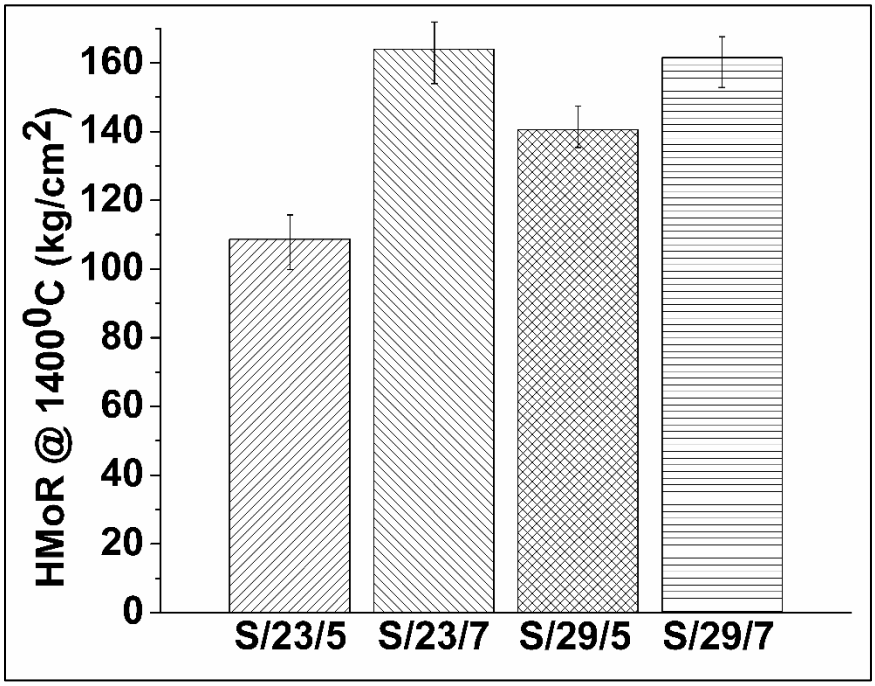

Figure 5.41: HMOR values of the spinel sol containing castables

5.4.2.5 Microstructural analysis: Along with phase constituents of a sintered ceramic material, the microstructural development during sintering i.e. the arrangement or distribution, relative amounts, size, shape and orientation of those phases, porosity, etc. is equally responsible for the developed properties [5.37]. To understand the microstructural development in the sintered samples, FESEM study of the fractured surface were done. The microstructure of fractured surface of castable composition S/23/7 sintered at 1650^{0}C is shown in figure 5.42 as a representative one. The FESEM image is showing highly compact microstructure with few little pores attributed to the better sintering between the matrix phase and refractory aggregates. The

high grain to grain contact is the result of better sintering and densification due to the presence of finer sol particles. This compact structure indicates the high strength of the sintered products.

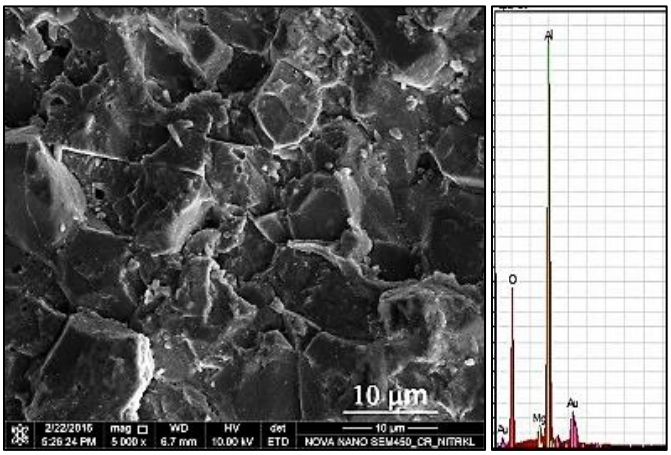

Figure 5.42: SEM photomicrograph of S/23/7 composition and EDX analysis

5.4.3 Summary of the section:

Stable spinel precursor sol was prepared by a simple wet chemical method using inorganic precursors and characterized for various properties. Spinel formation was confirmed by phase analysis from 600^{o}C. The developed sol was solely used as a binder at 5 and 7% level for making high alumina castables with two different particles size distributions. Conventional castable processing technique was used with a sintering temperature of 1650^{o}C. Well sintered density and strength and hot strength values were obtained for the castables with no sign of deformation and shrinkage. Much improved thermal shock resistance and corrosion resistance were also obtained for this spinel sol bonded compositions when compared with the silica sol bonded composition with similar purity and formulations. The absence of impurity and any liquid phase formation in the developed castable system makes it suitable for very high temperature applications.

5.5 Comparative study against commercial binders and their corrosion study

From the previous section, it is found that the batch A/23/8 from alumina sol bonded, B/23/8 from boehmite sol bonded, M/23/7 from mullite sol bonded and S/23/7 from spinel sol bonded compositions showed optimum properties for various refractory properties points of view. These compositions are, thus, selected for the comparative study of various refractory properties against commercially available silica sol bonded composition and conventional high alumina low cement castable (LCC) composition with similar particle size distribution, processed under similar conditions [5.38]. The compositions are further compared to their corrosion resistance against blast furnace (BF) slag.

Before going for the comparative study of the castables, a comparison of the various developed sols are given in the table 5.5 against commercial silica sol. The table shows that the developed sols have lower solid content in comparison to silica sol and thus they have higher water content. The lower solid content is responsible for lower green strength which is described in next section. The particle size analysis of the sols shows that the particle are having nano-dimensions with major fraction of all the sols below 100 nm size. The phase analysis of the calcined powders obtained from sols at 1000^0C confirms the formation of respective oxides.

Table 5.5: Properties of the developed sols against commercial silica sol

	Alumina sol	**Boehmite sol**	**Mullite sol**	**Spinel sol**	**Silica sol**
Appearance	translucent	translucent	transparent	transparent	transparent
Particle size range	10-60 nm	20-400 nm	10-100 nm	10-200 nm	10-80 nm
D_{50} (nm)	20	50	25	40	20
Solid content	6%	17%	12.5%	8%	31.5%
Phase analysis at 1000^0C	α-Alumina and γ-alumina phase	γ-alumina phase	α-alumina, γ-alumina and mullite phase	Spinel phase	Tridymite phase
Phase analysis at 1200^0C	α-Alumina phase	α-Alumina phase	mullite phase	Spinel phase	Tridymite phase

5.5.1 Bulk density: The variation of bulk density with temperature for the optimized batches of developed sol bonded castables and their comparison with commercial silica sol and cement bonded compositions are given in figure 5.43. The figure shows that at green stage, the developed sol bonded compositions have lower density values than commercial binders except for spinel sol bonded composition. The factor which might be responsible for higher BD values for spinel sol is the faster gelling due to high reactivity of the colloidal particles (homogenous mixture of Al and Mg hydroxides) formed at atomic level in the spinel sol. The faster gelling observed in the spinel sol is probably due to greater coagulation of colloidal particles resulted in better consolidation of the castable samples. Also, the physically absorbed water is not completely removed at 110^0C compared to other sols (confirmed from DSC-TG analysis), which might be resulted in higher density values.

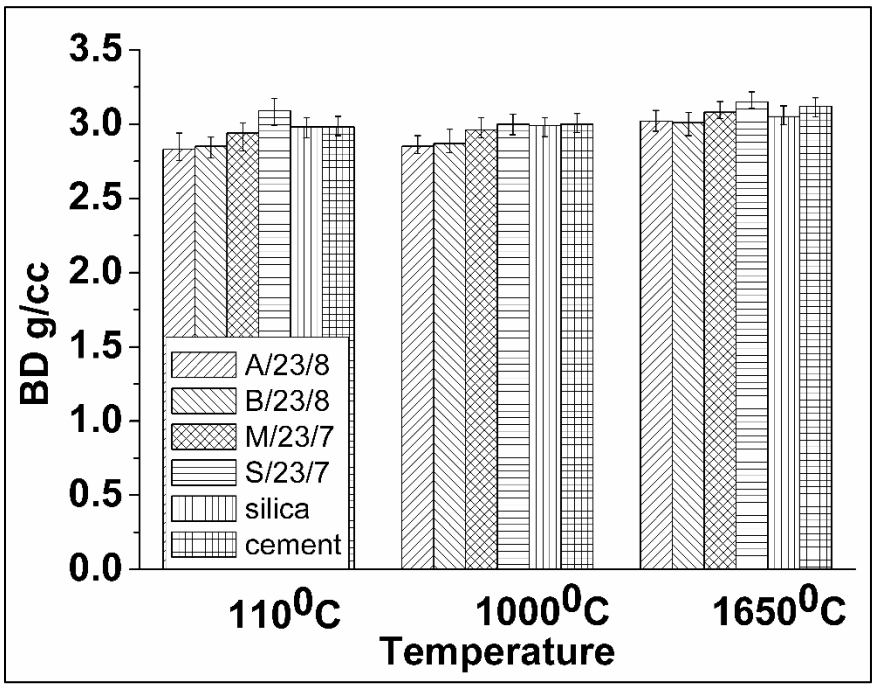

Figure 5.43: Bulk density of optimized batches against cement and silica sol bonded castables.

At the intermediate temperature of 1000ºC, the bulk density of all castables increases except that of spinel sol bonded. The removal of physically and chemically bonded water and other volatile matters resulted in a reduction of density but is compensated by the densification due to initiation of early sintering between the ultrafine sol particles and the finer matrix components in the sol-gel bonded compositions. In spinel sol bonded composition, the spinalization reaction which is

accompanied by volume expansion may be responsible for this reduction in density at the intermediate temperature. Even though there is a reduction in the density value for spinel bonded composition, still it is higher than all other castables. For mullite sol bonded compositions, the mullitization reaction which is also accompanied by volume expansion has taken place above 1100^{o}C (figure 5.27) hence, no reduction in density value is observed at 1000^{o}C.

At 1650^{o}C, again the spinel sol bonded compositions acquire the highest density. Density increases again for all the castable compositions due to the higher extent of sintering caused by the presence of ultrafine particles which increases the sintering effect and, thus increase in density. The density values of all the castables are found to be above 3.0 g/cc level. This indicates that the degradation of the quality of the castables at intermediate temperatures, as commonly observed for cement bonded compositions, is not prominent and the studied compositions can work better compared to the conventional cement and silica sol bonded castables.

5.5.2 CCS: The comparison of CCS of different optimized batches is given in figure 5.44. At the green stage, cement bonded composition, have the highest strength resulted from the stronger hydraulic bonding. All the sol bonded compositions have strength lower than cement bonded composition except the silica sol bonded composition which has strength only a little less than the cement composition. The strength in sol-gel bonding depends on the coagulation tendency of the colloidal particles and also on the number of particles (solid content) present in the sol. The silica sol has the solid content of about 30 percent which is much higher than all other synthesized sols hence have the greater green strength (coagulation bonding). The other sol compositions having lower solid content thus have low green strength due to weaker coagulation bonding. This trend continuous even at 1000^{o}C where sintering between ultrafine particles from sol and fine alumina particles from the matrix just started. Cement bonded compositions have the highest strength followed by silica sol bonded compositions. At the higher temperature of 1650^{o}C, again cement bonded compositions have the highest strength due to the greater amount of liquid phase sintering resulting in better densification and strength.

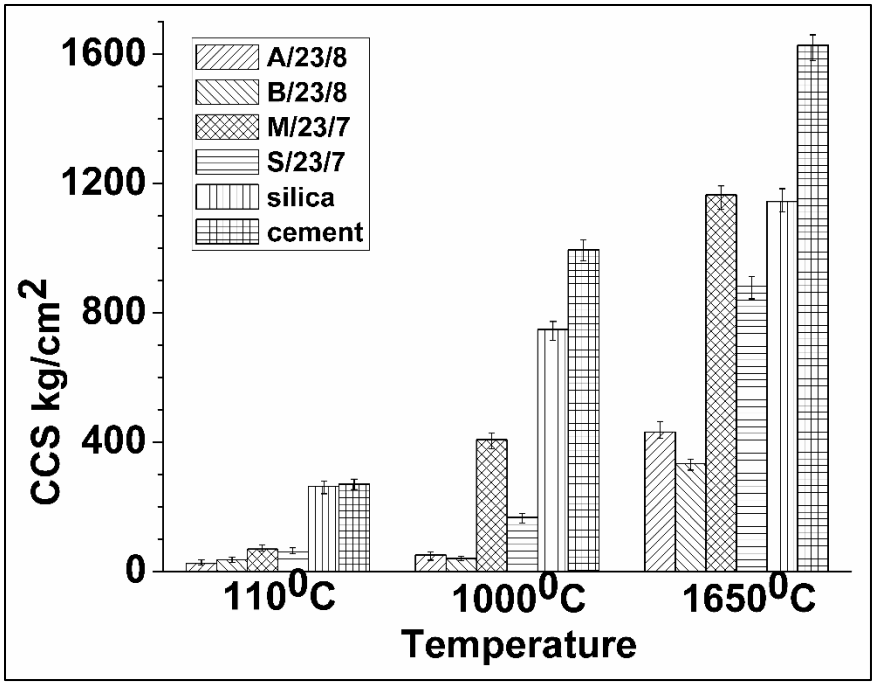

Figure 5.44: CCS of optimized batches against cement and silica sol bonded castables.

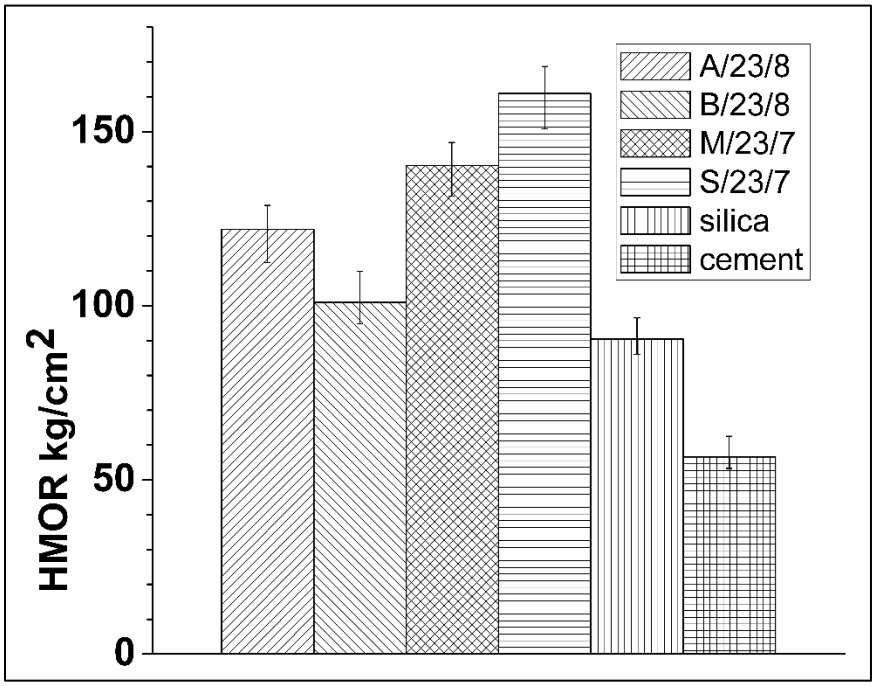

Figure 5.45: HMOR of optimized batches against cement and silica sol bonded castables.

Among sol bonded compositions, the strength increases significantly for all the castables at 1650^{o}C because of greater sintering between the ultrafine particles obtained from sol and the fine alumina matrix. The mullite sol bonded compositions have the highest strength greater than even commercially available silica sol bonded compositions though the later has higher solid content than mullite sol. This can be attributed to the presence of very ultrafine nano size particles in the mullite sol (a homogenized mixture of aluminum hydroxide and silicon oxide) which results in greater mullitization reaction imparting greater strength to the mullite sol bonded castables.

5.5.3 HMOR: The comparison of HMOR of different optimized batches is given in figure 5.45. The high hot strength values of above 100 kg/cm^2 or 10 MPa at 1400^{0}C are obtained for all the developed sol bonded compositions, which may be considered good for the refractory castables [5.24]. This higher strength further indicates a well compact microstructure developed within the castables without any liquid phase formation at high temperatures due to very high compositional purity present in all the developed sol bonded compositions. Among all the compositions spinel sol bonded castables has the highest HMOR value.

The cement bonded compositions have the lowest value among all the compositions. This can be attributed to the fact that some low melting phase or eutectic formation has taken place in the cement bonded composition due to the presence of CaO and SiO_2 which is mainly responsible for this degradation in hot strength. Among the sol bonded compositions, silica sol possess the lowest hot strength even though it has the highest solid content. It indicates that not all the colloidal silica particles are involved in mullite formation with the fine alumina matrix. Some remain as free silica and form low melting phases which result in low hot strength of the silica sol bonded compositions. All the developed sol bonded compositions have shown better hot strength values in comparison to silica sol bonded and cement bonded compositions due to highly pure chemistry of their composition which does not result in any low melting phase generation in the castables matrix and thus results in higher hot strength values.

5.5.4 TSR: Figure 5.46 shows the percent retention of strength of the different batches undergoing thermal shock after different numbers of thermal cycles. The increasing number of thermal cycle results in a greater extent of thermal shocks to the test samples, causing the greater extent of thermal cracks to be generated which is reflected in the retained strength values of the

samples. For spinel sol bonded composition, it can be observed that strength retainment capacity initially increases for the composition and then gradually decreases with the increasing number of thermal cycles. This may be due to differential thermal expansion character between alumina and spinel, resulting in micro-cracking within the sample matrix and resisting the propagation of the thermal cracks by acting as a crack inhibitor, as also reported in different literatures [5.39, 5.40]. But on further thermal cycles, the crack generated by the thermal shock overpowers the micro-cracking effect and results in deterioration in strength retainment properties. There is no sharp or drastic degradation observed till 8 cycles and even after 8 thermal cycles, the strength retainment by the castable is about 90% of its original strength. This indicates that the compositions are strong against thermal cycles of 1200^{o}C with water quenching.

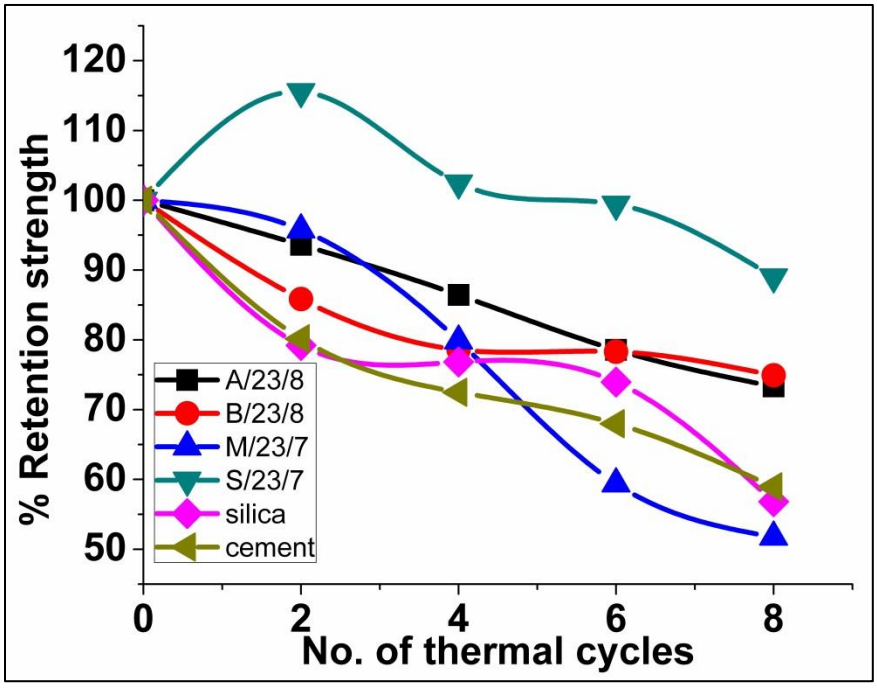

Figure 5.46: Retained strength of optimized batches after different number of thermal shock cycles against cement and silica sol bonded castables

For mullite sol bonded batch, there is no sharp or drastic degradation observed till 2nd cycle. This may also be due to the micro-cracking effect, as in the case of spinel sol bonded compositions, arising from the thermal mismatch of alumina and mullite in the matrix phase. The relatively greater difference between the thermal expansion coefficients of alumina and mullite particles resulted in higher thermal mismatch and thus, the microcracks extended at a higher

extent on increasing number of thermal shock cycles. This might have caused a rapid degradation in strength retainment capacity at higher thermal cycles (>2 cycles). But even after 8 thermal cycles, the strength retainment by the castable is more than 50 % of its original strength. Figure 5.47 shows the high magnified microstructural images of spinel and mullite sol containing compositions showing the presence of micro cracks formed due to the thermal expansion mismatch after 2nd cycle of thermal shock.

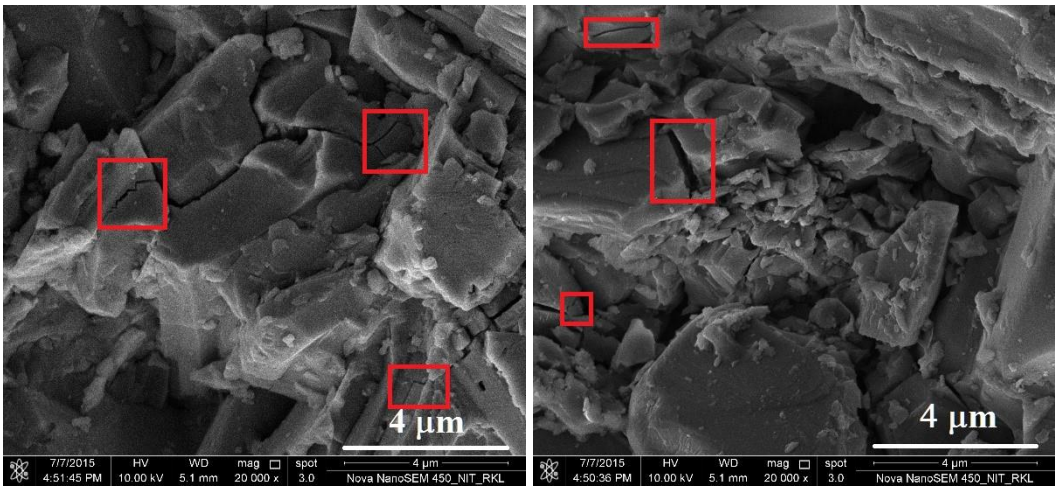

Figure 5.47: Microstructure showing microcracks in (a) spinel and (b) mullite sol containing compositions after 2nd thermal cycle.

For alumina and boehmite sol bonded compositions, the percent strength retainment capacity is comparatively higher even after 8 thermal cycles. The presence of comparatively higher porosity (lower BD among developed sol bonded compositions) might have balanced the effect of thermal shock. The gradual and slow degradation in strength retainment capacity of the two compositions might be due to higher porosity that caused crack blunting. Crack blunting is the phenomena in which thermal shock cracks lose their sharp crack tips or it is blunted, once interacted with a pore and thus the crack movement is restricted. Also, both the compositions are composed of only alumina particles, and hence the effect of thermal mismatching as in the case of mullite and spinel sol bonded compositions is absent.

For cement and silica sol bonded compositions, there is a drastic decrease of about 20% in the strength retainment capacity just after 2nd cycle of thermal shock. For both the compositions, the strength retainment capacity is less than 60% after 8 cycles of thermal shock. The presence and

formation of various phases with different thermal expansion behavior in the cement and silica sol bonded compositions resulted in a higher degree of the thermal mismatch within the matrix, thus not able to counter balance the thermal shock and is responsible for the drastic fall in the strength.

5.5.5 Slag Corrosion study:

For the corrosion study of the castables, blast furnace slag (composition given in table 5.6) of basicity (CaO/SiO_2) 1.02 and liquidus temperature 1430^0C was used. From the vertical cut cross-sections of the castables, shown in figure 5.48, the depth of corrosion and slag penetration (depth of discoloration) was determined for the compositions. The extent of slag penetration in terms of the area was noted by the graphical method and is shown in figure 5.49.

The slag resistance (slag penetration) of the developed castables was also compared with that of commercially available silica sol bonded castables and conventional cement bonded castables. It can be observed from the image of the slag corroded samples that the actual corrosion (eating away of the surface) by the slag is minimal in the case of all developed sol bonded compositions. This can be attributed to the highly compact grain structure obtained from a highly pure castable composition without any low melting phases or eutectics.

From the image, it can also be observed that the slag penetration and slag corrosion in the spinel sol bonded composition is minimum, while in silica sol bonded composition, it is maximum among all the sol bonded compositions. The higher bulk density or lower porosity and the highly pure chemistry of the spinel bonded composition are responsible for lower slag penetration and corrosion of the castables. In the case of silica sol bonded composition, the higher silica (SiO_2) content might be responsible, that has reacted with the impurity cations coming from the slag and cause for greater slag penetration.

Table 5.6: Chemical composition of blast furnace slag.

CaO	SiO_2	Al_2O_3	MgO	MnO	FeO	Sulphur
32.25 %	31.66 %	24.00 %	5.92 %	1.25 %	0.8 %	0.8 %

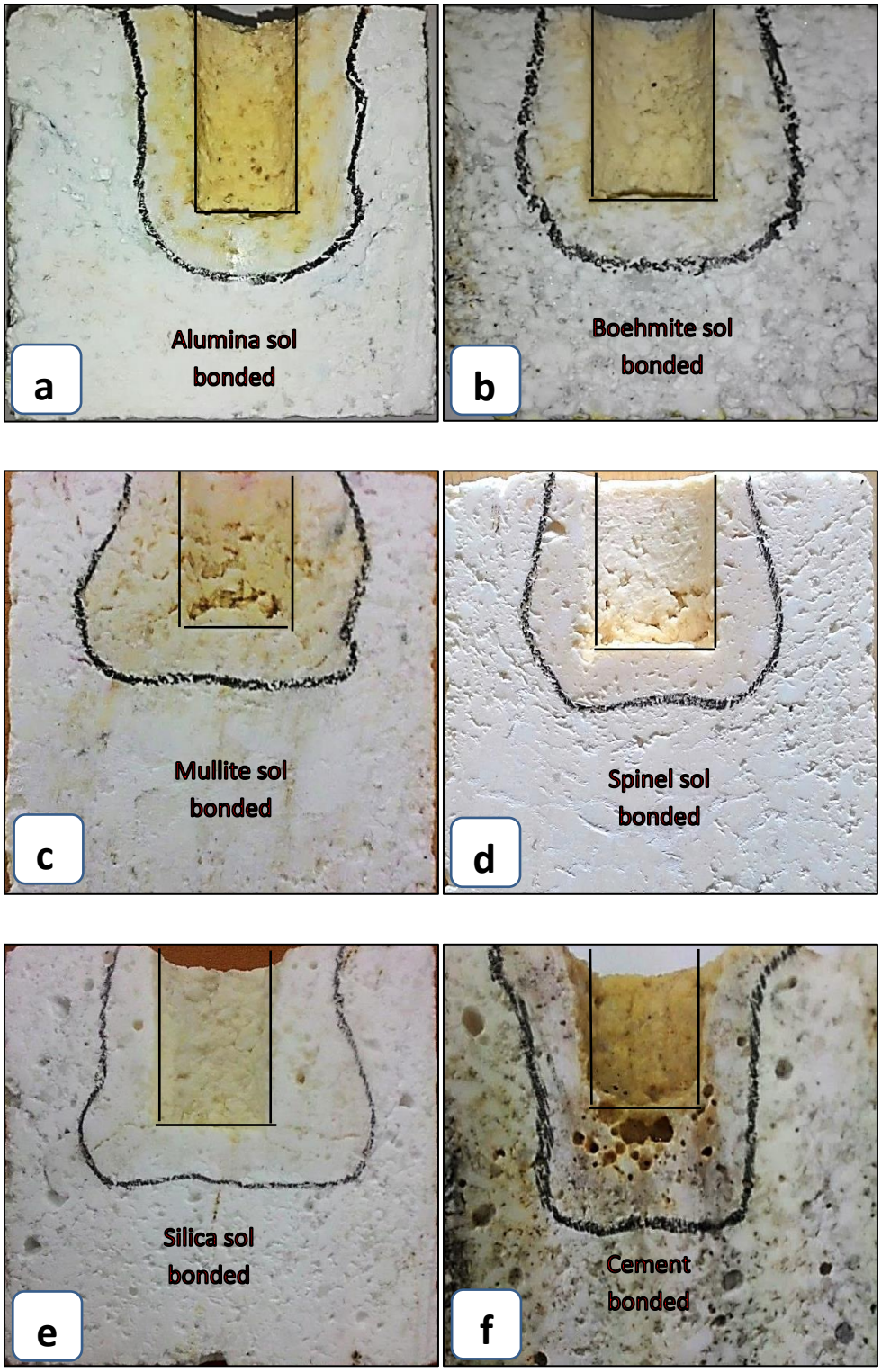

Figure 5.48: Slag corroded castables bonded by (a) alumina sol (b) boehmite sol (c) mullite sol (d) spinel sol (e) silica sol and (f) cement

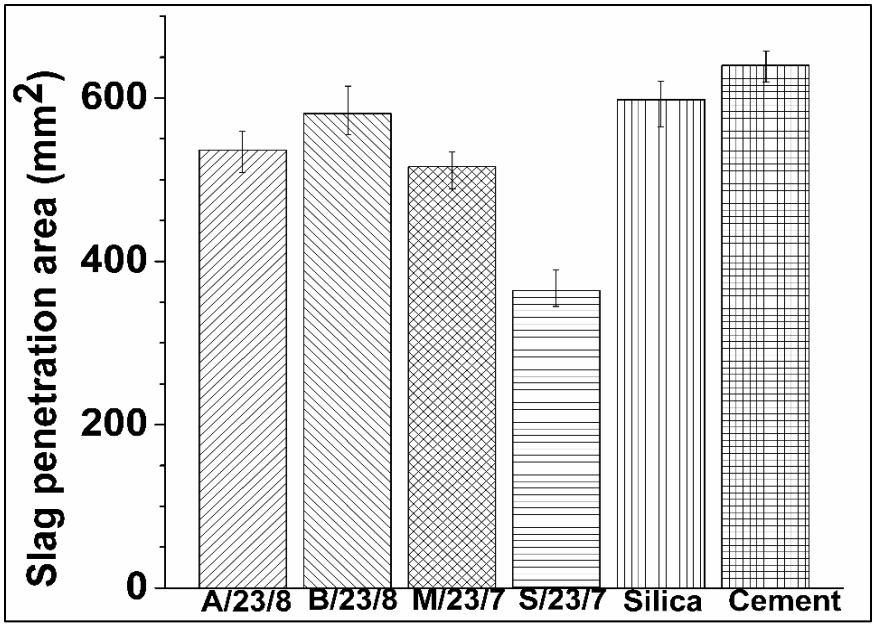

Figure 5.49: Slag penetration area of different castables

For cement bonded composition, it can be seen that besides higher slag penetration, there is also some corrosion (eating away of the surface) happening near the slag-refractory interphase. The presence of CaO and SiO_2, besides other impurities, in the cement binder and that coming from slag melt results in a number of low melting phases in the slag melt. The finer alumina matrix being soluble in these liquid phases, results in the higher corrosion of the cement bonded compositions. In all other batches, the binders have highly pure chemistry without the presence of any impurity phases and as a result, the amount of liquid phase generation is less and hence less penetration and corrosion activity is observed in the rest of the compositions.

5.5.6 Microstructural study of the slag corroded region

The microstructures of the slag corroded samples of the developed sol bonded compositions shows similar characteristics. All the microstructures (Figure 5.50 – 5.53) show some plate-like structures more or less homogenously distributed on the whole corroded surface. The elemental analysis of these plates like structures confirms the presence of only Al as the major element with some amount of Ca and O in it, indicating the formation of some high alumina bearing calcium aluminate phases. [Some Au (gold) peaks are also found coming from the coating done on the sample]. These are possibly calcium hexa-aluminate, CA_6 ($CaAl_{12}O_{19}$), crystals formed locally due to the reaction between the CaO component of the slag melt and fine reactive

alumina from the castable matrix. This plate-like CA_6 formation was also found by Chandradass and Nagaoka [5.41-5.42]. The elemental study of the matrix region of the corroded areas also shows Al as the major element with O and little amount of Ca and Si coming from the slag. The matrix thus may contain various other impurity oxides, mainly CaO and SiO_2, coming from the slag and may form low melting compounds in the system Al_2O_3-CaO-SiO_2, besides other impurities like MgO, MnO_2, TiO_2, Fe_2O_3, etc.

The microstructural and elemental analysis of the corroded region of the alumina and boehmite sol bonded compositions is similar in nature because of a similar chemical constituent. The corroding (penetrating) activity in alumina sol bonded composition is little less due to compact microstructure than boehmite sol bonded composition. In the case of mullite and spinel bonded compositions, the corroding activity is even less. The developed mullite (minor phase) phase, forming from the sol, with orthorhombic crystal structure has oxygen vacancies and is able to accommodate many cations like Ti, Mg, Fe, etc. The developed mullite thus adsorbed many cations from the liquid slag changing its composition and viscosity resulted in a decrease in slag penetration [5.43]. Similar to mullite, the in-situ spinel (minor) phase, formed from the precursor sol, with orthorhombic crystal structure has lattice vacancies and can entrap many cations like Ti, Mg, Fe, Mn, etc. The developed spinel, thus, adsorbed many cations from the infiltrating liquid slag, changing its composition and viscosity, and inhibit slag penetration [5.39, 5.43]. The formation of CA_6 in the slag corroded portion actually reduces the lime content of the slag composition, resulting in a CaO depleted slag having a higher viscosity which has less corroding activity with the refractory. Thus, the corrosion effect in sol bonded containing composition is further lowered.

In cement bonded compositions too, the microstructure (Figure 5.54a) contains the platy crystal structures but more in number. The high amount of CaO coming from the binder as well as from the slag dissolves the finer alumina matrix causing greater corrosion as can be evident from the image of the corroded sample in figure 5.48f. The matrix region (figure 5.54b) is fused with various low melting liquid phases formed from the reaction between the impurities coming from the slag and the binder cement. The formation of these low melting compounds is responsible for the reduction in strength values at high temperatures as can be seen from the HMoR and TSR values of the cement bonded compositions.

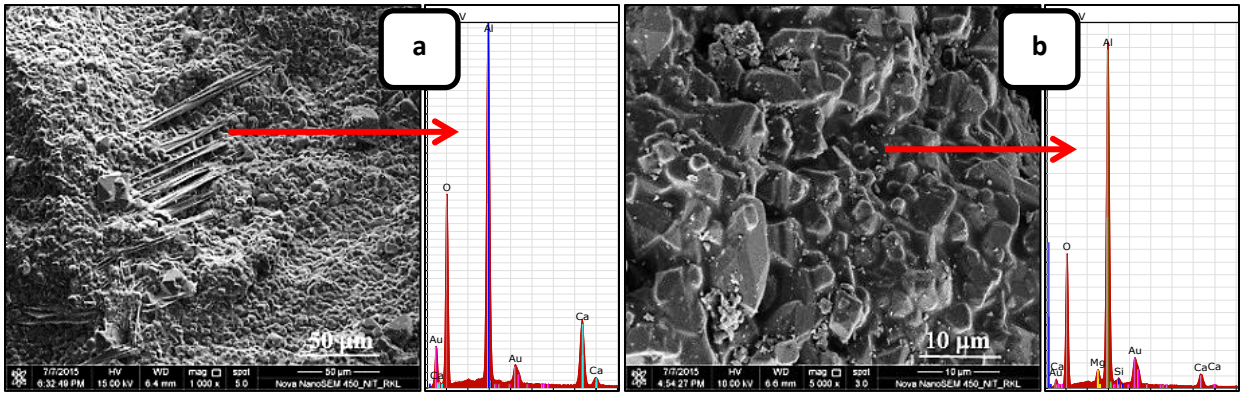

Figure 5.50 Microstructure and EDX analysis of (a) plate-like structure (b) matrix of corroded surface of alumina sol bonded composition.

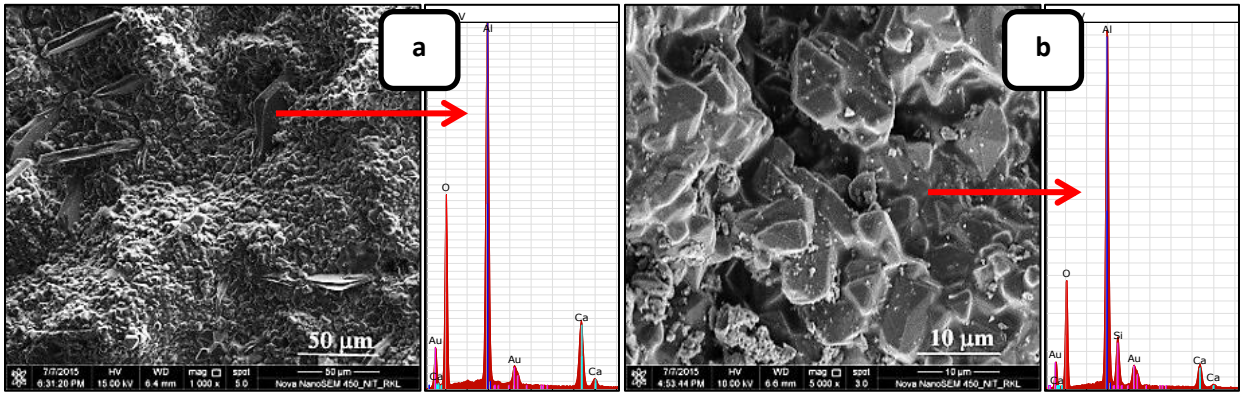

Figure 5.51 Microstructure and EDX analysis of (a) plate-like structure (b) matrix of corroded surface of boehmite sol bonded composition.

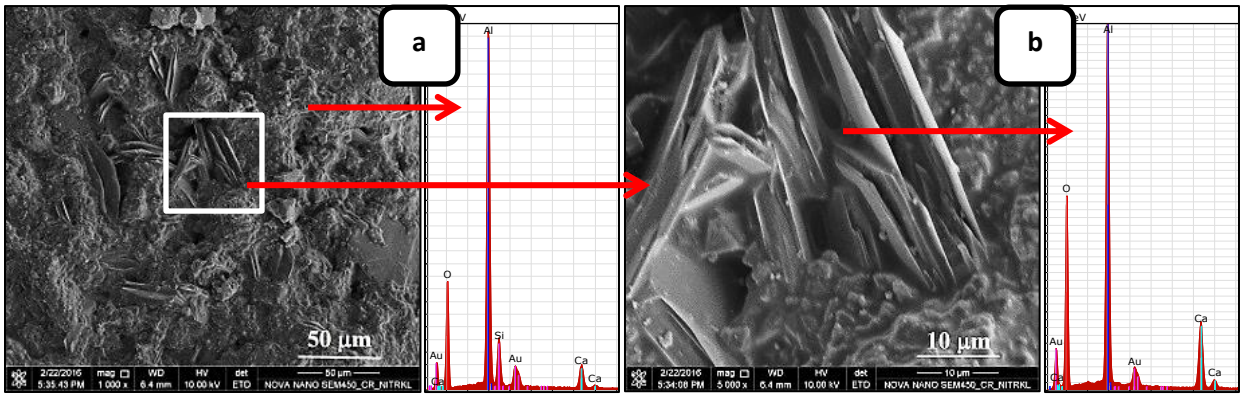

Figure 5.52 Microstructure and EDX analysis of (a) matrix (b) plate-like structure of corroded surface of mullite sol bonded composition.

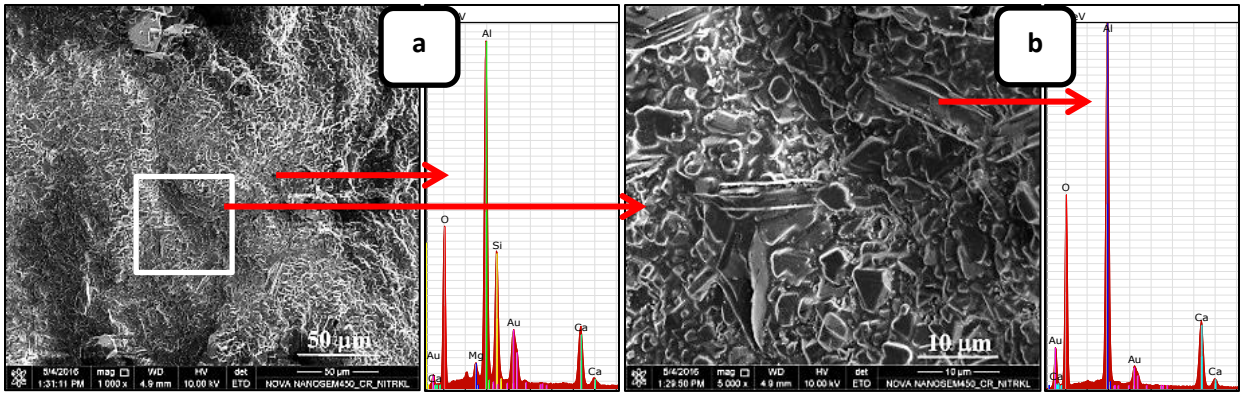

Figure 5.53 Microstructure and EDX analysis of (a) matrix (b) plate-like structure of corroded surface of spinel sol bonded composition.

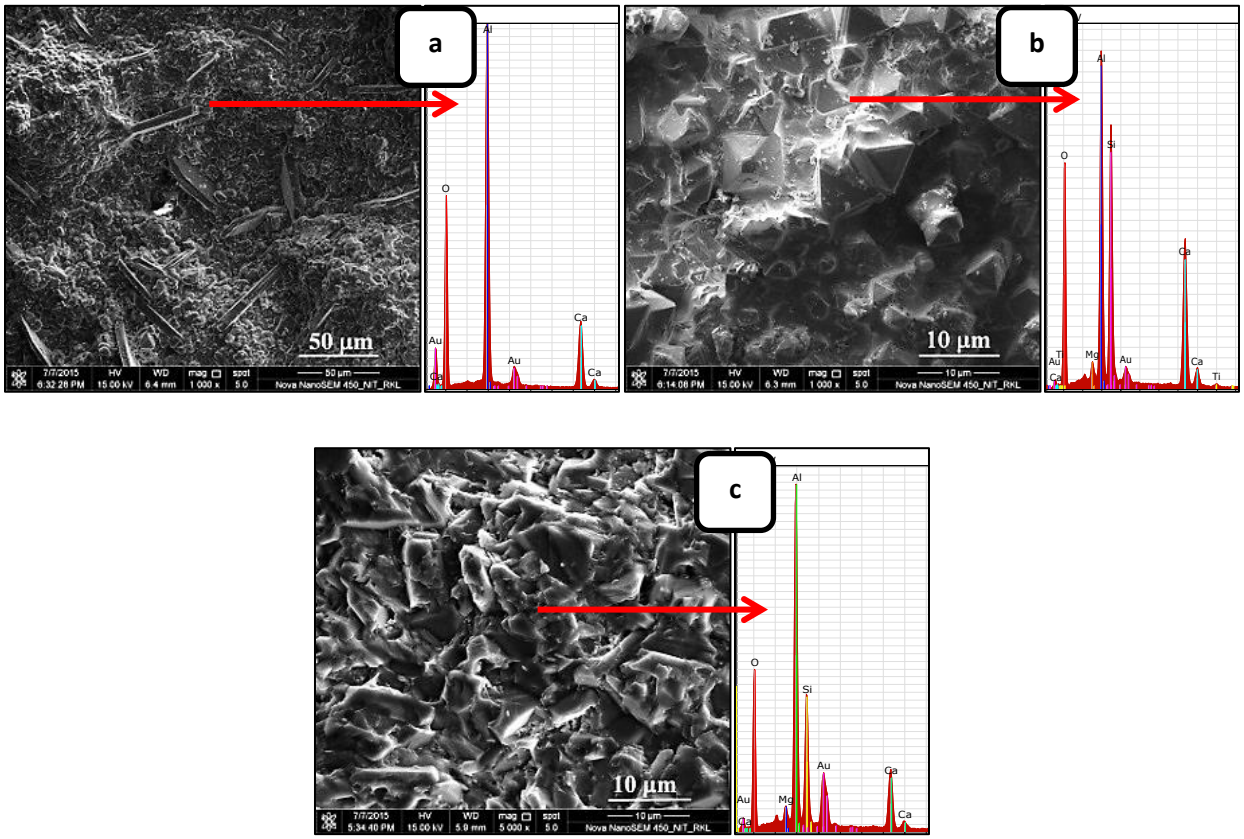

Figure 5.54 Microstructure and EDX analysis of (a) plate-like structure, and (b) matrix of corroded cement bonded composition and (c) matrix of corroded silica sol bonded composition.

For the silica sol bonded castable, the analysis of the slag corroded region in (figure 5.54c) shows a microstructure without sharp grain boundaries and edges with fused mass appearances over the entire surface due to the reaction between the fine castable matrix and the slag melt. The reaction between the fine castable matrix composed of alumina fines and silica (minor phase) coming from sol and the slag melt results in a number of low melting phases. The exact phase of the fused mass is difficult to determine but it is possibly a mixture of calcium aluminum and magnesium silicates as evident from the EDAX analysis. The presence of fused mass over the entire corroded surface is an indication of more amount of liquid phase generation during the reaction between the refractory component with higher silica content and slag melt.

5.5.7 Summary of the section:

The developed sol bonded compositions have bulk densities comparable to commercial silica and cement bonded compositions at all temperatures. The densities obtained in the developed sol bonded compositions are affected by the solid content of the developed sols as well as on the gelling tendency of the colloidal particles present in the sol. Among the developed sol bonded compositions, spinel sol bonded compositions acquired highest bulk density even greater than the commercial counterparts.

The strength obtained by the developed compositions at the green stage is quite low in comparison to the commercial binders. This can be attributed to the weak coagulation bonding in the developed sol bonded compositions due to lower solid content. The commercial silica sol bonded composition which has a higher solid content, obtained strength comparable to commercial cement binder at green stage. The developed sol bonded compositions do not show any reduction in strength at intermediate temperatures as generally observed for hydraulic cement binders due to early initiation of sintering between the particles of the sol binder and the finer matrix components resulting in early densification of the castables.

The strength obtained by the developed sol bonded compositions at the peak temperature of 1650^0C is dependent on various factors like the solid content, particles size, gelling tendency and the in-situ reaction taking place at higher temperatures. Among the developed sol, mullite sol bonded composition acquires the greatest strength at peak temperature. Though it is less than the

strength of the commercial cement bonded composition, but it is greater than the commercial silica sol bonded composition.

All the developed sol bonded compositions show better hot strength, than the commercial binders due to lack of any impurity in their composition. The presence of impurities resulted in low melting phase formation in the commercial binder compositions leading to a reduction in strength at the hot condition or at high temperature. Among the developed sol bonded composition, spinel and mullite sol bonded compositions shows better hot strength.

The thermal shock resistance of the developed compositions is also better than the commercial binders. The high permeability of the alumina and boehmite composition and the micro-cracking effect in the spinel and mullite composition resulted in better thermal shock resistance as compared to commercial binders. The spinel sol bonded composition shows the highest resistance to thermal shock compared to all other compositions. The mullite bonded composition resistance to thermal shock was better up to 4 cycles, but after than degraded abruptly.

All the developed sol bonded compositions show better corrosion resistance against blast furnace slag at 1500^0C compared to commercial binders. The low temperature sintering of the finer alumina matrix and the colloidal particles of the developed sols resulted in a compact and consolidated microstructure hindering the corroding activity (penetration) of the slag melt. Also, the absence of any impurity or low melting phase formation at higher temperature further increases the corrosion resistance of the developed compositions. Among the developed sol spinel bonded composition showed the highest corrosion resistance whereas the commercial cement bonded composition showed the least corrosion resistance.

Chapter 6

Conclusion

6.1 Conclusion:

1. **The developed alumina, boehmite, mullite and spinel sols showed stability for more than a month with least stability observed for spinel sols responsible for its higher gelling tendency.**

   The different sol systems were synthesized by the wet chemical method using simple inorganic precursors and were characterized for solid content, DSC-TG, FTIR, microstructure and phase analysis at different calcination temperatures.

2. **The various sol characterization techniques confirmed phase pure nano oxides formation after calcination from respective sols.**

   All the sol systems resulted in pure and desired oxide phase on calcination. The alumina and boehmite sol resulted in α-alumina phase on calcination above 1000^0C. The mullite formation from developed mullite sol takes place on calcination around 1100-1200^0C. Similarly, the formation of magnesium aluminate spinel phase from the developed sol is observed between 400-500^0C.

3. **The developed sol bonded castables showed well sintered density and strength compared to traditional cement and silica sol bonded castables. The densities (3.0-3.2 g/cc) obtained signifies a well compact microstructure, as also observed in the microstructural analysis.**

   The developed compositions obtained bulk densities comparable to commercial binders at all temperatures. The sol containing compositions showed lower green strength due to weak coagulation bonding and lower solid content of the sol. But strong sintering due to the presence of finer sol particles enhances the strength considerably on firing. The low temperature formation of various nano oxides phases resulted in the early initiation of sintering in the castable matrix.

4. **Considerably high hot strength and higher thermal shock resistance are observed for the developed sol containing compositions, higher than the commercial binders, due to the absence of any impurity phase.**

All the developed compositions have highly pure chemistry and lack any impurity phases in their composition. Impurities resulted in low melting phases at high temperature and affect the hot properties which are not observed in any of the developed compositions. Also, the lack of any thermal mismatch and high permeability (than other compositions) of the alumina and boehmite compositions and the micro-cracking effect in the spinel and mullite composition resulted in better thermal shock resistance as compared to commercial binders.

5. **Among the developed sol containing compositions, mullite sol bonded one showed highest compressive strength, whereas hot properties are better in spinel bonded compositions.**

   The compressive strength of the developed compositions is dependent on particle size distribution, the solid content of the developed sol, etc. The mullite sol bonded compositions showed the best performance for compressive strength, may be associated with the higher solid content. For hot strength, the spinel sol bonded composition performed better among all the compositions including traditional binders, dense structure and absence of any low melting phases in the system may be the reason for such improvement.

6. **Also, the corrosion resistance of the developed castables was found to be better than the commercial binder containing compositions and spinel bonded composition was found to produce best results.**

   All the developed compositions showed better corrosion resistance against blast furnace slag compared to commercial binders. High pure matrix phase and presence of finer particles in the developed sol containing systems resulted in a purer and compact structure thus reducing the corroding activity (penetration) of the slag melt. Formation of low melting phases in traditional binder systems resulted in poor corrosion properties.

7. **The developed compositions are suitable for applications at the temperature of 1650^0C and above.**

   All the developed sol containing compositions showed no deformation or any considerable shrinkage even on firing at 1650^0C, indicating its application at and above this temperature without any difficulty. However, conventional cement and silica containing compositions resulted in poor hot properties due to the formation of low melting compounds in the system.

6.2 Scope of future work:

- Increasing the solid content of the developed sols may further enhance the castable properties.
- Finding additives which enhance the green strength, without compromising the high temperature structural strength.
- Further characterizations of the developed compositions such as abrasion resistance, RUL, creep, etc.
- Analyzing corrosion behaviour by dynamic slag corrosion test like rotary slag test.
- Bulk manufacturing of the developed sols and industrial trial of the castable compositions.
- Development of other sol systems like magnesia, chromia, titania, zirconia, etc. to use as binders for refractory castables.
- Searching for sol synthesis with other routes like using urea or ammonia salts.

References

Chapter 1 Introduction

1.1 S. Musikant, What Every Engineer Should Know About Ceramics, Preface, Marcel Dekker Inc., New York, [1991].

1.2 W.D. Kingery, H.K. Bowen and D.R. Uhlmann, Introduction to Ceramics, pp.690, Wiley-Interscience, 2nd Edition, [2006].

1.3 C.A. Krause, Refractories: The Hidden Industry. American Ceramic Society, Columbus, OH, [1987].

1.4 G. Lewis, Applications for Traditional Ceramics, Refractories, pp.895–918 In, Engineered Materials Handbook, Vol. 4, Ceramics and Glasses. ASM International, OH, [1991].

1.5 W.E. Lee, R.E. Moore, Evolution Of In Situ Refractories in the 20th Century, J. Am. Ceram. Soc., 81[6], pp.1385–410, [1998].

1.6 A. Bhatia, Overview of Refractory Materials, PDH online Course M158 (3 PDH), PDH Centre, VA, US, [2012] (http://www.pdhonline.com/courses/m158/m158content.pdf).

1.7 Furnaces and Refractories (http://www.moderneq.com/pdf/Refractories.pdf).

1.8 Introduction To Refractories, Chapter 12, In, the Manual for Construction, Operation and, Troubleshooting for Glass Melting Pot Furnace, Complete Network for Small and Micro Learning Enterprise, India (http://www.cosmile.org).

1.9 Refractory Materials, Lecture 9, National Programme on Technology Enhanced Learning, MHRD, Govt. of India (http://nptel.ac.in/courses/113104059/lecture_pdf/Lecture%209.pdf).

1.10 O.P. Gupta, Refractories, In, Elements of Fuels. Furnaces and Refractories, Khanna Publishers, India, [2002].

1.11 J. H. Chesters, Refractories: Production And Properties, Iron And Steel Institute, London, [1973]

1.12 W. E. Lee, W. Vieira, S. Zhang, K. G. Ahari, H. Sarpoolaky and C. Parr, Castable Refractory Concrete, Intern. Mat. Rev., 46[3], pp.145-167, [2001].

1.13 Z. Li, G. Ye, Bonding and Recent Progress of Monolithic Refractories, Interceram. 41[3], pp.169-173, [1992].

1.14 S. Banerjee, Recent Developments in Monolithic Refractories, Ceram. Bull., 77[90], pp.59-63, [1998].

1.15 P. Pilate, J. Tirlocq, F. Cambier, Refractory Castables: An Overview, Ceramic Forum International, 84[6], pp.43-49, [2007].

1.16 M. Ishikawa, Refractory Castables, Taikabutsu, 51[4], pp.170-178, [1999].

1.17 K.M. Parker, J.H. Sharp, Refractory Calcium Aluminate Cements, Trans. Brit. Ceram., 81, pp.35–42, [1982].

1.18 M. R. Ismael, R. Salomao, V. C. Pandolfelli, A Combined Binding System For Refractory Castables Based On Colloidal Silica And Hydratable Alumina, American Ceramic Society Bulletin, 86[9], pp.58–61, [2007].

1.19 C. D. Parr, C. Revais, H. Fryda, The Nature Of Chemical Reactions That Occur During Castable Installation And Analytical Techniques Used To Follow These Reactions, Ceramic Transaction 12: Fundamentals Of Refractory Technology, Eds J.P.Bennett, J.D. Smith, Amer. Ceram Soc., pp.53-71, [2001].

1.20 C. Alt, C. Parr and C. Revais, The Effect of Environmental Temperature Conditions on the Rheology of Deflocculated Refractory Castable, Refrac. Appl. and News, 7[1], pp.9-15, [2002].

1.21 T.H. Bier, N.E. Bunt, C. Parr, Calcium Aluminate Bonded Castables – Their Advantages and Applications, Alafar proceedings, Bariloche, Argentina, Vol. 2, pp.73-84. [1996].

1.22 IFGL Refractories Product Datasheet, [2016].

1.23 TRL Krosaki Product Data Sheet, [2016].

1.24 S. Banerjee, Versatility of Gel-Bond Castable/Pumpable Refractories, Refractories Applications and News, 6[1], pp.3–5, [2001].

1.25 http://www.sevenrefractories.com/steel-ladle.

1.26 http://www.sevenrefractories.com/casthouse-engineering.

1.27 http://www.sevenrefractories.com/electric-arc-furnace.

…….

Chapter 2 Literature Review

…….

2.1 W.W. Perkins, Ceramic Glossary, The American Ceramic Society, pp.71, [1984].

2.2 Furnaces and Refractories (http://www.moderneq.com/pdf/Refractories.pdf).

2.3 Introduction To Refractories, Chapter 12, In the Manual for Construction, Operation and, Troubleshooting for Glass Melting Pot Furnace, Complete Network for Small and Micro Learning Enterprise, India (http://www.cosmile.org).

2.4 A. Bhatia, Overview of Refractory Materials, PDH online Course M158 (3 PDH), PDH Centre, VA, US, [2012]. (http://www.pdhonline.com/courses/m158/m158content.pdf).

2.5 Refractory Materials, Lecture 9, National Programme on Technology Enhanced Learning, MHRD, Govt. of India. (http://nptel.ac.in/courses/113104059/lecture_pdf/Lecture%209.pdf).

2.6 O.P. Gupta, Refractories, In, Elements of Fuels Furnaces and Refractories, Khanna Publishers, India, [2002].

2.7 J.H. Chesters, Refractories: Production and Properties, Iron and Steel Institute, London, [1973].

2.8 W.E. Lee, W. Vieira, S. Zhang, K.G. Ahari, H. Sarpoolaky and C. Parr, Castable Refractory Concrete, Intern. Mat. Rev., 46[3], pp.145-167, [2001].

2.9 Z. Li, Bonding and Recent Progress of Monolithic Refractories, Interceram. 41[3], pp.169-173, [1992].

2.10 R. Sarkar, Refractory Technology: Fundamentals and Applications, CRC Press, [2016].

2.11 J. Arnould, Un Ciment Hydraulique Refractaire, Chimie et Industrie, 15[2], [1922].

2.12 T.D. Robson, Refractory Concretes: Past Present And Future, Refractory Concrete, American Concrete Institute, Detroit, pp.1-10, [1978].

2.13 S. Banerjee, Monolithic Refractories: A Comprehensive Handbook, Wiley, [1998].

2.14 B. Clavaud, J.P. Kiehl, J.P. Radal, A new generation of low-cement Castables, pp.274-284, R.E. Fisher (Ed.), Advances in Ceramics, Vol.13, New Developments in Monolithic Refractories, Am. Ceram. Soc., Columbus, OH, [1985].

2.15 J.P. Kiehl , V. Jost and B. Clavaud, Low Lime Content Hydraulic Cements And Concretes Which Contain Them, US Patent 4111711, Sep 5 [1978].

2.16 S. Banerjee, Recent Developments in Monolithic Refractories, Ceram. Bull., 77 [90], pp.59-63, [1998].

2.17 M.R. Ismael, R. Salomao, V.C. Pandolfelli, A Combined Binding System For Refractory Castables Based On Colloidal Silica And Hydratable Alumina, American Ceramic Society Bulletin, 86, pp.58–61, [2007].

2.18 M. Ishikawa, Refractory Castables, Taikabutsu, 51[4], pp.170-178, [1999].

2.19 P. Pilate, J. Tirlocq, F. Cambier, Refractory Castables: An Overview, Ceramic Forum International, 84[6], pp.43-49, [2007].

2.20 K.M. Parker, J.H. Sharp, Refractory Calcium Aluminate Cements, Trans. Brit. Ceram., 81, pp.35–42, [1982].

2.21 W.T. Bakker, Refractory Concrete, American Concrete Institute Publication, SP- 57, 2, pp.11, [1978].

2.22 http://www.mdpi.com/1996-1073/8/11/12329/htm

2.23 Kenneth A. McGowan, Calcium aluminate clinker as a refractory aggregate with and without barium addition and use thereof US 8123853 B2, Feb 28, 2012

2.24 Y. Hongo, ρ-Alumina Bonded Castable Refractories, Taikabutsu Overseas, 40[4], pp.226–229, [1988].

2.25 W. Ma, P.W. Brown, Mechanisms of Reaction of Hydratable Aluminas, Journal of the American Ceramic Society, 82[2], pp.453–456, [1999].

2.26 B. Myhre and B. Sandberg, Mullite formation in tabular alumina based refractory castables with hydraulic alumina as binder, In: The 97th Annual Meeting of the American Ceramic Society, Ohio, USA, [1995].

2.27 B. Myhre and K. Sunde, Alumina based castables with very low contents of hydraulic compound. Part I: The effect of binder and particle-size distribution on flow and set. In Proc. UNITECR-95, pp.309-316, Kyoto Japan, [1995].

2.28 B. Myhre and K. Sunde, Alumina based castable with very low contents of hydraulic compound. Part II: Strength and high temperature reactions of no cement castables with hydraulic alumina and micro silica. In Proc. UNITECR-95, pp.317-324, Kyoto Japan, [1995].

2.29 S.C. Maestrelli, L.L.H.C. Ferreira and J.B. Baldo, The Effect Of Cement Substitution for ρ-Alumina Partial Additions On The Thermo-Mechanical Properties Of A Low Cement Refractory Concrete, In Proc. UNITECR-95, pp.337-345, Kyoto Japan, [1995].

2.30 M.W. Vance, K.J. Moody, Use Of Hydratable Alumina Binders In Refractory Compositions And Related Applications, Presented At The 97th American Ceramic Society Annual Meeting And Exposition, May 1, [1995].

2.31 F.A. Cardoso, M.D.M. Innocentini, M.F.S. Miranda, F.A.O. Valenzuela, V.C. Pandolfelli, Drying Behavior Of Hydratable Alumina-Bonded Refractory Castables, Journal Of The European Ceramic Society, 24[5], pp.797–802, [2004].

2.32 M.D.M. Innocentini, A.R.F. Pardo, V.C. Pandolfelli, Permeability Of High-Alumina Refractory Castables Based On Various Hydraulic Binders, Journal Of The American Ceramic Society, 85[6], pp.1517–1521, [2002].

2.33 R. Lorenz, G. Buchel, A. Buhr, J. Aronni., R. Racher, Improved Workability Of Calcia Free Alumina Binder Alphabond For Non-Cement Castables, In, Proceedings Of The 47th International Colloquium On Refractories, pp.67–71, Aachen, Germany, [2004].

2.34 New Almatis Alphabond 300 Global Product Data Sheet, Gp-Rcp/015/R04/1207/Msds 834, [2004]. (http://www.almatis.com/media/4024/gp-rcp_015_alphabond_300_0812.pdf).

2.35 C. Parr, C. Wohrmeyer, The advantages of calcium aluminate cement as a castable bonding system, In, Proceedings of St Louis Section Meeting of American Ceramic Society, St Louis USA, [2006].

2.36 W.D. Kingery, Fundamental Study of Phosphate Bonding In Refractories: 1, J. Am. Cera. Soc., 33[8], pp.239-241, [1950].

2.37 C. Toy and O.J. Whittemore, Phosphate Bonding with Several Calcined Aluminas, Ceramics International, 15, pp.167-171, [1989].

2.38 J.W. Lyon, G.J. Mac Ewan and C.D. Siebenthal, Phosphoric Acid in Soil Stabilization II. Secondary Additives, Acid Source and Mechanism, Highway Research Board Bulletin, 318, pp.15-24, [1962].

2.39 A.M. Gonçalves, A.M. Segadães, Unshaped Refractories with Chemical Bonding, Materials Science Forum, 34, pp.705-709, [1988].

2.40 W.D. Kingery, Phosphate Bonding in Refractories, D.Sc. thesis, MIT, [1950]. (https://dspace.mit.edu/bitstream/handle/1721.1/77868/29893269-MIT.pdf?sequence=2)

2.41 J.L. Dolph, Refractory Bonding Mortar, US Patent 3179526A, 20 Apr. [1965].

2.42 R.S. Kalyoncu, Chemically Bonded Refractories – A Review of the State of the Art, Bureau of Mines Information Circular 8878, pp. 1–20, Department of the Interior, US [1982].

2.43 M. Kataoka, Unshaped / Monolithic Refractories, In Refractories Handbook, The Technical Association of Refractories, Japan 1998, pp.215-238

2.44 S. Yue, Y. Qiu, P. Fan, P. Zhang and N. Zhang, Sodium Metasilicate Cemented Analogue Material and Its Mechanical Properties, Advances in Materials Science and Engineering, Vol. 2016, Article ID 3716145, 17 pages, [2016]. (http://dx.doi.org/10.1155/2016/3716145).

2.45 M. Nouri-Khezrabad, M.A.L. Braulio, V.C. Pandolfelli, F. Golestani-Fard, H.R. Rezaie Et Al, Nano-Bonded Refractory Castables, Ceramics International, 39[4], pp.3479–3497, [2013].

2.46 R.G. De Sa and W.E. Lee, Nanotechnology For The Refractories Industry—A Foresight Perspective, The Refractories Engineer, May, pp.12–19, [2007].

2.47 A.M. Garbers-Craig, Presidential Address: How cool are refractory materials?, J. S. Afr. Inst. Min. Metall., 108[9], pp.491–506, [2008].

2.48 V. Antonovic, I. Pundiene, R. Stonys, J. Cesniene and J. Keriene A Review Of The Possible Applications Of Nanotechnology In Refractory Concrete, Journal Of Civil Engineering And Management, 16[4], pp.595–602. [2010].

2.49 M.R. Ismael, R.D. Anjos, R. Salomao, V.C. Pandolfelli, Colloidal Silica As A Nanostructured Binder For Refractory Castables, Refractories Applications And News, 11[4], pp.16–20, [2006].

2.50 M.A.L. Braulio, C. Tontrup, J. Medeiros, V.C. Pandolfelli, Colloidal Alumina As A Novel Castable Bonding System, Refractories World-Forum, 3[3], pp.135–141, [2011].

2.51 M. Anderson, Better Refractories through Nanotechnology, Ceramic Industry Magazine, 155[10], pp.29–35, [2005].

2.52 T.R. Lipinski, E. Drygalska, C. Tontrup, The Influence Of Additions Of Nanostructured Al_2O_3 Powder On The High Temperature Strength Of High Alumina Refractories, In, Proceedings of UNITECR-09, pp.3, Salvador, Brazil, [2009].

2.53 T.R. Lipinski, C. Tontrup, The Use Of Nano-Scaled Alumina In Alumina-Based Refractory Materials, In, Proceedings of UNITECR-07, pp.391–393, Dresden, Germany, [2007].

2.54 M.A.L. Braulio, J.F.R. Castro, C. Pagliosa, L.R.M. Bittencourt, V.C. Pandolfelli, From Macro To Nano Magnesia: Designing The In Situ Spinel Expansion, Journal of The American Ceramic Society, 91[9], pp.3090–3093, [2008].

2.55 H.E. Bergna and W.O. Roberts, Colloidal Silica: Fundamentals and Applications, CRC Press, Tylor and Francis, Florida USA [2005].

2.56 S. Lin, M. Khine, Patterning Silica Islands Onto Thermoplastic Shrink Film, United States Patent Application, 20160169877, 16 June [2016].

2.57 S. Banerjee, Versatility of Gel-Bond Castable/Pumpable Refractories, Refractories Applications and News, 6[1], pp.3–5, [2001].

2.58 S. Ghosh, R. Majumdar, B.K. Sinhamahapatra, R.N. Nandy, M. Mukherjee and S. Mukhopadhyay, Micro Structures Of Refractory Castables Prepared With Sol Gel Additives, Ceram. Int., 29[6], pp.671–677, [2003].

2.59 J.E. Kopanda, G. MacZura, Production processes, properties and applications for calcium aluminate cements, L.D. Hart (Ed.), Alumina Chemical Science and Technology Handbook, pp.171–184, American Ceramic Society, Westerville, OH [1990].

2.60 H. Schneider, K. Okada and J.A. Pask, Mullite and Mullite Ceramics, John Wiley & Sons, New York, [1994].

2.61 A. Souri, F. Kashaninia, H. Sarpoolaki, Improving Thermo-Mechanical Properties Of Tabular Alumina Castable Via Using Nano-Structured Colloidal Silica, In, Proceedings Of 1st International Conference On Nanomaterials: Applications And Properties, pp.254–259, Crimea, Ukraine, [2011].

2.62 X. Jaquan, P. Yuntao, X. Dayong, M. Xuesong, The Characteristics Of Silica-Sol Combining Refractories, Advanced Materials Research, 396–398, pp.288–291, [2011].

2.63 M.A.L. Braulio, C. Tontrup, J. Medeiros, V.C. Pandolfelli, Colloidal Alumina as a Refractory Binder, In: Proceedings of 35th Alafar Congress, Lima, Peru, [2010].

2.64 P.C. Nordine, J.K. Richard Weber and J.J. Felten, Glass fiber having compositions of alumina-lanthana and made from undercooled molten materials, US6484539 B1, Nov 26, [2002].

2.65 R.K. Iler, The Chemistry of Silica: Solubility, Polymerization, Colloid and Surface Properties and Biochemistry, pp.866, Wiley-Blackwell, New York, [1979].

2.66 R.D. Dos Anjos, M.R. Ismael, R. Salomao, V.C. Pandolfelli, Rheometric Techniques Applied To Refractory Ceramic Suspensions, Refractories Applications and News, 11[2] pp.8-13, [2006].

2.67 M. Shojaie-Bahaabad, E. Taheri-Nassaj, Economical Synthesis Of Nano Alumina Powder Using An Aqueous Sol–Gel Method, Materials Letters, 62, pp.3364–3366, [2008].

2.68 J. Chengbin, Z. Xiujian and T. Haizheng, The Synthesis Of Stable, High Solid Content Alumina Sol, Journal Of Sol-Gel Science And Technology, 38[1], pp.19–23, [2006].

2.69 D.J. Suh, T-J Park, J.H. Kim and K.L. Kim, Fast Sol-Gel Synthetic Route To High-Surface-Area Alumina Aerogels, Chem. Mater., 9[9], pp.1903-1905, [1997].

2.70 K.R. Han, C.S. Lim, M-J Hong, J.W. Jang and K.S. Hong, Preparation Method of Sub-Micrometer-Sized α-Alumina by Surface Modification of γ-Alumina with Alumina Sol, J. Am. Ceram. Soc., 83[4], pp.750–754, [2000].

2.71 N. Dilsiz and G. Akovali, Study of Sol–Gel Processing For Fabrication of Low Density Alumina Microspheres, Materials Science and Engineering: A, 332[1-2], pp.91–96, [2002].

2.72 S. Zhang, W.E. Lee, Improving the Water-Wettability and Oxidation Resistance of Graphite Using Al2o3/Sio2 Sol-Gel Coatings, Journal of the European Ceramic Society, 23, [2003] pp.1215–1221.

2.73 J. Chandradass, M. Balasubramanian, Sol–Gel Processing of Alumina Fibres, Journal of Materials Processing Technology, 173[3], pp.275–280, [2006].

2.74 S. Yilmaz, Y. Kutmen-Kalpakli, E. Yilmaz, Synthesis and Characterization of Boehmitic Alumina Coated Graphite by Sol–Gel Method, Ceramics International, 35[5], pp.2029–2034, [2009].

2.75 F. Mirjalili, L.C. Abdullah, H. Mohamad, A. Fakhru'l-Razi, A.B.D. Radiah, and R. Aghababazadeh, Process For Producing Nano-Alpha-Alumina Powder, ISRN Nanotechnology, [2011], Article Id 692594, [2011]. (doi:10.5402/2011/692594).

2.76 T. Maki and S. Sakka, Preparation of Alumina Fibers by Sol-Gel Method, Journal of Non-Crystalline Solids, 100[1-3], pp.303-308, [1988].

2.77 R. Venkatesh, P.K. Chakrabarty, B. Siladitya, M. Chatterjee and D. Ganguli, Preparation Of Alumina Fibre Mats By A Sol-Gel Spinning Technique, Ceramics International, 25[6], pp.539-543, [1999].

2.78 M. Chatterjee, M.K. Naskar, P.K. Chakrabarty and D. Ganguli, Sol-Gel Alumina Fibre Mats For High-Temperature Applications, Materials Letters, 57[1], pp.87– 93, [2002].

2.79 A. Sedaghat, E. Taheri-Nassaj, R. Naghizadeh, An Alumina Mat With A Nano Microstructure Prepared By Centrifugal Spinning Method, Journal Of Non-Crystalline Solids, 352[26-27], pp.2818–2828, [2006].

2.80 P.V. Krivoshapkin, E.F. Krivoshapkina and B.N. Dudkin, Growth and Structure of Microscale Fibers as Precursors Of Alumina Nanofibers, Journal Of Physics And Chemistry Of Solids, 74[7], pp.991–996, [2013].

2.81 E. Ponthieu, E. Payen And J. Grimblot, Ultrafine Alumina Powders Via A Sol-Emulsion-Gel Method, Journal Of Non-Crystalline Solids, 147&148, pp.598-605, [1992].

2.82 E. Morgado, Jr., Y.L. Lam and L.F. Nazar, Formation of Peptizable Boehmites by Hydrolysis of Aluminum Nitrate in Aqueous Solution, Journal of Colloid and Interface Science, 188[2], pp.257–269, [1997].

2.83 N. Yao, G. Xiong, Y. Zhang, M. He and W. Yang, Preparation of Novel Uniform Mesoporous Alumina Catalysts by the Sol–Gel Method, Catalysis Today, 68[1-3], pp.97–109, [2001].

2.84 M.I.F. Macedo, C.C. Osawa and C.A. Bertran, Sol-Gel Synthesis Of Transparent Alumina Gel And Pure Gamma Alumina By Urea Hydrolysis Of Aluminum Nitrate, Journal Of Sol-Gel Science And Technology, 30[3], pp.135–140, [2004].

2.85 M.R. Karim, M.A. Rahman, M.A.J. Miah, H. Ahmad, M. Yanagisawa and M. Ito, Synthesis of γ–Alumina Particles And Surface Characterization, The Open Colloid Science Journal, 4[5], pp.32-36, [2011].

2.86 J. Li, Y. Pan, C. Xiang, Q. Ge and J. Guo, Low Temperature Synthesis Of Ultrafine α-Al_2O_3 Powder By A Simple Aqueous Sol–Gel Process, Ceramics International 32[5], pp.587–591, [2006].

2.87 A. Rajaeiyan and M.M. Bagheri-Mohagheghi, Comparison Of Urea And Citric Acid Complexing Agents And Annealing Temperature Effect On The Structural Properties Of γ- And α-Alumina Nanoparticles Synthesized By Sol-Gel Method, Advances In Materials Science And Engineering, Vol. 2013, Article Id 791641, 9 Pages [2013]. (http://dx.doi.org/10.1155/2013/791641).

2.88 B.P. Singh, S. Bhattacharjee and L. Besra, Influence Of Surface Charge On Maximizing Solids Loading In Colloidal Processing Of Alumina, Materials Letters, 56[4], pp.475–480, [2002].

2.89 B.P. Singh, R. Menchavez, C. Takai, M. Fuji and M. Takahashi, Stability Of Dispersions Of Colloidal Alumina Particles In Aqueous Suspensions, Journal Of Colloid And Interface Science, 291[1], pp.181–186, [2005].

2.90 L. Chera, E. Palcevskis, M. Berzins, A. Lipe and I. Jansone, Dispersion of Nanosized Ceramic Powders in Aqueous Suspensions, Journal of Physics: Conference Series, 93[1], pp.1-5, [2007].(doi:10.1088/1742-6596/93/1/012010).

2.91 M. Thiruchitrambalam, V.R. Palkar and V. Gopinathan, Hydrolysis of Aluminum Metal and Sol–Gel Processing of Nano Alumina, Materials Letters, 58[24], pp.3063–3066, [2004].

2.92 K.R. Han S.W. Park, C.S. Kim and J.O. Yang, Unshaped Refractory Composition Added With Alumina Sol Binder, International Patent WO 2011/115352, [2011].

2.93 S. Mukhopadhyay, S. Dutta, M. Majumdar, A. Kundu, S.K. Das, Synthesis And Characterization Of Alumina Bearing Sol For Application In Refractory Castables, Industrial Ceramics, 20[2], pp.88-92, [2000].

2.94 S. Mukhopadhyaya and S.K. Das, Role of Alumina Sol on the Physical Properties of Low Cement Castables, Transactions of the Indian Ceramic Society, 59[3], pp.68-74, [2000].

2.95 S. Mukhopadhyay, S. Mahapatra, P. Mukherjee, T. Dasgupta and S.K. Das, Effect Of Alumina Sol In No-Cement Refractory Castables, Transactions Of The Indian Ceramic Society, 60[2], pp.63-67, [2001].

2.96 S. Mukhopadhyay, M. K. Mahapatra, P.K. Mondal and S.K. Das, Alumina and Silica Sols as Binders In A Typical ULC Castable, Transactions Of The Indian Ceramic Society, 62[2], pp.106-111, [2003].

2.97 E. Yilmaz and S. Yilmaz, Investigation of Properties of Boehmitic Sol Coated Graphite Added Alumina-Low Cement Castables, Journal of Ceramic Processing Research, 11[1], pp.56-60, [2010].

2.98 K.R. Han, S.W. Park, C.S. Kim and J.O. Yang, Alumina Bonded Unshaped Refractory and Manufacturing Method Thereof, Int. Patent, WO 2011/115353, [2011].

2.99 M.A.L. Braulio, G.G. Morbioli, J. Medeiros, J.B. Gallo, V.C. Pandolfelli, Nano-Bonded Wide Temperature Range Designed Refractory Castables, J. Am. Ceram. Soc., 95[3], pp.1100–1104, [2012].

2.100 P.C. Dokko, J.A. Pask and K.S. Mazdiyasni, High-Temperature Mechanical Properties of Mullite under Compression, J. Am. Ceram. Soc., 60[3-4], pp.150–155, [1977].

2.101 I. Jaymes, A. Douy, D. Massiot and J.P. Coutures, Characterization of Mono- And Diphasic Mullite Precursor Powders Prepared By Aqueous Routes, ^{27}Al and ^{29}Si MAS-NMR Spectroscopy Investigations. J Mater Sci., 31[17], pp.4581–4589, [1996].

2.102 L.S. Cividanes, T.M.B. Campos, L.A. Rodrigues, D.D. Brunelli and G.P. Thim, Review Of Mullite Synthesis Routes By Sol–Gel Method, J. Sol-Gel Sci. Technol., 55[1], pp.111-125, [2010].

2.103 C.C. Osawa, Efeito do pH e da uréia na síntese de mulita pelo método sol-gel, a partir de sóis de sílica e alumina, Diss. Mestrado, Universidade Estadual de Campinas - Unicamp, Campinas, SP, Brasil [2004] (In Portuguese).

2.104 I. Jaymes, A. Douy, D. Massiot and J-P. Busnel, Synthesis of a Mullite Precursor from Aluminum Nitrate and Tetraethoxysilane via Aqueous Homogeneous Precipitation: An ^{27}Al and ^{29}Si Liquid- And Solid-State NMR Spectroscopic Study, J. Am. Ceram. Soc., 78[10], pp.2648–2654, [1995].

2.105 S. Sundaresan and I.A. Aksay, Mullitization of Diphasic Aluminosilicate Gel, J. Am. Ceram. Soc., 74[10], pp.2388–2392, [1991].

2.106 I.A. Aksay, D.M. Dabbs and M. Sarikaya, Mullite for Structural, Electronic and Optical Applications. J. Am. Ceram. Soc., 74[10], pp.2343–2358, [1991].

2.107 S-H. Hong and G.L. Messing, Anisotropic Grain Growth in Diphasic-Gel-Derived Titania-Doped Mullite. J. Am. Ceram. Soc., 81[5], pp.1269–1277 [1998].

2.108 C. Airoldi and R.F. de Farias, Alcoxidos Como Precursores Na Sintese De Novos Materiais Atraves Do Processo Sol-Gel. Quimica Nova 27[1], pp.84–88, [2004]. (In Portuguese)

2.109 R. Roy, Aids In Hydrothermal Experimentation: II. Methods Of Making Mixtures For Both ‘‘Dry’’and ‘‘Wet’’ Phase Equilibrium Studies, J. Am. Ceram. Soc., 39[4], pp.145–146, [1956].

2.110 A.K. Chakraborty, Aluminosilicate Formation in Various Mixtures of Tetra Ethyl Orthosilicate [TEOS] And Aluminum Nitrate [ANN], Thermochimica Acta, 427[1-2], pp.109–116, [2005].

2.111 N.T. da Silva, Síntese, Caracterizacao e Cinética De Cristalizacao De Pós Precursores De Cordierita Por Sol-Gel Coloidal Sob Ação De Ácido Cítrico, Diss. Ph.D. Thesis, Iq/Unicamp, Brazil, [2003]. (http://repositorio.unicamp.br/jspui/handle/REPOSIP/249992).

2.112 F. Mizukami, K. Maeda, M. Toba, T. Sano, S-I. Niwa, M. Miyazaki, K. Kojima, Effect of Organic Ligands Used In Sol-Gel Process on the Formation of Mullite. J. Sol–Gel Sci. Techno., 8[1], pp.101–106, [1997].

2.113 V.V. Vol'khin, I.L. Kazakova, P. Pongratz and E. Halwax, Mullite Formation from Highly Homogeneous Mixtures of Al_2O_3 and SiO_2. Inorg. Mat., 36[4], pp.375–379, [2000].

2.114 M. Niederberger, G. Garnweitner, Organic Reaction Pathways in the Nonaqueous Synthesis of Metal Oxide Nanoparticles, Chem. Eur. J., 12[28], pp.7282–7302, [2006].

2.115 W-C. Wei, J.W. Halloran, Transformation Kinetics of Diphasic Aluminosilicate Gels, J. Am. Ceram. Soc., 71[7], pp.581–587, [1988].

2.116 D.X. Li, W.J. Thomson, Mullite Formation Kinetics of a Single-Phase Gel, J. Am. Ceram. Soc., 73[4], pp.964–969, [1990].

2.117 J.C. Huling and G.L. Messing, Hybrid Gels for Homoepitactic Nucleation of Mullite, J. Am. Ceram. Soc., 72[9], pp.1725–1729, [1989].

2.118 H. Zhao, K. Hiragushi and Y. Mizota, Mullite Formation of Colloidal Matrix Hybrid Aluminosilicate Gel, J. Sol-Gel Sci. Techno., 27[3], pp.287–291, [2003].

2.119 T. Ban, S. Hayashi, A. Yasumori and K. Okada, Characterization of Low Temperature Mullitization, J. Eur. Ceram. Soc., 16[2], pp.127–132, [1996].

2.120 J. Leivo, M. Linden, CV. Teixeira, J. Puputti, J. Rosenholm, E. Levanen and TA. Mantyla, Sol-Gel Synthesis of a Nanoparticulate Aluminosilicate Precursor for Homogeneous Mullite Ceramics. J. Mater. Res., 21[5], pp.1279–1285, [2006].

2.121 T. Nishio, K. Kijima, K. Kajiwara and Y. Fujiki, Influence Of Preparation Procedure In The Mullite Preparation By Solution Method To The Mixing Of Al And Si And The Crystallization Behavior, J. Ceram. Soc. Japan, 102[5], pp.462–470, [1994].

2.122 T. Nishio and Y. Fujiki, Preparation of Mullite Fiber by Sol-Gel Method, Nippon Seramikkusu Kyokai Gakujutsu Ronbunshi (J. Ceram. Soc. Japan), 99, pp.654–659, [1991].

2.123 A.K. Chakraborty, Effect of pH on 980^0C Spinel Phase Mullite Formation of Al_2O_3-SiO_2 Gels, J. Mater. Sci., 29[6], pp.1558–1568, [1994].

2.124 D. Voll, A. Beran and H. Schneider, Temperature-Dependent Dehydration of Sol-Gel-Derived Mullite Precursors: An FTIR Spectroscopic Study, J. Eur. Ceram. Soc., 18[8], pp.1101–1106, [1998].

2.125 E.R. Sola, F. Estevan, F.J. Torres and J. Alarcon, Effect of Thermal Treatment on the Structural Evolution of 3:2 and 2:1 Mullite Monophasic Gels, J. Non-cryst. Solids, 351[14-15], pp.1202–1209, [2005].

2.126 I. Jaymes and A. Douy, New Aqueous Mullite Precursor Synthesis: Structural Study by ^{27}Al and ^{29}Si NMR Spectroscopy. J. Eur. Ceram. Soc., 16[2], pp.155–160, [1996].

2.127 B. Simendic and L.J. Radonjic, Formation of Sol-Gel Nanostructured Mullite by Additions of Fluoride Ion, J. Therm. Anal. Calorim., 79[3], pp.487–492, [2005].

2.128 B. Bagchi, S. Das, A. Bhattacharya, R. Basu, and P. Nandy, Nanocrystalline Mullite Synthesis at A Low Temperature: Effect of Copper Ions, J. Am. Ceram. Soc., 92[3], pp.748-751, [2009].

2.129 D.W. Hoffman, R. Roy and S. Komarneni, Diphasic Xerogels, a New Class of Materials: Phases in the System Al_2O_3-SiO_2, J. Am. Ceram. Soc., 67[7], pp.468–471, [1984].

2.130 D.R. Volllet, D.A. Donatti, R.N. Domingos and I. Oliveira, Monolithic Diphasic Gels of Mullite by Sol-Gel Process under Ultrasound Stimulation, Ultrason. Sonochem., 5[2], pp.79–81, [1998].

2.131 A. Beran, D. Voll and H. Schneider, Dehydration and Structural Development of Mullite Precursors: An FTIR Spectroscopic Study, J. Eur. Ceram. Soc., 21[14], pp.2479–2485, [2001].

2.132 P. Padmaja, G.M. Anilkumar, P. Mukundan, G. Aruldhas and K.G.K. Warrier, Characterization of Stoichiometric Sol–Gel Mullite by Fourier Transform Infrared Spectroscopy, International J. Inorg. Mat., 3[7], pp.693–698, [2001].

2.133 E. Tkalcec, H. Ivankovic, R. Nass and H. Schmidt, Crystallization Kinetics Of Mullite Formation In Diphasic Gels Containing Different Alumina Components, J. Eur. Ceram. Soc., 23[9], pp.1465–1475, [2003].

2.134 Y.X. Huang, A.M.R. Senos, J. Rocha and J.L. Baptista, Gel Formation in Mullite Precursors Obtained Via Tetraethylorthosilicate [TEOS] Pre-Hydrolysis, J. Mater. Sci., 32[1], pp.105–110, [1997].

2.135 G.M. Anilkumar, P. Mukundan, A.D. Damodaran and K.G.K. Warrier, Effect Of Precursor pH On The Formation Characteristics Of Sol-Gel Mullite, Materials Letters, 33[3–4], pp.117-122, [1997].

2.136 J-E Lee, J-W Kim, Y-G Jung, C-Y Jo and U. Paik, Effects Of Precursor pH And Sintering Temperature On Synthesizing And Morphology Of Sol–Gel Processed Mullite, Ceramics International, 28[8], pp.935–940, [2002].

2.137 C.C. Osawa and C.A. Bertran, Mullite Formation from Mixtures of Alumina and Silica Sols: Mechanism and pH Effect, J. Brazil. Chem. Soc., 16[2], pp.251–258, [2005].

2.138 G.P. Thim, C.A. Bertran, V.E. Barlette, M.I.F. Macedo and M.A.S. Oliveira, Experimental and Monte Carlo Simulation: The Role of Urea in Mullite Synthesis, J. Eur. Ceram. Soc., 21[6], pp.759–763, [2001].

2.139 A.L. Campos, N.T. Silva, F.C.L. Melo, M.A.S. Oliveira and G.P. Thim, Crystallization Kinetics of Orthorhombic Mullite from Diphasic Gels, J. Non-cryst. Solids, 304[1-3], pp.19–24, [2002].

2.140 L.S. Cividanes, T.M.B. Campos, C.A. Bertran and G.P. Thim, Effect of Urea on the Mullite Crystallization, J. Non-cryst. Solids, 356[52–54], pp.3013–3018, [2010].

2.141 T.M.B. Campos, L.S. Cividanes, R.B.R. Garcia, E.Y. Kawachi and G.P. Thim, Efeito Do Tratamento Térmico e Do Ácido Cítrico Na Cristalizaçao Da Mulita, In: Proceedings Of The 63 Congresso Anual Da ABM, Santos, SP, Brazil, [2008].

2.142 G.M. Anilkumar, U.S. Hareesh, A.D. Damodaran & K.G.K. Warrier, Effect Of Seeds On The Formation Of Sol-Gel Mullite, Ceramics International, 23[6], pp.537-543, [1997].

2.143 S-H. Hong and G.L. Messing, Anisotropic Grain Growth in Boria-Doped Diphasic Mullite Gels, J. Eur. Ceram. Soc., 19[4], pp.521–526, [1999].

2.144 J. Roy, N. Bandyopadhyay, S. Das and S. Maitra, Role Of Cr_2O_3 On The Mullitization Of Di-phasic Al_2O_3-SiO_2 Gel, Cerâmica, 56[339], pp.273-278, [2010].

2.145 S. Ghosh, R. Majumdar, B.K. Sinhamahapatra, R.N. Nandy, M. Mukherjee and S. Mukhopadhyay, Microstructures Of Refractory Castables Prepared With Sol–Gel Additives, Ceramics International, 29[6], pp.671–677, [2003].

2.146 S. Mukhopadhyay, S. Ghosh, M.K. Mahapatra, R. Mazumder, P. Barick, S. Gupta and S. Chakraborty, Easy-To-Use Mullite And Spinel Sols As Bonding Agents In A High-Alumina Based Ultra Low Cement Castable, Ceramics International, 28[7], pp.719–729, [2002].

2.147 F. Cao, S. Long, X. Wu and R. Telle, Properties of Sol–Gel Bonding Castables, Key Engineering Materials, 336-338, pp.1484-1487, [2007].

2.148 B. Mandal, R. Sarkar and P. K. Daspoddar, Effect Of Different Mullite Precursors On The Properties Of Low Cement High Alumina Castable, Industrial Ceramics, 31[3], pp.217-222, [2011].

2.149 M.A.L. Braulio, M. Rigaud, A. Buhr, C. Parr and V.C. Pandolfelli, Spinel-Containing Alumina-Based Refractory Castables, Ceram. Int., 37[6], pp.1705–1724, [2011].

2.150 J.F. Pasquier, S. Komarneni and R. Roy, Synthesis of $MgAl_2O_4$ Spinel: Seeding Effects on Formation Temperature, Journal of Materials Science, 26[14], pp.3797–3802, [1991].

2.151 J. Guo, H. Lou, H. Zhao, X. Wang and X. Zheng, Novel Synthesis Of High Surface Area $MgAl_2O_4$ Spinel As Catalyst Support, Materials Letters, 58[12–13], pp.1920–1923, [2004].

2.152 Y. Yuan, S. Zhang and W. You, Synthesis of $MgAl_2O_4$ Spinel Nanometer Powder via Biology Polysaccharide Assisted Sol-Gel Process, Journal of Sol-Gel Science and Technology, 30[3], pp.223–227, [2004].

2.153 H. Zhang, X. Jia, Z. Liu and Z. Li, The Low Temperature Preparation Of Nanocrystalline $MgAl_2O_4$ Spinel By Citrate Sol–Gel Process, Mater. Lett., 58[10], pp.1625-1628, [2004].

2.154 H. Zhang, X. Jia, Y. Yan, Z. Liu, D. Yang and Z. Li, The Effect Of The Concentration Of Citric Acid And pH Values On The Preparation Of $MgAl_2O_4$ Ultrafine Powder By Citrate Sol–Gel Process, Mater. Res. Bull., 39[6], pp.839–850, [2004].

2.155 J. Xiaolin, Z. Haijun, Y. Yongjie and L. Zhanjie, Effect of the Citrate Sol–Gel Synthesis on the Formation of $MgAl_2O_4$ Ultrafine Powder, Mater. Sci. Eng. A, 379[1-2], pp.112–118, [2004].

2.156 M.K. Naskar and M. Chatterjee, Magnesium Aluminate ($MgAl_2O_4$) Spinel Powders from Water-Based Sols, Journal of the American Ceramic Society, 88[1], pp.38-44, [2005].

2.157 A. Saberi, F. Golestani-Fard, M. Willert-Porada, Z. Negahdari, C. Liebscher and B. Gossler, A Novel Approach To Synthesis Of Nanosize $MgAl_2O_4$ Spinel Powder Through Sol–Gel Citrate Technique And Subsequent Heat Treatment, Ceramics International, 35[3], pp.933–937, [2009].

2.158 M.Y. Nassar, I.S. Ahmed and I. Samir, A Novel Synthetic Route For Magnesium Aluminate ($MgAl_2O_4$) Particles Using Sol-Gel Auto Combustion Method And Their Photocatalytic Properties, Spectrochimica Acta Part A: Molecular And Biomolecular Spectroscopy, 131, pp.329-334, [2014].

2.159 L-Z. Pei, W-Y. Yin, J-F. Wang, J. Chen, C-G. Fan and Q-F. Zhang, Low Temperature Synthesis of Magnesium Oxide and Spinel Powders by a Sol-Gel Process. Materials Research, 13[3], pp.339-343, [2010].

2.160 N.M. Khalil, M.B. Hassan, E.M.M. Ewais and F.A. Saleh, Sintering, Mechanical And Refractory Properties Of MA Spinel Prepared Via Co-Precipitation And Sol–Gel Techniques, Journal Of Alloys And Compounds, 496[1–2], pp.600–607, [2010].

2.161 O. Varnier, N. Hovnanian, A. Larbot, P. Bergez, L. Cot and J. Charpin, Sol Gel Synthesis Of Magnesium Aluminum Spinel From A Heterometallic Alkoxide, Mat. Res. Bull., 29[5], pp.479–488 [1994].

2.162 J. Parmentiera, M. Richard-Ploueta and S. Vilminot, Influence Of The Sol-Gel Synthesis On The Formation Of Spinel $MgAl_2O_4$, Materials Research Bulletin, 33[11], pp.1717–1724, [1998].

2.163 M.M. Amini, M. Mirzaee and N. Sepanj, The Effect Of Solution Chemistry On The Preparation Of $MgAl_2O_4$ By Hydrothermal-Assisted Sol–Gel Processing, Materials Research Bulletin, 42[3], pp.563–570, [2007].

2.164 W. Liu, D. Wu and J. Yang, Preparation Of Nanometer Magnesium Aluminate Spinel Powders By Sol-Gel Method, International Journal Of Materials And Product Technology, 37[3-4], pp.297-304, [2010].

2.165 W. Liu, J. Yang, H. Xu, Y. Wang, S. Hu and C. Xue, Effects Of Chelation Reactions Between Metal Alkoxide And Acetylacetone On The Preparation Of $MgAl_2O_4$ Powders By Sol–Gel Process, Advanced Powder Technology, 24[1], pp.436–440, [2013].

2.166 D. Lepkova, A. Batarjav, B. Samuneva, Y. Ivanova and L. Georgieva, Preparation And Properties Of Ceramics From Magnesium Spinel By Sol-Gel Technology, Journal Of Materials Science, 26[18], pp.4861–4864, [1991].

2.167 G. Ye, and T. Troczynski, Mechanical Activation of Heterogeneous Sol–Gel Precursors for Synthesis of $MgAl_2O_4$ Spinel, Journal of the American Ceramic Society, 88[10], pp.2970–2974, [2005].

2.168 G. Ye, G. Oprea, and T. Troczynski, Synthesis of $MgAl_2O_4$ Spinel Powder by Combination of Sol–Gel and Precipitation Processes, Journal Of The American Ceramic Society, 88[11], pp.3241–3244, [2005].

2.169 C. Păcurariu, I. Lazău, Z. Ecsedi, R. Lazău, P. Barvinschi and G. Mărginean, New Synthesis Methods Of $MgAl_2O_4$ Spinel, Journal Of The European Ceramic Society, 27[2–3], pp.707–710, [2007].

2.170 R. Sarkar, Particle Size Distribution for Refractory Castables: A Review, Interceram, International Ceramic Review, 65[3], pp.82–86, [2016].

2.171 J. Homeny and R.C. Dradt, Aggregate Distribution Effects on the Mechanical Properties and Thermal Shock Behavior of Model Monolithic Refractory Systems. In: Fisher R, Ed. Advances in Ceramics Vol. 13. New Development in Monolithic Refractories, Westerville, OH, The American Ceramic Society, pp.110–130, [1985].

2.172 B. Myhre and A. Hundere, The Use Of Particle Size Distribution In Development Of Refractory Castables, Proceedings Of The XXV ALAFAR Congress, San Carlos de Bariloche, Argentina, 1-4 Dec, [1996].

2.173 G. Maczura, V. Gnauck and P.T. Rothenbuehler, Fine Aluminas for High Performance Refractories, The First International Conference on Refractories, pp.560–575, Technical Association of Refractories, Tokyo, Japan, 15-18 Nov, [1983].

2.174 A.H.M. Andreasen, Zur Kenntnis Des Mahlgutes, Kolloidchemische Beihefte, 27[6–12], pp.349–458, [1928]. (In German)

2.175 A.H.M. Andreasen, Üeber Die Gültigkeit Des Stokes'schen Gesetzes Für Nicht Kugelförmige Teilchen, Kolloid-Zeitschrift, 48[2], pp.175–179, [1929]. (In German)

2.176 A.H.M. Andreasen, Ueber Die Beziehung Zwischen Kornabstufung Und Zwischenraum, In: Produkten Aus Losen Körnern [Mit Einigen Experimenten], Kolloid-Zeitschrift, 50[3] pp.217–228, [1930]. (In German)

2.177 D.R. Dinger and J.E. Funk, Particle Packing II– Review of Packing of Polydisperse Particle Systems, Interceram, 41[2], pp.95–97, [1992].

2.178 R. Sarkar and A. Parija, Effect of Alumina Fines on Vibratable High Alumina Low Cement Castable, Interceram, 63[3], pp.113–116, [2014].

2.179 R. Sarkar and A. Parija, Effect of Alumina Fines on High Alumina Self-Flow Low Cement castables, Refractories World Forum, 6[1], pp.73–77, [2014].

2.180 R. Sarkar and A. Parija, Low Cement High Alumina Castable: Effect Of Distribution Coefficient, International Conference on Advances in Refractories and Clean Steel Making, RDCIS, Ranchi, India, 26–28 June [2013].

2.181 R. Sarkar, Particle Size Distribution and Distribution Coefficient of Castables, Invited Talk, National Seminar On Advances In Refractory Raw Materials And Monolithics (ARMM 2013), Kolkata, India, 12–13 Nov. [2013].

…….

Chapter 5 Result and Discussion

…….

5.1 X. Du, Y. Wang, X. Su and J. Li, Influences Of pH Value On The Microstructure And Phase Transformation Of Aluminum Hydroxide, Powder Tech., 192, pp.40-46, [2009].

5.2 M.N. Barroso, M.F. Gomez, L.A. Arrúa and M.C. Abello, Reactivity of Aluminum Spinels in the Ethanol Steam Reforming Reaction, Catal. Lett., 109, pp.13-19, [2006].

5.3 T. Meher, A.K. Basu and S. Ghatak, Physicochemical Characteristics of Alumina Gel In Hydroxyhydrogel and Normal Form, Ceram. Int., 31[6], pp.831-838, [2005].

5.4 M. Rokita, M. Handke and W. Mozgawa, The $AlPO_4$ Polymorphs Structure In The Light Of Raman And IR Spectroscopy Studies, J. Mol. Struct., 555[1-3], pp.351-356, [2000].

5.5 H.W. Van Der Marel and H. Buetelspacher, Atlas Of Infrared Spectroscopy Of Clay Minerals And Their Admixtures, pp.194, 226 and 228, Elsevier Scientific Publishing Company, Amsterdam, Oxford, New York [1976].

5.6 G. Herzberg, Spectra Of Diatomic Molecules, pp.504, D. Van Nostrand Co. Inc., New York, USA [1950].

5.7 V.C. Farmer, The Infrared Spectra of Minerals, pp.147, The Mineralogical Society, London, UK [1974].

5.8 S. Mukhopadhyay, S. Dutta, M. Majumdar, A. Kundu and S.K. Das, Synthesis And Characterization Of Alumina Bearing Sol For Application In Refractory Castables, Ind. Ceram., 20[2], pp.88-92, [2000].

5.9 P.K. Kiyohara, H.S. Santos, A.C.V. Coelho and P.S. Santos, Structure, Surface Area And Morphology Of Aluminas From Thermal Decomposition Of $Al[OH][CH_3COO]_2$ Crystals, An. Acad. Bras. Cienc, 72[4], pp.471-495, [2000].

5.10 M. Thiruchitrambalam, V. R. Palkar and V. Gopinathan, Hydrolysis Of Aluminium Metal And Sol–Gel Processing Of Nano Alumina, Mater. Lett., 58[24], pp.3063-3066, [2004].

5.11 K.R. Han, C.S. Lim, M-J. Hong, J.W. Jang and K.S. Hong, Preparation Method of Submicrometer-Sized α-Alumina by Surface Modification of γ-Alumina with Alumina Sol, J. Am. Ceram. Soc., 83[4], pp.750-754, [2000].

5.12 K. Prabhakaran, S. Ananthakumar and C. Pavithran, Gel Casting Of Alumina Using Boehmite As A Binder, J. Eur. Ceram. Soc., 19[16], pp.2875-2881, [1999].

5.13 A. Beran, D. Voll and H. Schneider, Dehydration and Structural Development of Mullite Precursors: An FTIR Spectroscopic Study, Journal of the European Ceramic Society, 21[14], pp.2479–2485, [2001].

5.14 E.R. De Sola, F. Estevan, F.J. Torres and J. Alarcon, Effect Of Thermal Treatment On The Structural Evolution Of 3:2 And 2:1 Mullite Monophasic Gels, Journal Of Non-Crystalline Solids, 351[14–15], pp.1202–1209, [2005].

5.15 Y. Hirata, K. Sakeda, Y. Matsushita, K. Shimada and Y. Ishihara, Characterization And Sintering Behavior Of Alkoxide-Derived Aluminosilicate Powders, J. Am. Ceram. Soc. 72[6], pp.995-1002, [1989].

5.16 K. Okada and N. Otsuka, Characterization of the Spinel Phase from SiO_2-Al_2O_3 Xerogels and the Formation Process of Mullite, J. Am. Ceram. Soc., 69[9], pp.652-656, [1986].

5.17 H.J. Percival, J.F. Duncan and P.K. Foster, Interpretation Of The Kaolinite-Mullite Reaction Sequence From Infrared Absorption Spectra, J. Am. Ceram. Soc., 57[2], pp.57-61, [1974].

5.18 X-H. Jin, L. Gao and J-K. Guo, The Structural Change of Diphasic Mullite Gel Studied by XRD and IR Spectrum Analysis, Journal of the European Ceramic Society, 22[8], pp.1307–1311, [2002].

5.19 J-E. Lee, J-W. Kim, Y-G. Jung, C-Y. Jo, and U. Paik, Effects of Precursor pH And Sintering Temperature on Synthesizing and Morphology of Sol–Gel Processed Mullite, Ceramics International, 28[8], pp.935–940, [2002].

5.20 A.K. Singh and R. Sarkar, High Alumina Castables: Effect of Alumina Sols and Distribution Coefficients, Trans. Ind. Ceram. Soc., 74[4], pp.225-231, [2015].

5.21 R.W. Grimshaw, The Chemistry and Physics of Clays and Allied Ceramic Materials, pp.977, Fourth Edition, Ernest Benn Ltd, London, [1971].

5.22 S. Sen, Ceramic Whitewares: Their Technologies and Applications, pp.25-26, Oxford & IBH Publishing Co. Pvt. Ltd., Calcutta, [1992].

5.23 S. Mukhopadhyay, S. Ghosh, M.K. Mahapatra, R. Mazumder, P. Barick, S. Gupta and S. Chakraborty, Easy-To-Use Mullite And Spinel Sols As Bonding Agents In A High-Alumina Based Ultra Low Cement Castable, Ceramics International, 28[7], pp.719–729, [2002],

5.24 M.A.L. Braulio, G.G. Morbioli, J. Medeiros, J.B. Gallo and V.C. Pandolfelli, Nano-Bonded Wide Temperature Range Designed Refractory Castables, J. Am. Ceram. Soc., 95[3], pp.1100–1104, [2012].

5.25 S. Ghosh, R. Majumdar, B.K. Sinhamahapatra, R.N. Nandy, M. Mukherjee and S. Mukhopadhyay, Microstructures Of Refractory Castables Prepared With Sol–Gel Additives, Ceramics International, 29[6], pp.671–677, [2003].

5.26 A. Saberi, F. Golestani-Fard, H. Sarpoolaky, M. Willert-Porada, T. Gerdes and R. Simon, Chemical Synthesis Of Nanocrystalline Magnesium Aluminate Spinel Via Nitrate-Citrate Combustion Route, J. Alloy. Compd., 462[1-2], pp.142–146, [2008].

5.27 J. Guo, H. Lou, H. Zhao, X. Wang and X. Zheng, Novel Synthesis of High Surface Area $MgAl_2O_4$ Spinel as Catalyst Support, Mater. Lett., 58[12-13], pp.1920–1923, [2004].

5.28 D. Lepkova, A. Batarjav, B. Samuneva, Y. Ivanova and L. Georgieva, Preparation and Properties of Ceramics from Magnesium Spinel by Sol-Gel Technology, J. Mater. Sci., 26[18], pp.4861–4864, [1991].

5.29 M.F. Zawrah, H. Hamaad and S. Meky, Synthesis and Characterization of Nano $MgAl_2O_4$ Spinel by the Co-Precipitated Method, Ceram. Int., 33[6], pp.969–978, [2007].

5.30 M.K. Naskar and M. Chatterjee, Magnesium Aluminate ($MgAl_2O_4$) Spinel Powders from Water-Based Sols, J. Am. Ceram. Soc., 88[1], pp.38–44, [2005].

5.31 H. Zhang, X. Jia, Z. Liu and Z. Li, The Low Temperature Preparation Of Nanocrystalline $MgAl_2O_4$ Spinel By Citrate Sol–Gel Process, Mater. Lett., 58[10], pp.1625–1628, [2004].

5.32 N.M. Khalil, M.B. Hassan, E.M.M. Ewais and F.A. Saleh, Sintering, Mechanical and Refractory Properties of MA Spinel Prepared Via Co-Precipitation and Sol–Gel Techniques, J. Alloy. Compd., 496[1-2], pp.600–607, [2010].

5.33 K.F. Waldner, R.M. Laine, S. Dhumrongvaraporn, S. Tayaniphan and R. Narayanan, Synthesis Of A Double Alkoxide Precursor To Spinel ($MgAl_2O_4$) Directly From $Al[OH]_3$, MgO, And Triethanolamine And Its Pyrolytic Transformation To Spinel, Chem. Mater., 8[12], pp.2850–2857, [1996].

5.34 T. Shiono, K. Shiono, K. Miyamoto and G. Pezzotti, Synthesis and Characterization of $MgAl_2O_4$ Spinel Precursor from a Heterogeneous Alkoxide Solution Containing Fine MgO Powder, J. Am. Ceram. Soc., 83[1], pp.235–237, [2000].

5.35 G. Ye, G. Oprea and T. Troczynski, Synthesis of $MgAl_2O_4$ Spinel Powder by Combination of Sol–Gel and Precipitation Processes, J. Am. Ceram. Soc., 88[11], pp.3241–3244, [2005].

5.36 J-G. Li, T. Ikegami, J-H. Lee, T. Mori and Y. Yajima, A Wet Chemical Process Yielding Reactive Magnesium Aluminate Spinel Powder, Ceram. Int., 27[4], pp.481–489, [2001].

5.37 S. Mukhopadhyaya, P.K. Daspoddar, Effect Of Preformed and In-Situ Spinels on Microstructure and Properties of A Low Cement Refractory Castable, Ceram. Int. 30, pp.369–380, [2004].

5.38 A.K. Singh, R. Sarkar, Effect of Binders and Distribution Coefficient on the Properties of High Alumina Castables, J. Aust. Ceram. Soc., 50[2], pp.93–98, [2014].

5.39 M.A.L. Braulio, M. Rigaud, A. Buhr, C. Parr and V.C. Pandolfelli, Spinel-Containing Alumina-Based Refractory Castables, Ceram. Int., 37[6], pp.1705–1724, [2011].

5.40 S. Zhang, W.E. Lee, Spinel-containing refractories, In: Refractories Handbook, pp.215–258, C.A. Schacht, Marcel Dekker, Monticello, [2004].

5.41 J. Chandradass, D.S. Bae and K.H. Kim, Synthesis of Calcium Hexa-aluminate ($CaAl_{12}O_{19}$) Via Reverse Micelle Process, Journal of Non-Crystalline Solids, 355[48–49], pp.2429–2432, [2009].

5.42 T. Nagaoka, T. Tsugoshi, Y. Hotta, M. Yasuoka and K. Watari, Forming And Sintering Of Porous Calcium Hexa-aluminate Ceramics With Hydraulic Alumina, Journal Of Materials Science, 41[22], pp.7401-7405, [2006].

5.43 W.E. Lee, Theory Experiment And Practice Of Slag Attack Of Refractories, Tehran International Conference On Refractories, 4-6 May [2004].

Dissemination

- **Patent: Filed**
  - A.K. Singh and R. Sarkar, Mullite bonded high alumina refractory castable using mullite precursor sol, IN Patent App. 1321/KOL/2015.
- **Journal Publication: Published**
  - A. K. Singh and R. Sarkar; High alumina castables: a comparison among various sol-gel bonding systems; Journal of the Australian Ceramics Society; accepted.
  - A. K. Singh and R. Sarkar; Development of spinel sol bonded high pure alumina castable composition; Ceramics International; 42[15], 17410–17419; [2016].
  - A. K. Singh and R. Sarkar; Nano mullite bonded refractory castable composition for high temperature applications; Ceramics International; 42[11], 12937–12945; [2016].
  - A. K. Singh and R. Sarkar; High alumina Castables: Effect of alumina sols and distribution coefficients; Transactions of the Indian Ceramic Society; 74[4], 225-231; [2016].
  - A. K. Singh and R. Sarkar; Synthesis and Characterization of Alumina Sol and Its Use as Binder in No Cement High-Alumina Refractory Castables; International Journal of Applied Ceramic Technology; 12[S3], E54-E60; [2015].
  - A. K. Singh and R. Sarkar; Effect of Binders and Distribution Coefficient on the Properties of High Alumina Castables; Journal of the Australian Ceramics Society; 50[2], 93–98; [2014].
- **Conference:**
  - A. K. Singh and R. Sarkar; Effect of Different Sol Systems on High Alumina Castable Refractory; Research Scholar's Week (RSW) 2016; NIT Rourkela; 2016.
  - A. K. Singh and R. Sarkar, High Alumina Castables: Effect of alumina sol and distribution coefficient, 78th Annual Session of Indian Ceramic Society, Jamshedpur; 2015.
  - A. K. Singh and R. Sarkar, High Alumina Castables: Comparative Study between Binders and Distribution Coefficients, 77th Annual Session of Indian Ceramic Society, Jamshedpur, 2013.